TAMPEREEN TEKNILLINEN YLIOPISTO
TAMPERE UNIVERSITY OF TECHNOLOGY

Antti Vehkaoja

Unobtrusive Monitoring of Heart Rate and Respiration Rate during Sleep

Julkaisu 1285 • Publication 1285

Tampere 2015

Tampereen teknillinen yliopisto. Julkaisu 1285
Tampere University of Technology. Publication 1285

Antti Vehkaoja

Unobtrusive Monitoring of Heart Rate and Respiration Rate during Sleep

Thesis for the degree of Doctor of Science in Technology to be presented with due permission for public examination and criticism in Sähkötalo Building, Auditorium S4, at Tampere University of Technology, on the 27th of February 2015, at 12 noon.

Tampereen teknillinen yliopisto - Tampere University of Technology
Tampere 2015

ISBN 978-952-15-3470-6 (printed)
ISBN 978-952-15-3475-1 (PDF)
ISSN 1459-2045

Abstract

Sleep deprivation has various adverse psychological and physiological effects. The effects range from decreased vigilance causing an increased risk of e.g. traffic accidents to a decreased immune response causing an increased risk of falling ill. Prevalence of the most common sleep disorder, insomnia can be, depending on the study, as high as 30 % in adult population. Physiological information measured unobtrusively during sleep can be used to assess the quantity and the quality of sleep by detecting sleeping patterns and possible sleep disorders. The parameters derived from the signals measured with unobtrusive sensors may include all or some of the following: heartbeat intervals, respiration cycle lengths, and movements. The information can be used in wellness applications that include self-monitoring of the sleep quality or it can also be used for the screening of sleep disorders and in following-up of the effect of a medical treatment. Unobtrusive sensors do not cause excessive discomfort or inconvenience to the user and are thus suitable for long-term monitoring. Even though the monitoring itself does not solve the sleeping problems, it can encourage the users to pay more attention on their sleep.

While unobtrusive sensors are convenient to use, their common drawback is that the quality of the signals they produce is not as good as with conventional measurement methods. Movement artifacts, for example, can make the detection of the heartbeat intervals and respiration impossible. The accuracy and the availability of the physiological information extracted from the signals however depend on the measurement principle and the signal analysis methods used.

Three different measurement systems were constructed in the studies included in the thesis and signal processing methods were developed for detecting heartbeat intervals and respiration cycle lengths from the measured signals. The performance of the measurement systems and the signal analysis methods were evaluated separately for each system with healthy young adult subjects. The detection of physiological information with the three systems was based on the measurement of ballistocardiographic and respiration movement signals with force sensors placed under the bedposts, the measurement of electrocardiographic (ECG) signal with textile electrodes attached to the bed sheet, and the measurement of the ECG signal with non-contact capacitive electrodes. Combining the information produced by different measurement methods for improving the detection performance was also tested.

From the evaluated methods, the most accurate heartbeat interval information was obtained with contact electrodes attached to the bed sheet. The same method also provided the highest heart rate detection coverage. This monitoring method, however, has a limitation that it requires a naked upper body, which is not necessarily acceptable for everyone. For respiration cycle length detection, better results were achieved by using signals recorded with force sensors placed under a bedpost than when extracting the respiration information from the ECG signal recorded with textile bed sheet electrodes. From the data quality point of view, an ideal night-time physiological monitoring system would include a contact ECG measurement for the heart rate monitoring and force sensors for the respiration monitoring. The force sensor signals could also be used for movement detection.

Acknowledgements

I wish to thank my supervisor, Professor Jukka Lekkala for the guidance he has provided and for the trust he has shown towards my abilities of doing this research independently. I am very grateful to the pre-examiners of the thesis, Professor Kwang Suk Park from Seoul National University and Professor Pasi Karjalainen from University of Eastern Finland for their valuable comments and also to my colleagues who kindly volunteered to comment the thesis manuscript and suggest improvements. I want to express my gratitude also to the co-authors of the publications included in the thesis, especially to Mikko Peltokangas and Jarmo Verho who have had a remarkable contribution in almost all of them. I want to thank people of the Department of Automation Science and Engineering for providing inspiring working atmosphere as well as people from other departments, institutions and companies with whom I have had a change to collaborate during this process.

The research presented in this thesis was started at the Department of Automation Science and Engineering at Tampere University of Technology in the summer 2010. Between years 2011 and 2014 I had a change to work as a teaching associate in the department, which offered me a possibility to work with this same research topic and to prepare this thesis. I am very grateful for this opportunity. During years 2011–2013 we also had one research project which dealt partially with the same topic as the thesis. This project, named MotoSD was funded by the Finnish Funding Agency for Innovation (Tekes) and Finnish companies. I would also like to acknowledge the financial support provided by Finnish Cultural Foundation and its Pirkanmaa

Regional Fund, Jenny and Antti Wihuri Foundation, Finnish Foundation of Automation, and Finnish Electronics Engineers Foundation in the form of working, support, and travelling grants.

Finally, I want to thank my family; my wife Nina for her patience during this process and our daughter Stella and recently our yet to be named son who have helped in putting the things in life into right order of importance.

Nokia, February 2015,

Antti Vehkaoja

Contents

List of publications

This thesis is based on the following publications, which are referred to in the text as Publications I – V. The publications are reprinted with the permission of the copyright holders. The publications have not been used as a part of other doctoral theses.

I. Peltokangas, M., Verho, J., and Vehkaoja, A., “Night-time EKG and HRV monitoring with bed sheet integrated textile electrodes," *IEEE Transactions on Information Technology in Biomedicine*, vol. 16, no. 5, pp. 935–942, Sept. 2012.

II. Vehkaoja, A., Rajala, S., Kumpulainen, P., and Lekkala, J., “Correlation approach for the detection of the heartbeat intervals by using bed integrated force sensors,” *Journal of Medical Engineering & Technology*, vol. 37, no. 5, pp. 327–333, July 2013.

III. Vehkaoja, A., Peltokangas, M., Verho, J., and Lekkala, J., “Combining the information of unconstrained electrocardiography and ballistography in the detection of night-time heart rate and respiration rate,” *International Journal of Monitoring and Surveillance Technologies Research (IJMSTR), Special Issue on Biomedical Monitoring Technologies*, vol. 1, no. 3, pp. 52–67, July-Sept. 2013.

IV. Vehkaoja, A., Peltokangas, M., and Lekkala, J., “Extracting the respiration cycle lengths from ECG signal recorded with bed sheet electrodes,” *Journal of Physics: Conference Series, Joint IMEKO TC1–TC7–TC13 Symposium*, vol. 459, no. 1, 2013, 6 pages.

V. Vehkaoja, A., Salo, A., Peltokangas, M., Verho, J., Salpavaara, T., and Lekkala, J., “Unconstrained night-time heart rate monitoring with capacitive electrodes,” in *Proceedings of XIII IFMBE Mediterranean Conference on Medical and Biological Engineering and Computing 2013*, vol. 41, 2014, pp. 1511–1514.

Author’s contribution

In Publication I, the author was closely supervising the development process of the monitoring system. The author participated in the designing of the system, the development of the signal analysis methods, conducting the test measurement, the analysis of the results, and writing the manuscript.

In Publication II, the author constructed the measurement setup, developed the signal processing methods, analyzed the data, and wrote most of the article.

In Publication III, the author further developed the measurement setup presented in Publication I and the related signal processing methods, developed the signal processing method for respiration detection, conducted the data collection, did the data analysis, and wrote most of the article.

In Publication IV, the author developed the signal processing methods for respiration detection based on the ECG signal, did the data analysis using the dataset collected originally for Publication III, and wrote most of the article.

In Publication V, the author participated in the designing of the measurement setup and collecting the data. The author also made the data analysis and wrote most of the article.

List of abbreviations

ADC	analog-to-digital conversion
Ag/AgCl	silver-silver chloride (electrode)
ANS	autonomous nervous system
BBI	beat-to-beat interval
BCG	ballistocardiogram, ballistocardiography
bpm	beats per minute
ECG	electrocardiography, measurement of the electrical activity of the heart
EDR	ECG derived respiration
EEG	electroencephalography, measurement of the electrical activity of the brain
EMFi	electro mechanical film
EMG	electromyography, measurement of the electrical activity of muscles
EOG	electro-oculography, measurement of the electrical signal resulting from eye movements
GND	ground
HF	high frequency
HR	heart rate

HRV	heart rate variability
LF	low frequency
MAE	mean absolute error
N1, N2, N3	NREM sleep phases
NREM	non-rapid eye movement (sleep phase)
NTC	negative temperature coefficient
OSA	obstructive sleep apnea
PSD	power spectral density
PSG	polysomnography
PVDF	polyvinylidene fluoride
QRS	certain waveform in an ECG signal
R-peak	middle point of the QRS waveform
RCL	respiration cycle length
REM	rapid eye movement (sleep phase)
RMSE	root mean square error
RRI	R-R-interval, time interval between two ECG R-peaks
RR	respiration rate
RSA	respiratory sinus arrhythmia
SNR	signal-to-noise ratio
SCSB	static charge sensitive bed
USB	universal serial bus

List of symbols

C1	capacitor 1
E	expected value
m_x	sample mean value of x
N	number of values
ρ	correlation coefficient
R1	resistor 1
$R1$	resistance of R1
R_{in}	input resistance
σ_x	variance of x
s_x	sample standard deviation of x
s_x^2	sample variance of x
s_{xy}	sample covariance of x and y
τ	delay
U1	operational amplifier 1
$V+$	positive supply voltage

$V-$	negative supply voltage
V_{in}	input voltage
V_{out}	output voltage
x	one element of a variable or vector X
X	vector X
μ	expected value
y	one element of a variable or vector Y
Y	vector Y

1 Introduction

We sleep roughly one third of our lives. The amount and the quality of sleep strongly affect our performance during the other two thirds. Everyone knows from their own experience how physical and mental performance is decreased after a badly slept night. Adequate amount of good quality sleep is needed for several bodily functions. The fundamental reason why we sleep is, however, still not completely understood. Theories suggest that sleep is needed to restore the energy balance in the brain (Scharf et al., 2008) and to conserve the total energy expenditure of the body (Mignot, 2008). Sleep also has an important role in learning and improvement of motor performance, since newly experienced things convert as memories during sleep (Hill et al., 2008; Stickgold, 2005).

Sleep deprivation or sleep loss has a variety of adverse physiological and mental effects such as decreased vigilance (Lim and Dinges, 2008), increased fatigue and stress (Dinges et al., 1997), mood disturbances (Kahn-Greene et al., 2006; Kamphuis et al., 2012), disturbed thermoregulation (Romeijn et al., 2012), and decreased cognitive performance (Alhola and Polo-Kantola, 2007; Harrison and Horne, 2000). Sleep deprivation has also been associated with interferences in metabolic function causing an increased risk of obesity and type 2 diabetes (Knutson and Van Cauter, 2008). The amount of sleep also affects to the immunity system and smaller amount of sleep or poorer sleep efficiency has been shown to expose to viral infections (Cohen et al., 2009; Irwin et al., 1996; Patel et al., 2012).

Monitoring of sleep and assessing sleep quality could be used to motivate people to pay more attention to their sleeping habits. For this purpose, continuous long-term monitoring that enables observing sleep trends and illustrates the effects of good sleep understandably is desirable. However, in order to be accepted by the users, the monitoring technology needs to be minimally obtrusive and require as little additional effort from the user as possible. Other possible applications for long-term night-time physiological monitoring include the screening of sleeping disorders, follow-up of the effects of sleep disorder treatment, elderly monitoring in nursing homes, and monitoring of newborns.

In order to give maximum value to the user, whether the user is the person being monitored or a sleep physician, the data provided by the monitoring system should be as accurate as possible and there should be as few temporal gaps or breaks in the data as possible. In many applications, the measured physiological information about the heart rate or respiration rate is further refined to some higher level information such as sleep phases or sleep quality information before shown to the user. The user is primarily interested in the correctness of the provided information. The uncertainty in the initial data is, however, inevitably reflected in the uncertainty of the end results. The correctness of the data is particularly important aspect in the medical screening or follow-up application areas.

The thesis combines and compares the results of five research papers that present measurement systems and signal processing methods for monitoring night-time physiological signals and deriving heartbeat interval and respiration cycle length information from them. Measurement systems of three different kind were constructed and used for recording the physiological signals. The constructed systems are based on the measurement of ballistocardiographic (BCG) and respiration signals with force sensors placed under the bedposts, the measurement of electrocardiographic (ECG) signal using textile electrodes that are attached to the bed sheet and the measurement of ECG signal with non-contact capacitive electrodes.

1.1 Objectives and contribution of the thesis

The main objective of the thesis is to evaluate and compare the aforementioned techniques for unobtrusive monitoring of physiological signals during sleep. A large part of the contribution of the thesis are the developed signal processing methods, which are partially different for each monitoring technique.

The following research questions are studied in the thesis:

1. What kind of unobtrusive measurement principles and sensor setups are suitable for unobtrusive monitoring of heart rate and respiration rate and what limitations do the methods have?
2. What specific requirements do the investigated sensing methods set for the signal processing algorithms used for extracting the heart rate and the respiration information from the measurement data?
3. How do the developed monitoring methods perform in the detection of the physiological parameters and are there noticeable differences in their performances?
4. What kind of a measurement system would suit best for unobtrusive respiration and heart rate detection?

The scientific contributions of the thesis are:

- the developed unobtrusive bed-integrated measurement systems,
- the signal processing algorithms developed for the detection of heartbeat intervals from the ballistocardiographic and electrocardiographic signals,
- the signal processing algorithms developed for the detection of respiration cycle lengths from the force sensor and electrocardiographic signals.

1.2 Structure of the thesis

The thesis is structured as follows: Chapter 2 provides the background for the presented work. It briefly revises the applications of the night-time physiological monitoring and presents previously developed methods for collecting this information focusing on the unobtrusive techniques that are suitable for long-term monitoring. Chapter 3 presents the measurement systems developed and used in the studies of Publications I – V and the signal processing techniques developed for extracting physiological information from the measured data. Chapter

4 presents the results obtained with the measurement systems and discusses the findings of the thesis. Chapter 5 presents the conclusions and gives answers to the research questions.

2 Background

This chapter briefly revises the most important and interesting applications for the night-time physiological monitoring and presents the most common methods for collecting the night-time physiological information. The focus is on unobtrusive monitoring techniques that are suitable for long-term monitoring and especially in the methods similar to those presented in Publications I – V. The state-of-the-art in the signal analysis methods developed for detecting the heart rate and respiration rate from the signals of unobtrusive sensors is also presented.

2.1 Applications of unobtrusive night-time physiological monitoring

Automatic monitoring of night-time physiological information, especially the heart rate, respiration rate, and movements can be used for several purposes. An important application is the classification of sleep stages or phases, which further enables the assessment of sleep quantity and quality. Traditionally, sleep is classified into different phases using the data from a polysomnographic recording i.e. polysomnography (PSG). This classification is called sleep staging and the resulting graph that shows sleep stages as a function of time is called hypnogram. PSG is briefly introduced in Section 2.2.1. According to the currently used rules, sleep is divided into five stages, one of which is awake. The actual sleep time consists of REM (rapid eye movement) sleep and NREM (non-rapid eye movement) sleep. The latter is further divided into three stages (N1, N2, N3) according to the depth of the sleep, N3 being the deepest sleep stage (Iber et al., 2007).

The sleep stages have been defined mainly according to the features present in the electroencephalographic (EEG) signals that result from the electrical activity of brain. Also electro-oculographic (EOG) and electromyographic (EMG) activity from eyes and muscles are used in sleep staging (Iber et al., 2007). None of these signals is available when using unobtrusive sensors for the measurement. The sleep stages can, however, be estimated by using the heart rate, respiration rate and movement information, which all can be collected using unobtrusive sensors (Choi et al., 2009; Chung et al., 2009; Kortelainen et al., 2010; Paalasmaa et al., 2012). This information can be further used to evaluate the quality of sleep as in (Paalasmaa et al., 2012). The information about the quality and the quantity of sleep measured unobtrusively can be used in self-monitoring applications to give the user feedback and to encourage the user to pay more attention to the importance of sleep (Paalasmaa 2014a).

Another application domain for unobtrusive night-time physiological monitoring methods is the screening of medical disorders. Currently, the unobtrusive methods are not yet widely adopted for this application domain but there is research evidence supporting their usage. For example, signals measured with unobtrusive sensors have been used to detect sleep related breathing disorders. Examples include the screening of sleep apnoea (Ayas et al., 2003; Roche et al., 1999) and also other types of sleep disordered breathing (Alametsä et al., 2006; Tenhunen et al., 2011). Tenhunen et al. showed that the increase in respiration effort can be detected with a force sensor placed under the thoracic area of a sleeping person (Tenhunen et al., 2011). In (Beattie et al., 2013) the apnea-hypopnea index was estimated with high accuracy using load-cell type bedpost sensors. Psychophysiological stress can be estimated from the night-time heart rate variability (HRV) information (Hall et al., 2004) and also atrial fibrillations have been detected using BCG signals (Brüser et al., 2013a). Information received by sleep staging, e.g. sleep onset latency can be further used in the screening of insomnias, which form the most prevalent group of sleep disorders affecting even as much as 30 % of adult population (Ohayon and Bader, 2010a; Ohayon and Sagales, 2010b). Unobtrusive bed integrated force sensors have also been successfully used for the detection of periodic limb movements, which is another prevalent sleep disorder (Rauhala, 2009).

All in all, the unobtrusive sensors and measurement systems enable longitudinal monitoring of sleep without causing discomfort to the user and therefore provide completely new aspects for sleep research.

2.2 Monitoring methods

This section presents different measurement methods that are suitable for unobtrusive night-time monitoring. The gold standard methods currently used for medical examination and diagnosis, polysomnography and wrist actigraphy, are introduced first.

2.2.1 Polysomnography

PSG is the standard method for collecting reliable and multiparametric data from a sleeping person and it is considered as the gold standard in sleep measurements. It can be used in the diagnosis of various medical disorders such as: sleep related breathing disorders, other respiratory disorders, narcolepsy, parasomnias, sleep related seizure disorders, restless legs syndrome, periodic limb movement sleep disorder, depression with insomnia, and circadian rhythm sleep disorders (Kushida et al., 2005). The biggest drawback of the polysomnographic examination is its high cost, which is a result of the requirement of specialized medical personnel and dedicated examination facilities. As a result, all the potential sleep disorder patients are, in practice, not examined and the monitoring is usually done during one night only. The discomfort caused by wearing the measurement equipment may also affect the sleep and skew the results. The signals or channels commonly measured and the sensors commonly used in full PSG recording include at least: three to six EEG channels, two EOG channels, one chin and one or more limb EMG channels, one or two airflow channels with temperature and/or flow pressure sensors, two respiration effort channels with respiratory inductance plethysmography sensors, microphone as snoring sensor, an ECG channel, blood oxygen saturation sensor, and body position sensor (Iber et al., 2007; Kushida et al., 2005).

In ambulatory PSG, a portable polysomnographic recording device is used. Most of the sensors are installed at the hospital but the patient spends the night at home and installs the rest of the sensor before going to bed (Leivo, 2007). This may be a more comfortable arrangement for some people but still does not remove the burden of wearing the multitude of sensors while in bed and does not enable a practical monitoring of more than one night. The reliability of the recording is also decreased when it is performed in unattended conditions (Gagnadoux et al., 2002; Portier et al., 2000).

Simpler portable sleep monitoring devices also exist. They can be used for recording of a subset of the physiological parameters of the full polysomnography. An example of such a device is WatchPAT from Itamar Medical (WatchPAT), which is able to detect obstructive sleep apnoea (OSA) events from the signals recorded only from the wrist. Unattended use of portable monitors of this kind for making clinical diagnosis of OSA, for instance, is still questioned (Collop et al., 2007).

2.2.2 Wrist actigraphy

Wrist actigraphy is another examination technique used for medical sleep analysis. It can be used in a variety of sleep studies including longitudinal monitoring of sleep patterns and circadian rhythm in the natural sleeping environment of the patient (Martin and Hakim, 2011). As the name implies, wrist actigraphy monitors patient's activity through a wrist-worn device using accelerometers. The benefit is that the device is relatively unobtrusive and the data can therefore be collected for extended periods of time, e.g. for one week. According to the recommendations of the American Association of Sleep Medicine, wrist actigraphy can be used in monitoring of several sleep disorders that are related to sleep rhythm (Morgenthaler et al., 2007). Still, it only offers one modality of information, activity, which limits its usability and the achievable accuracy of the results. For example, it is difficult to differentiate sleep from lying still in the bed and wrist actigraphy has been reported to overestimate the amount of sleep and sleep efficiency (Pollak et al., 2001).

2.2.3 Ballistocardiography

Ballistocardiography measures the mechanical signal caused by the cardiac activity. The main components of the BCG signal result from the movement of blood in the heart and in aorta. BCG was discovered in the late 19th century and developed during the first half of the 20th century to be used as a tool to analyze cardiac function (Pinheiro et al., 2010). Cardiac analysis through ECG recordings and other techniques such as ultrasound, however, displaced the BCG as a diagnostic tool by the end of the 1970s (Giovangrandi et al., 2011).

Another application area for BCG recordings has been night-time monitoring of physiological signals. In these applications, the interest is in the detection of heartbeat intervals instead of the exact waveform of the BCG signal. Already in late 70's Alihanka et al. developed a method of using a static charge sensitive bed (SCSB) for measuring the physiological parameters of a person during sleep (Alihanka et al., 1981). The lack of powerful automated signal analysis methods however led to the diminishing of the interest towards night-time BCG monitoring for almost a couple of decades. Later, the development of technology, especially the signal analysis methods and an increase in computation power, has brought new interest towards ballistocardiography especially in the area of unobtrusive night-time physiological monitoring.

In the original applications that were aiming for the evaluation of the cardiac function, the exact waveform of the ballistocardiographic signal was important and therefore the measurement setup had to be strictly controlled (Scarborough et al., 1956). In long-term night-time monitoring, the measurement conditions cannot be controlled because the person being monitored has to have a possibility to e.g. change the sleeping posture. Therefore, the measured waveforms are usually not consistent with the textbook examples of BCG signals. The measurements made with bed integrated sensors are still commonly called as ballistocardiography. An alternative and more general term for these measurements is ballistography, but it is rarely used. It was, however, applied in Publication III to emphasize that not only cardiac but also respiration related information was extracted from the measured signals.

There are several possibilities for the placement of the BCG sensors to the bed. They can be installed under the bedposts (Brink et al., 2006; Kärki and Lekkala 2009; Mack et al., 2009a; Publication II), to the bed frame (Brüser et al., 2011), on top of the mattress (Jacobs et al., 2004; Niizeki et al., 2005; Paalasmaa 2014b; Siivola, 1989), or under the pillow (Chen et al., 2008). Also special mattresses with integrated sensors have been developed (Alihanka et al., 1981; Chee et al., 2005; Kortelainen et al., 2010). Sensor location has an effect on how different physiological signals are coupled to the sensors and how the signals produced by another person possibly sleeping in the same bed affect the measurement. For example, the sensors located under the bedposts are more prone to interferences caused by the movements of another person than the sensors located right under the person being monitored (Paalasmaa 2014a). Also the structure of the bed has an effect on the coupling of the signals.

A large variation in the operational principles of the developed ballistocardiographic sensors also exists. Film type sensors made of piezoelectric polymer, polyvinylidene fluoride (PVDF) have been used in (Jacobs et al., 2004; Kortelainen et al., 2012; Niizeki et al., 2005; Paalasmaa et al., 2014b; Wang et al., 2003). Another film type force sensor material, permanently charged electret polymer material EMFi (Electro Mechanical Film), has been used in (Alametsä et al., 2006; Brüser et al., 2013b; Kortelainen et al., 2010; Publication II). Bedpost sensors based on the optical detection of beam deflection were used in (Brink et al., 2006) and strain gauges attached to a slat under the mattress were used in (Brüser et al., 2011). Sensor structures consisting of a mat or tubes filled either with water or air have been used in (Chee et al., 2005; Chen et al., 2008; Rosales et al., 2012; Tanaka et al., 2002). Yet another type of sensor for ballistocardiographic recording has been proposed in (Böhm et al., 2013). It is comprised of light emitting diodes and a photo detector located inside the mattress topper. The ballistocardiographic movements alter the amount of light scattered back to the photo detector. A similar system, but using the modulation of ultrasound, was proposed in (Mukai et al., 2009).

There are some commercially available products in the market that use ballistocardiographic signals for monitoring sleep. These include e.g. Emfit IP-9150 non-contact vital signs monitor by EMFit Ltd. (EMFit), Beddit sleep tracker by Beddit Ltd (Beddit), and Touch-free Life Care™ smart bed sensor by BAM Labs Inc (BAM Labs).

2.2.4 Unobtrusive monitoring of the electrical activity of the heart

Another researched method for obtaining physiological information from a sleeping person is to measure the electrical signal of the heart, the ECG. While attaching conventional disposable ECG electrodes containing adhesives to the body every night is beyond being unobtrusive, other possible monitoring techniques include using wearable monitoring systems with reusable textile electrodes, attaching the electrodes to the bed sheet, or using capacitively coupled non-contact electrodes placed on top of the mattress.

ECG monitoring with wearable sensors

Slightly less obtrusive technique than attaching conventional adhesive electrodes to the body every night is to use a vest or shirt that includes the electrodes and also carries the measurement device as in (Yang et al., 2009). Such system was also tested in (Vehkaoja et al., 2012). A regular heart rate belt is another option to be used as the platform for wearable sensors. Choi and Jiang combined the measurement of wearable ECG and respiration in a measurement belt that included textile electrodes and a force sensor made of piezoelectric PVDF material (Choi and Jiang, 2008). For many users, wearable devices are, however, too disturbing to be used continuously, especially if the person does not have any special motivation to do so, such as the screening of medical disorder or follow-up of the effect of a treatment.

Contact electrodes embedded into the bed

An unobtrusive way of recording a contact ECG signal is to attach the electrodes to the bed. A system using two large area textile electrodes, one acting also as the pillow case and the other covering the foot of the bed was presented in (Devot et al., 2007). Similar electrode setup was used in (Ishijima, 1997). Park et al. also used pillow and foot electrodes but they added another two large electrode areas to both sides of the bed providing another ECG channel (Park et al., 2008). The measurement setup proposed in Publications I and III has eight textile electrodes attached transversally to the bed sheet. The drawback of this approach is that in order to have a galvanic contact between the electrodes and the skin, the user cannot wear a shirt or pajamas. There is no such requirement with the approach proposed by Devot et al. and Ishijima but in their systems the pillow always has to be used under the head and having hair between the electrode and the skin may block the galvanic contact and disturb the signals.

Capacitive electrodes embedded into the bed

Capacitive electrodes do not have a galvanic contact with the skin. Their benefit is that the electrodes can be designed so that the user can wear clothes. The drawback of the capacitive electrodes is that they are very sensitive to the motion artifacts because the skin-electrode capacitance varies due to movements, which together with triboelectricity may cause strong interferences to the signals. For these reasons, the capacitive electrodes are not commonly used in applications where a large amount of movement is present, although a capacitive heart rate monitoring has been successfully applied to a car seat (Wartzek et al., 2011). The amount of movements is limited during sleep and therefore capacitive electrodes provide an interesting possibility for night-time heart rate monitoring.

Systems using capacitive electrodes in the measurement of a night-time ECG signal have been proposed in (Ishida et al., 2007; Lim et al., 2007; Publication V; Wu and Zhang, 2008). Large area capacitive textile electrodes measuring one ECG channel were used in the studies by Ishida et al. and Wu and Zhang. The systems presented in (Lim et al., 2007 and Publication V) included several small area active electrodes placed transversally in the bed. The same electrode setup as used in (Lim et al., 2007) was also successfully used for the detection of sleeping postures in (Lee et al., 2013). The system proposed by Ishijima included, besides contact electrode ECG monitoring, also large area capacitive electrodes under the body for measuring the movements caused by respiration through the changes in the capacitances between the electrodes and the body (Ishijima, 1997).

2.2.5 Other techniques

The thesis focuses on the evaluation and comparison of the developed monitoring systems that are based on the aforementioned monitoring techniques; ballistocardiography and electrocardiography with contact and capacitive electrodes. There are also other possible methods for unobtrusive night-time physiological monitoring.

Microwave radar

Microwave radars have been used for measuring respiration and heart rate (Droitcour, 2006; Xiaomeng et al., 2012; Zakrzewski et al., 2012). An Irish company Biancamed, a part of ResMed Inc. has a product SleepMinder, which uses microwave radar in the detection of respiration and further, analysis of sleep quality. The device is also able to detect periods of sleep disordered breathing and estimate the apnoea-hypopnoea index (Zaffaroni et al., 2013). The principle of operation of the microwave radars is based on the Doppler phenomenon.

Infra-red and video imaging

Respiration can also be detected by an infra-red video imaging and monitoring the changes of temperature near nostrils caused by inhaling and exhaling (Abbas et al., 2011; Murthy et al., 2004). Respiration detection using normal visible light and near infra-red video imaging has also been studied (Bartula et al., 2013).

Accelerometers

In addition to wrist worn actigraphy devices, accelerometers have also been utilized in other ways for night-time physiological monitoring. Phan et al. studied the measurement of respiratory waveform and heart rate using an accelerometer attached to the chest of a person (Phan et al., 2008). Also other studies of using wearable accelerometer for heart rate detection have been reported and the technique is able to provide sporadic heart rate readings also during day time activities (Kwon et al., 2011). The signal recorded by an accelerometer attached to the chest has been called seismocardiogram. The main origin of the measured signal is the physical contraction of the heart muscle rather than from the movement of the blood as in ballistocardiography.

The accelerometer does not necessarily need to be worn for detecting a heart rate during sleep. An accelerometer placed inside the duvet was used in (Okada et al., 2006). Woodward et al. used accelerometers placed into the mattress topper (Woodward et al., 2007). They called the method as kinetocardiogram. Murata Ltd. has recently introduced a module that includes their low noise inclinometer and embedded digital signal processor for extracting heart and respiration rate when the module is placed under the mattress toper (Murata). In this case the accelerometer measures the vibrations of the bed caused by the BCG force and changes in the inclination of the sensor caused by the respiration movements. Besides these examples, using bed integrated accelerometers for night-time heart rate monitoring has not been extensively reported. A probable reason for this is that the acceleration signal caused by heartbeats is weak and the measurement therefore requires very low noise accelerometer to be used. Also the structure and the mass of the bed affect how strong acceleration the ballistocardiographic forces cause to the bed.

Sleep Cycle Alarm Clock is an iPhone application that uses the accelerometer of the mobile device to estimate the depth of sleep and adjusts the actual time of the wake-up alarm within a time window based on the estimated sleep depth. The alarm is triggered when the movements of the person become stronger and more frequent showing a lighter phase of sleep (Sleep Cycle). Similar application, Sleep as Android, is available for the Android devices (Sleep as Android). Also other such applications exit. The smartphone applications may also take an advantage of using the microphone of the device for recording respiration sounds and snoring (Hao et al., 2013; Krejcar et al., 2011).

Besides the actigraphy devices intended for medical investigations, a number of wrist-worn devices that use accelerometers for sleep evaluation have also been developed for wellness sector. These include for example Fitbit Flex, Jawbone UP, and SleepTracker (Kelly et al., 2012). Two former ones are also intended for daytime activity monitoring.

2.3 Algorithms for heartbeat interval and respiration cycle length detection

This section presents the background and the state-of-the-art of the signal processing techniques developed for detecting the heart rate or the heartbeat intervals and the respiration cycles from the BCG and the ECG signals. There are two different strategies for the detection of these parameters. One can detect the average value of the heart or the respiration rate over a certain time period, for example one epoch of sleep analysis, or one can try to detect individual events i.e. every heartbeat or respiration cycle. The latter approach is generally more demanding and requires more sophisticated signal analysis methods.

In the applications of night-time monitoring, there is usually no need for on-line signal analysis, especially when the person being monitored is using or reviewing the data him- or herself. Exceptions are e.g. monitoring of people suffering from dementia where an important application could be the detection of the person leaving the bed, or monitoring of a newborn for detecting possible signs of a sudden infant death syndrome. If it is desired that the results of the overnight sleep are ready as soon as possible after the awakening, the data can be processed in smaller batches and each batch can be processed as off-line data. All signal processing techniques presented in the thesis have been developed for off-line use.

2.3.1 Heartbeat interval detection

Algorithms for ballistocardiogram based heartbeat interval detection

Various signal processing techniques have been developed to detect beat-to-beat intervals from BCG signals. Difficulty in ballistocardiogram based heartbeat detection is that the signal waveform varies substantially between the subjects and also depends on the measurement conditions, e.g. the bed, the sleeping posture, and the location of the person in the bed. The signal waveform, however, stays fairly constant when all the aforementioned conditions remain constant. For these reason, any predefined waveform should not be looked from the signal when trying to detect the heartbeats but rather recognize repeating patterns in the signal.

Figure 1 shows examples of different BCG waveforms recorded from different subjects and postures with a film type force sensor placed under a bedpost.

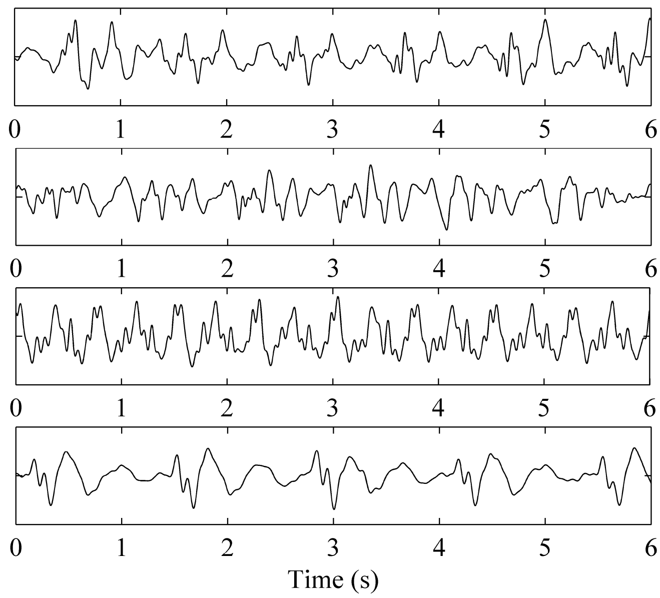

Figure 1. *Examples of different BCG waveforms. The figure is adopted from Publication II.*

Clustering of feature vectors formed from the morphology of the measured BCG signal to form a template for heartbeat detection has been used in (Brüser et al., 2011; Paalasmaa and Ranta, 2008; Paalasmaa et al., 2014b; Rosales et al., 2012). The templates were further used in (Brüser et al., 2011 and Paalasmaa et al., 2014b) as a part of a multi-phase beat-to-beat interval detection process. In (Paalasmaa 2014b) beat-to-beat intervals were searched by constructing a synthetic signal that includes two heartbeats based on the template and evaluating its correlation with the measured BCG signal. In (Brüser et al., 2011), three indicators were calculated and used together to find the heartbeats. The template found by clustering was used to find the heartbeats by cross correlation. This was combined with the calculation of the Euclidean distance between the feature vectors formed from the BCG signal and the cluster center, and heartbeat locations suggested by the so called heart valve signal.

Brüser et al. have also published another method for inter-beat interval detection where they used a sliding search window and the results of autocorrelation, average magnitude difference function, and maximum amplitude pair as probabilistic estimators of the heartbeat interval

(Brüser et al., 2013b). The methods developed by Brüser et al. and Paalasmaa et al. can be considered as the state-of-the-art in beat-to-beat interval detection from a single channel BCG signal.

Other, simpler methods for beat-to-beat heart rate detection have included e.g. using of wavelet decomposition for signal preprocessing as in (Jin et al., 2009; Wang et al., 2003; Zhu 2006). Wang et al. used wavelet decomposition in preprocessing the BCG signal and a smoothed square of a certain wavelet component to highlight the heartbeat complexes, which were then recognized by adaptive thresholding (Wang et al., 2003).

Brink et al. used a moving window with variable length to detect the highest peaks with suitable distance in the signal (Brink et al., 2006). A method for beat-to-beat interval detection based on k-means clustering was proposed in (Rosales et al., 2012). In (Friedrich et al., 2010) heartbeat intervals were first detected using heart valve signal, modeled beat-to-beat interval trend, and a stochastic HRV model. The estimates were then further refined by using correlation. Cross-correlation between a heartbeat template and the BCG signal recorded with SCSB sensor was used already in (Jansen et al., 1991).

An interesting method for heartbeat detection from multiple BCG signals was proposed in (Kortelainen et al., 2007). The method is based on using a signal cepstrum, which is the inverse Fourier transforms of the logarithm of the estimated spectrum of the signal. Heartbeat frequency and its harmonics form a peak into the cepstrum at the time point that corresponds to the time interval of two heartbeats. Kortelainen et al. also used averaging of multiple measurement channels in order to reduce the variance of the cepstra and to improve the accuracy of the method. A multichannel extension of the method proposed in (Brüser et al., 2013b) was compared with Kortelainen's method in (Brüser et al., 2015). Using the multiple channels of BCG data significantly improved the performance of Brüser's algorithm by increasing both, the detection coverage and the accuracy of the beat-to-beat interval detection. The multichannel version of Brüser's algorithm was showing similar coverage but smaller error than Kortelainen's algorithm.

Heart rate detection from the electrocardiogram

The analysis of ECG signals has been under a lot of research for several decades because of its clinical importance. The detection of the R-peak or the QRS complex from the ECG signal is one of the most basic tasks in automated ECG analysis and it serves as a basis for the detection of other ECG waveforms. A huge variety of different methods have been developed for the detection of the QRS complexes in the ECG signal (Elgendi et al., 2014; Kohler et al., 2002). The developed methods include for example the use of signal derivative, filters, and adaptive thresholds (Elgendi, 2013; Pan and Tomkins, 1985), hidden Markov models (Andreão et al., 2006), wavelet decomposition (Park et al., 2008; Zidelmal et al., 2012), neural networks (Maglaveras et al., 1998), or a combination of the previous two (Abibullaev and Seo, 2011). Many authors have, besides robustness, also emphasized the computational simplicity when developing methods for the QRS detection (Darrington, 2006; Elgendi, 2013; Pan and Tompkins, 1985; Yeh and Wang, 2008; Zhengzhong et al. 2011). One of the most well-known database for testing the performance of the developed QRS detection algorithms is MIT-BIH Arrhythmia Database (Moody and Mark, 2001), which is available through Physionet database archive (Goldberger et al., 2000). A large number of other ECG databases are also available through Physionet (Physionet).

The aforementioned R-peak detection methods have been usually developed for signals recorded with regular, e.g. disposable Ag/AgCl gel electrodes but the same algorithms can be used to detect heart rate from signals recorded with unobtrusive bed integrated textile or capacitive electrodes. However, the quality of the ECG signals acquired with textile or capacitive electrodes is often not as good as what is achieved with gel electrodes. The noise level in the signals is usually higher due to the properties the skin-electrode interface (e.g. lack of electrolyte in case of the textile electrodes). The measurement lead varies according to the sleeping posture, which changes the appearance of the recorded signal affecting also to the polarity and the morphology of the QRS complex. These issues need to be taken into account when designing or selecting an algorithm for the R-peak detection. If the measurement system includes multiple measurement channels from which the best one is preferably used for the heart rate detection, the signal quality assessment and channel selection should also be done carefully. Another possibility is to detect the heartbeats from all the channels and combine the results. In both cases the computational complexity of the QRS detection algorithm should be considered when selecting the algorithm.

2.3.2 Respiration cycle length detection

Detection of the respiration cycle length from a force sensor signal

Many authors who have developed ballistocardiographic methods for the detection of night-time physiological parameters have developed, besides heartbeat detection, also methods for respiration rate (RR) or respiration cycle length (RCL) detection from the same signals. Paalasmaa et al. used multiple band-pass filters with different cut-off frequencies for filtering the signal measured with a piezo-electric bedpost sensor and then calculated the RCLs using the output of the filter that produced the breathing signal with the most consistent amplitude (Paalasmaa et al., 2011). Wang et al. used a single component of the wavelet transformed force sensor signal and an adaptive threshold to count the breathing cycles (Wang et al., 2003). Signal preprocessing with wavelet decomposition was also used in (Zhu 2006 and Chen et al., 2008). Shin et al. used autocorrelation to compute the mean respiration rate in 30 second epochs (Shin et al., 2010). Force signal preprocessing by principal component analysis was used in (Kortelainen et al., 2012). The first principal component of the signals of eight sensor channels was used in their study for the respiration detection.

Detection of the respiration cycle length from the ECG signal

Breathing rate can also be detected from the ECG signal. The signals produced using the ECG to resemble respiration are usually called ECG derived respiration (EDR) signals. One commonly used respiration related feature in the ECG is the respiratory sinus arrhythmia (RSA), which is caused by the autonomous nervous system's (ANS) regulation of sinoatrial node of the heart (Berntson et al., 1993). Several other features can be derived from the physical modulation of the direction of the mean electrical axis of the heart due to filling and emptying of the lungs (Moody et al., 1985). This effectively modulates the morphology of the QRS complexes and affects to the baseline of the measured ECG signal. The respiration related features that have been derived from this physical modulation and used for respiration detection include ECG baseline changes, the amplitude of the R-peak, R-S-amplitude, area of the QRS complex, and the kurtosis of the distribution of ECG signal sample values between consecutive R-peaks (Boyle et al., 2009; Ding et al., 2004; O'Brien and Heneghan, 2007, Park et al., 2008; Widjaja et al., 2010).

Orphanidou et al. used the power density spectrum of the R-R-interval (RRI) signal to find the frequency of the RSA and combined that with the spectrum of the signal formed using R-peak amplitudes (Orphanidou et al., 2013). They used the method for estimating the average respiration rate in one minute time windows. The same EDR signals were used in (Cysarz et al., 2008) to calculate the mean respiration rate in 5 minute epochs. Avci et al. evaluated the performance of six different ECG based respiration detection methods in average and instantaneous respiration cycle length detection. From the evaluated methods, a combination of the RSA signal and ECG baseline signal band-pass filtered with 0.2 Hz–0.8 Hz performed the best (Avci et al., 2011). The same conclusion was drawn by Boyle et al. when evaluating methods for ECG based respiration detection during several daily activities (Boyle et al., 2009).

From the aforementioned studies, the one conducted by Park et al. is the only one that used electrodes attached to the bed. They, however, used a controlled setup where the person was lying only in the supine position. The other authors have used electrodes that have been fixed to certain locations on the body. Therefore the proposed methods do not necessarily perform equally well with signals recorded using an unconstrained bed integrated ECG measurement setup.

It should be noticed that most of the EDR methods provide only one sample of data for each heartbeat, which means that e.g. in case of heart rate being 60 bpm and respiration rate 20 cycles per minute, only three samples for each respiration cycle are received. According to the Nyquist-Shannon sampling theorem, the sampling rate should be at least twice the highest sinusoidal frequency component in the signal (Shannon, 1949). The waveform of the respiration signal, however, is not exactly sinusoidal and it therefore includes also frequency components higher than the fundamental respiration frequency. This leads to the distortion of the respiration waveform that is reconstructed using the sparsely sampled data and thus increases the uncertainty of the detected instantaneous respiration cycle lengths. Further problems may occur if the respiration rate is particularly high compared to the heart rate. Relatively good results can, however, be achieved by using polynomial or spline interpolation, which has been used by most of the authors in reconstructing the respiration signals, e.g. (Avci et al., 2011; Cysarz et al., 2008; Park et al., 2008; Publications III and IV; Widjaja et al., 2010).

A minor detail worth knowing when combining the EDR signals based on the RSA and the physical modulation of the ECG signal is that they are not in the same phase, and furthermore, the phase difference is not constant because of the complex regulation mechanisms of the ANS. The phase difference has been found to vary, for example, depending on the sleep stage (Thomas et al., 2005).

3 Developed monitoring systems

This chapter presents the measurement systems used for signal collection in Publications I – V and the developed signal processing methods.

Three different methods for detecting heartbeat intervals with bed integrated sensors were investigated in the attached publications. The methods are: ballistocardiography that is measured with sensors placed under the bedposts (Publication II), contact ECG measurement with textile sensors attached to the bed sheet (Publication I; Publication III), and the measurement of the ECG with capacitive electrodes (Publication V). Detection of the respiration cycle lengths by using force sensor signals (Publication III) and features extracted from the contact ECG signal (Publication IV) were also investigated. The recordings were made in all studies using custom made data acquisition devices that have 16 bit measurement resolution and using 250 Hz sampling rate. The signal processing in all developed systems has been done off-line using MATLAB software from MathWorks Inc., Natick, MA, USA.

3.1 Methods developed for unobtrusive heartbeat interval detection

3.1.1 Ballistocardiographic heartbeat interval detection

Publication II presents the monitoring system and the developed signal processing method for detecting heartbeat intervals with force sensors placed under the bedposts. The dynamic force sensors selected for the system were commercial products from EMFit Ltd. (S-series sensors) manufactured from EMFi material. EMFi is a permanently charged cellular film material made of polypropylene (Paajanen et al., 2000). Its main difference compared with the piezoelectric polymers like PVDF is that it is fairly insensitive to other forces than the force component normal to its surface.

One EMFi sensor was placed under each bedpost. Albeit the main component of the BCG signal is in the direction of the torso, the mechanics of the bed in practice converts the force so that it can be measured with the EMFi sensor as changes in the normal force. A non-inverting voltage amplifier with a gain of 100 was used to amplify the signals and decrease the impedance level of the signal. High-pass cut-off frequency was set to 0.15 Hz by setting the input resistance of the amplifier to 100 MΩ with a bias resistor and the capacitance to approximately 11 nF. Figure 2 shows the EMFi film sensor placed under a bedpost.

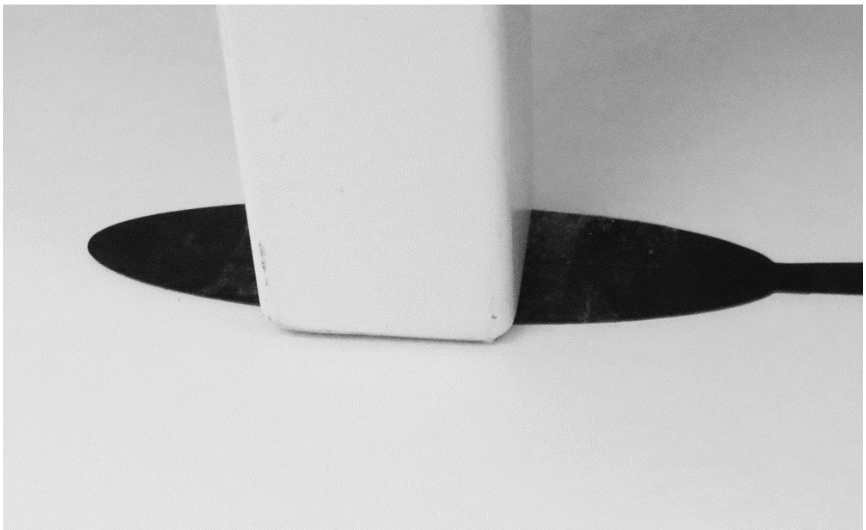

Figure 2. *An EMFi sensor placed under a bedpost.*

In digital signal processing, the sensor signals were first low-pass filtered with a cut-off frequency of 20 Hz because no content relevant to the heartbeat detection was considered existing above this frequency. This also removes the 50 Hz power line interference from the signals. Then a difference was taken from the signals by subtracting the value of preceding sample from each sample in the signal. The signal waveforms or complexes caused by the heartbeats are emphasized in the difference signal thus improving the recognition of the heartbeat intervals. The difference signal was also used in (Brüser et al., 2013b; Paalasmaa and Ranta, 2008; Paalasmaa et al., 2014b).

The signal produced by movements can be orders of magnitude higher than the signal produced by the ballistocardiographic forces. It is practically impossible to find the heartbeats or heartbeat intervals if there are simultaneously artifacts caused by strong movements in the signal. Admitting this fact, the amplifier and the data acquisition device used in Publication II were adjusted so that stronger movements e.g. changing the sleeping posture caused the amplifier to saturate. The limits of saturation were used to detect the movements and the signal preprocessing step removed these sections in addition to two second safety margins from further processing.

The methods found in literature for detecting heartbeats or heartbeat intervals usually try to find the exact locations of the waveforms that correspond to the heartbeats. The heartbeat detection method proposed in Publication II does not try to find individual beats but only the repetition interval of the main component in the signal that is in the same frequency range as the normal resting heart rate.

The method is based on finding the delay that produces the maximum correlation between two consecutive signal segments. The sample correlation coefficient ρ between two sequences as a function of the delay τ is calculated according to Equation 1.

$$\rho_{XY}(\tau) = \frac{E[(X-\mu_X)(Y_\tau - \mu_Y)]}{\sqrt{E[(X-\mu_X)^2]}\sqrt{E[(Y-\mu_Y)^2]}} = \frac{\frac{1}{N-1-\tau}\sum_{i=1}^{N-\tau}(x_i - m_x)(y_{i+\tau} - m_y)}{s_x s_y}, \tag{1}$$

where E[·] is the expected value of the expression inside the brackets, X and Y are signal vectors, μ_X and μ_Y are the expected values of X and Y, x and y are the two consecutive signal segments of length N, m_x and m_y are the sample mean values of the segments, and s_x and s_y are the corresponding sample standard deviations defined as:

$$s_x = \sqrt{\frac{1}{N-1}\sum_{i=1}^{N}(x_i - m_x)^2}\ . \tag{2}$$

The assumption is that the heartbeat interval may vary between 0.5 – 1.5 seconds, which corresponds the heart rate values of 45 – 120 beats per minute. The optimal lengths of the consecutive data segments depend on the prevailing heart rate and therefore the algorithm uses several different segment lengths simultaneously and finds the correlation maximum for each case. This is repeated for all four sensors under the bedposts. Only correlation coefficients above a fixed threshold (0.75 in Publication II) are considered and the median of the beat-to-beat intervals (BBI) suggested by the five highest correlation coefficient values is considered as the BBI value for that time instance. The computation is done every 0.5 seconds and thus an equally spaced BBI vector is formed. Figure 3 shows an example of the difference of a ballistocardiogram signal and the resulting correlation sequence when the cross correlation between the two signal segments identified by the vertical lines is calculated.

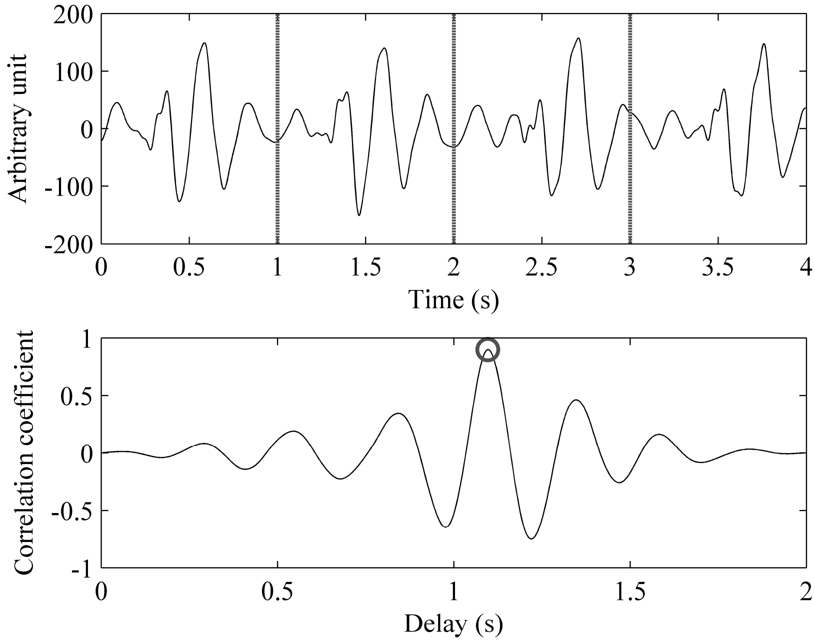

Figure 3. *An example of the difference of the ballistocardiogram signal (upper trace) and the correlation sequence calculated from the signal segments between 1–2 s and 2–3 s. The figure is adopted from Publication II.*

The formed beat-to-beat interval signal is then post-processed to remove clearly erroneous detections and to make the continuously detected BBI segments longer. Because the BBI is calculated for every 0.5 seconds there should not be single values that deviate much from the surrounding values. A true, deviant beat-to-beat interval should be seen in more than one detected BBI values. Therefore, if there is a single value in the continuous BBI signal that differs more than 100 ms from both values around it, the value is considered as an outlier. In these cases, the value is replaced with the average of the two surrounding BBI values. Also the gaps in the BBI series caused by single missing BBI values are filled with the mean value of the preceding and following BBIs.

There are also cases where only one or two consecutive BBI values have been detected. In these cases, the values are discarded because the scattered BBI detections indicate that the recorded BCG signals are not of good quality and the detected BBI values are more likely to be incorrect than the values in a continuously detected BBI signal.

3.1.2 Heart rate monitoring with bed sheet integrated textile electrodes

Publication I presents a measurement system and a signal processing method that was developed for measuring and analyzing ECG signals recorded with textile electrodes attached to the bed sheet. In Publication III, the measurement system was modified by decreasing the inter-electrode distance and the signal processing method was further developed. Also a simple method for deploying movement information to assist in the R-R-interval detection from the ECG signal processing was tested.

In Publication I, eight electrodes were attached to the bed sheet transversally with approximately 10 cm spacing. The voltage signal was measured between two adjacent electrodes thus forming seven signals in total. The person lying on the bed is not in contact with all the electrodes at the same time and usable signal is therefore available only in some of the measurement channels. Figure 4 shows the measurement setup.

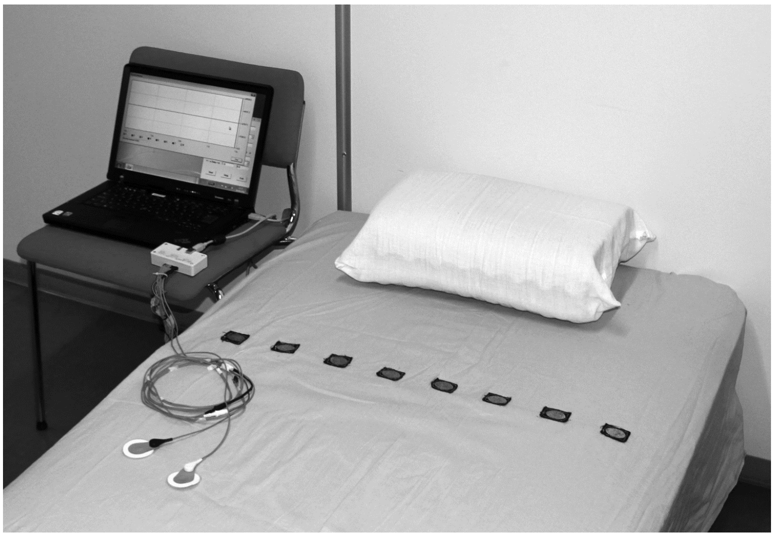

Figure 4. *Bed sheet ECG recording system with integrated textile electrodes. The figure is adopted from (Peltokangas et al., 2011)*

Before trying to detect the QRS complexes from the measured ECG signals, the signals are preprocessed by low-pass filtering with a cut-off frequency of 30 Hz and high-pass filtering with a non-linear filter that removes a 100 ms moving median from the signals. This essentially removes any baseline wander and even lower frequency physiological ECG features like P- or T-wave but leaves the high frequency QRS complex untouched. The method was proposed in (Keselbrener et al., 1997) for ECG preprocessing.

The filtered signals are then processed with a channel selection algorithm, which chooses the channel with the best signal quality to be used in the RRI detection. The best channel is selected by investigating a 10 second signal sample taken from all the channels. The 10 second samples are divided into 2 second segments and the peak with the highest amplitude is searched from each segment. The amplitudes and the maximum derivatives of the peaks' rising and falling edges are marked. The average peak amplitude and the average maximum derivatives are then used to set thresholds for the peak detector. All peaks satisfying the criteria are searched from the 10-second signal samples.

Next, the noise level in the signals is determined by comparing the amplitude of the found peaks with the variance of the remaining baseline signal. For those signals that fulfill the maximum noise criterion, the physiological rationality of the found R-peaks is verified. From the channels that contain only physiologically reasonable peaks, the one with the highest ratio between the average peak amplitude and the variance of the remaining signal is selected and used in the R-peak detection. If none of the signals fulfill the minimum requirements of the signal quality, the channel selection is tried again after one second.

The actual R-peak detection is done using the same method as in the channel selection. The thresholds for the R-peak and derivative amplitudes are updated with the values of recently detected R-peaks. The channel selection procedure is repeated if the signal quality of the currently used channel decreases too much or if the R-peaks are no longer found in the signal. Finally, polynomial fitting is used to refine the R-peak location estimates for achieving sub-sample interval accuracy. The R-peak detection algorithm was modified from the method proposed in (Zhengzhong et al., 2011). A more detailed description of the algorithm is found in Publication I.

The feasibility of using movement information to assist in the RRI detection was tested as a part of the study presented in Publication III. The assumption was that if the degradation of the signal quality is not caused by movement, the channel reselection criteria can be adjusted to tolerate a smaller signal-to-noise ratio (SNR). This was implemented by setting another threshold for the ECG signal quality indicator. When the first threshold was met, the value of a movement indicator calculated from the signal of a force sensor located under a bedpost was checked. If it showed no movement, the measurement was continued. Only if the ECG signal quality indicator went under the second threshold, the channel reselection was initiated even when the movement was not present.

Combining the measurement channels

The effect of combining the bed sheet ECG channels to the R-R-interval detection coverage and accuracy was tested as a part of the work reported in Publication III. To increase the number of electrodes simultaneously in contact with the monitored person, the inter-electrode distance was also decreased from 10 cm to 5 cm.

Combining the signals of the adjacent bed sheet ECG channels increases the signal quality in two ways. Firstly, the noise caused by the measurement electronics and the interferences in the skin-electrode interfaces are independent between the channels if at least three channels are combined (for two combined channels the interference associated with the common electrode is not independent) whereas the ECG signal is not independent and the R-peaks are seen practically at the same time in all channels where they are visible. This increases the SNR by the square root of the number of the combined channels, when assuming that the signal component is identical in the channels. In practice the effect is smaller because the signals are not exactly the same. The more important source of the improvement is the increased distance of the measuring electrodes, which according to the lead field theory, increases the measurement sensitivity deeper in the torso where the signal source, the heart, is located (Puurtinen, 2012). Figure 5 illustrates the effect of increased inter-electrode distance to the measurement lead field.

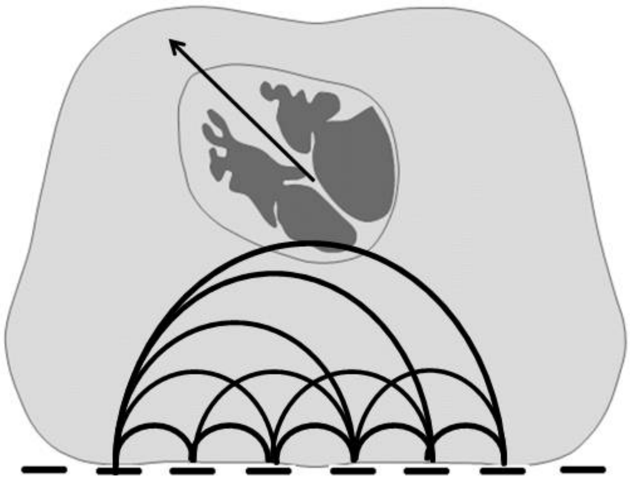

__Figure 5.__ The principle of the measurement sensitivity with different combination of the electrode pairs (all combinations are not shown for clarity). The picture is for illustration only and does not correspond to the actual lead field of the measurement. The figure is modified from (Malmivuo J. and Plonsey R., 1995).

Combining the measurement channels is simply done by adding the recorded signals together after low-pass filtering with 30 Hz cut-off frequency. This can be done because each electrode, excluding the outermost electrodes, is common to two adjacent measurement channels. In addition to the original seven measurement channels, the combining produces six combinations of two channels, five combinations of three channels and so on. Altogether 21 channel combinations in addition to the original seven channels are thus formed. The best channel for the R-peak detection is selected from all 28 possibilities in the same way as in Publication I. Figure 6 shows an example of the improvement of the signal-to-noise ratio of the bed sheet ECG signal when the signals of three adjacent measurement channels are combined.

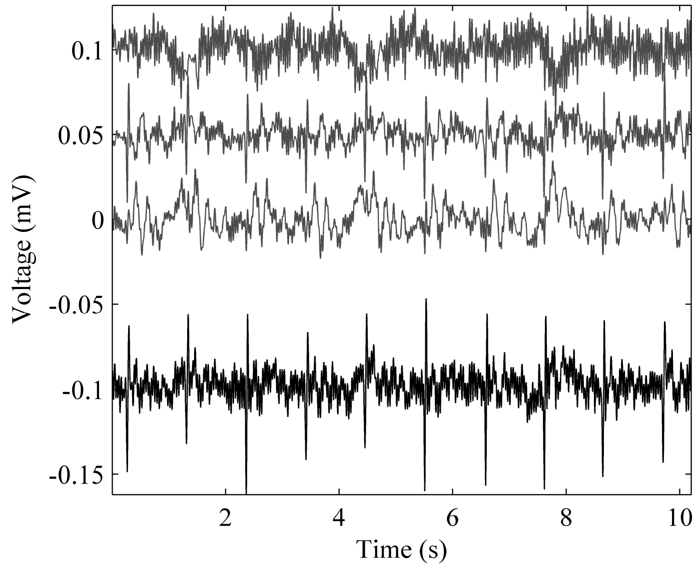

Figure 6. *An example of the effect of combining the measurement channels. Three upper traces are signals from individual measurement channels and the lowest trace is the combined signal. The signals are off-set for clarity. The figure is adopted from Publication III.*

3.1.3 Heart rate monitoring with capacitive electrodes

The drawback of using the bed sheet integrated textile electrodes for measuring the night-time ECG and heart rate is the requirement of direct skin contact and therefore basically a naked upper body. To overcome this drawback, a system that uses capacitive active electrodes was designed and tested as a bed integrated ECG recording device.

The system reported in Publication V includes four capacitive electrodes that are located transversally with five centimeter distances on the bed sheet similarly as the textile electrodes in Publication III. The setup however differs from the textile electrodes in a sense that with the capacitive electrodes, the potentials measured by the electrodes are not compared with each other but the signal from each electrode is formed with respect to a large common capacitive ground electrode. The capacitive ground electrode is realized by placing a conductive textile sheet, covering the whole bed, under the bed sheet.

The high-pass frequency of a capacitive electrode is determined by the capacitance between the electrode and the measured person, and the input resistance of the electrode. The diameter of the active electrodes used was 25 mm. Assuming that the person being measured is wearing a 0.5 mm thick cotton shirt that has the relative permittivity of 2, the skin-electrode capacitance becomes approximately 20 pF. Together with a 110 GΩ input resistance used in the capacitive electrodes, the high-pass cut-off frequency becomes approximately 0.08 Hz.

The circuit diagram of one capacitive active electrode is shown in Figure 7. The input resistance of 110 GΩ is formed by using a bootstrap connection which effectively multiplies the input impedance via positive feedback (Jung, 2004). The input resistance of the electrode in Figure 7 is calculated as:

$$R_{in} = (\frac{R5}{R4} + 1) \cdot R1 + R3 \tag{3}$$

The operational amplifier used in the capacitive electrodes, OPA129, has a non-standard pinout, which supports an efficient guarding of the input terminals. It also has a very small input bias current which allows using a large value of bias resistance.

In addition to protect the input from leakage currents, the guard also decreases the parasitic capacitance of the circuit board layout. The input capacitance of the amplifier component and some parasitic capacitance still remain, which together with the capacitance of the electrode form a capacitive voltage division, which changes the pass-band gain of the active electrode. A capacitive positive feedback was used to compensate these remaining input capacitances. The gain of the feedback is adjusted by the variable resistor R2. When a test signal is fed to the active electrode, the gain of the electrode is adjusted to the set value, 0.9 in this case. Figure 8 shows the capacitive active electrode.

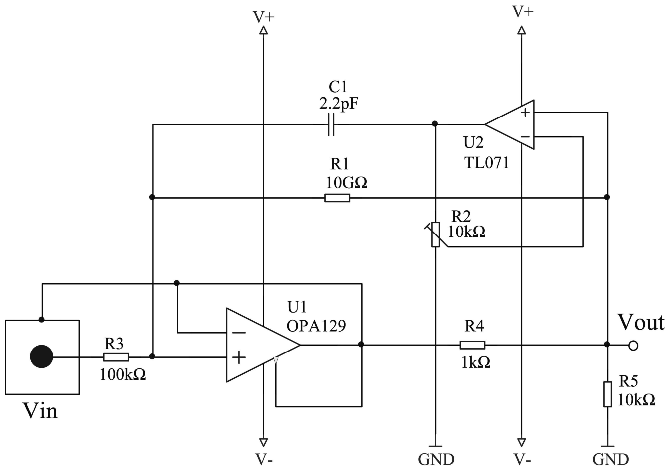

Figure 7. *Schematic of the capacitive active electrode. The figure is adopted from Publication V.*

Figure 8. The capacitive active electrode. The active area with the diameter of 25 mm is surrounded by a guard ring. The electronics is protected with an enclosure made of copper.

The capacitive ECG measurement is very sensitive to movements. Movements, like changing the sleeping posture or even a movement of a limb can cause so strong disturbances to the measured signal that the recognition of the R-peaks is impossible. Also smaller artefacts that were synchronous with the heartbeats were often seen in the signals when testing the capacitive monitoring system. One explanation for these is that they result from the movements caused by ballistocardiographic forces. Capacitively measured ECG signals containing this kind of artefact component are illustrated in the upper panel of Figure 9.

Often these small artifacts are seen similarly in more than one channel while the ECG component in the signals is different because of the different electrode location on the body. Combining the measurement channels by subtracting their signals can therefore attenuate the common mode interference significantly as shown in the lower panel of Figure 9. All channel combinations were calculated and the same channel selection algorithm as was used with the textile electrodes was then let to select the best signal for R-peak detection. Also the original signals were used as possible alternatives for the R-peak detection.

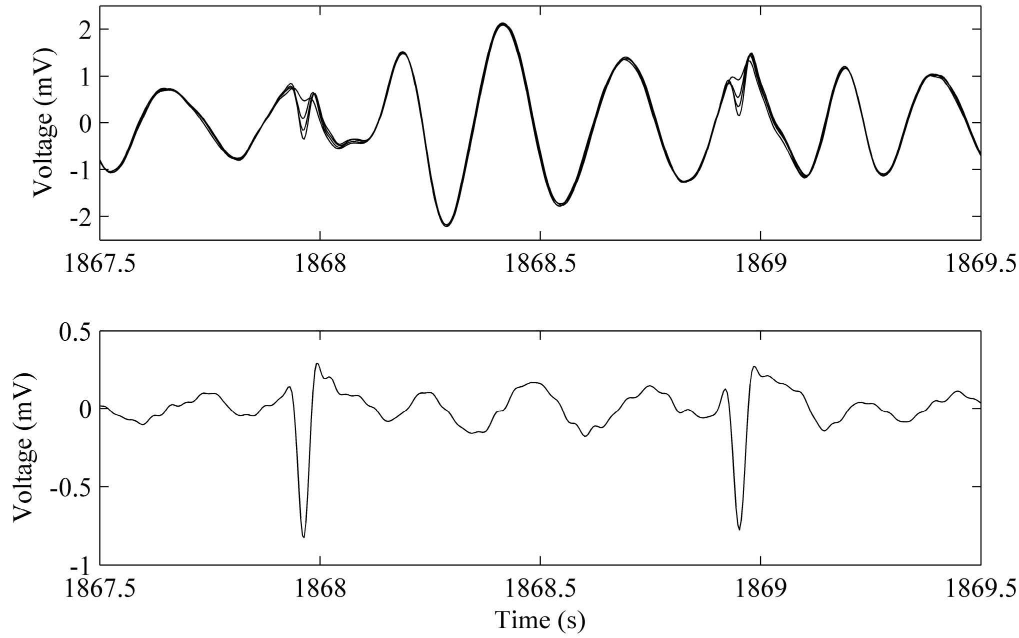

Figure 9. *Four signals recorded with the capacitive electrodes (upper panel). Common mode artifacts in the signals are caused by small movements. The lower panel shows how the R-peaks are emphasized when subtracting those two signals that differ the most at the R-peak locations. The figure is adopted from Publication V.*

3.2 Methods developed for unobtrusive respiration detection

Two methods were developed for detecting respiration cycle lengths by using physiological signals of different origin. The first method, using force sensors placed under a bedpost was studied in Publication III. The other method, using ECG signals recorded with bed sheet integrated textile electrodes, was studied in Publication IV. It was also tested in Publication III if combining these two methods and measurement modalities would improve the detection results.

3.2.1 Respiration detection from the force sensor signals

Dynamic force sensors made of EMFi were used also in the detection of respiration cycle lengths. Two EMFi sensor elements were used in Publication III and they were placed under the same bedpost. Using of two sensors provides data redundancy but does not complicate the measurement system significantly. The high-pass cut-off frequency of the respiration measurement setup was set to 0.05 Hz, which is more suitable for the low frequency respiration signal than the cut-off frequency of 0.15 Hz that was used in the heartbeat interval detection in Publication II.

Disturbances caused by movements were recognized in Publication III by using the variance calculated in a 4-second sliding window. A threshold was empirically set at 20 times of the average variance of the recording. 5-second safety margins were used before and after the detected disturbance instead of the 2-second margins used in the heartbeat interval detection because of the lower cut-off frequency and frequency content of the signal that was under investigation.

The algorithm developed for detecting the RCLs is based on using filters with different pass-bands to preprocess the force sensor signals. Filtering the force sensor signals for respiration detection with several pass-bands was earlier used in (Paalasmaa et al., 2011). The pass-bands of the filters were: 0.05–0.154 Hz, 0.1–0.22 Hz, 0.1–0.33 Hz, and 0.1–0.5 Hz. The low-pass frequency of 0.33 Hz was erroneously reported as 0.433 Hz in Publication III. The reason for using filters with different pass-bands is that the signal measured with force sensors and low-pass filtered for respiration detection often contains a certain kind of distortion or skew at one half period of the signal as can be seen in the panel b of Figure 10. The frequency of these distortion components is approximately two times the respiration frequency. It is desirable that the cut-off frequency is between the main frequency and the frequency of the distortion. The respiration cycle length normally varies between two and ten seconds, which corresponds to 0.1–0.5 Hz. If the low-pass cut-off is lower than the respiration frequency, it will attenuate the actual signal. If the cut-off is higher than two times the respiration frequency, it will not remove the undesired component. The filter order has to be high enough so that the undesired component of the signal is attenuated but the amplitude of the basic component caused by the respiration is not affected significantly. On the other hand, the filter order should not be too high so that it does not distort the shape of the signal when the respiration frequency is close to the cut-off. Fourth order filters with Butterworth response gave good results in tests and were used in Publication III.

After filtering with four different pass-bands, simple features: local maxima, local minima, and rising and falling zero crossings are recognized from all resulting signals. RCL suggestions are generated as the repetition intervals of these features. With two sensors and four filters, eight signals are formed and by calculating four features from each signal, 32 RCL suggestion vectors are generated. The RCL suggestion vectors are then interpolated linearly to one second sample intervals.

For each time instance, the RCL is determined to be in the middle of a cluster that is formed by those six suggestions that are closest to each other. If the square distance of the six closest suggestions is too high, the uncertainty of the suggested RCL value is considered too large and no RCL value is given for that time instance. It is still checked in the post-processing phase that there is no single time instance where the selected RCL value deviates too much (1 s) from the surrounding values. Different phases of the RCL detection process are illustrated in Figure 10. Panel a of Figure 10 shows a reference respiration signal that was measured using a thermistor placed inside a breathing mask.

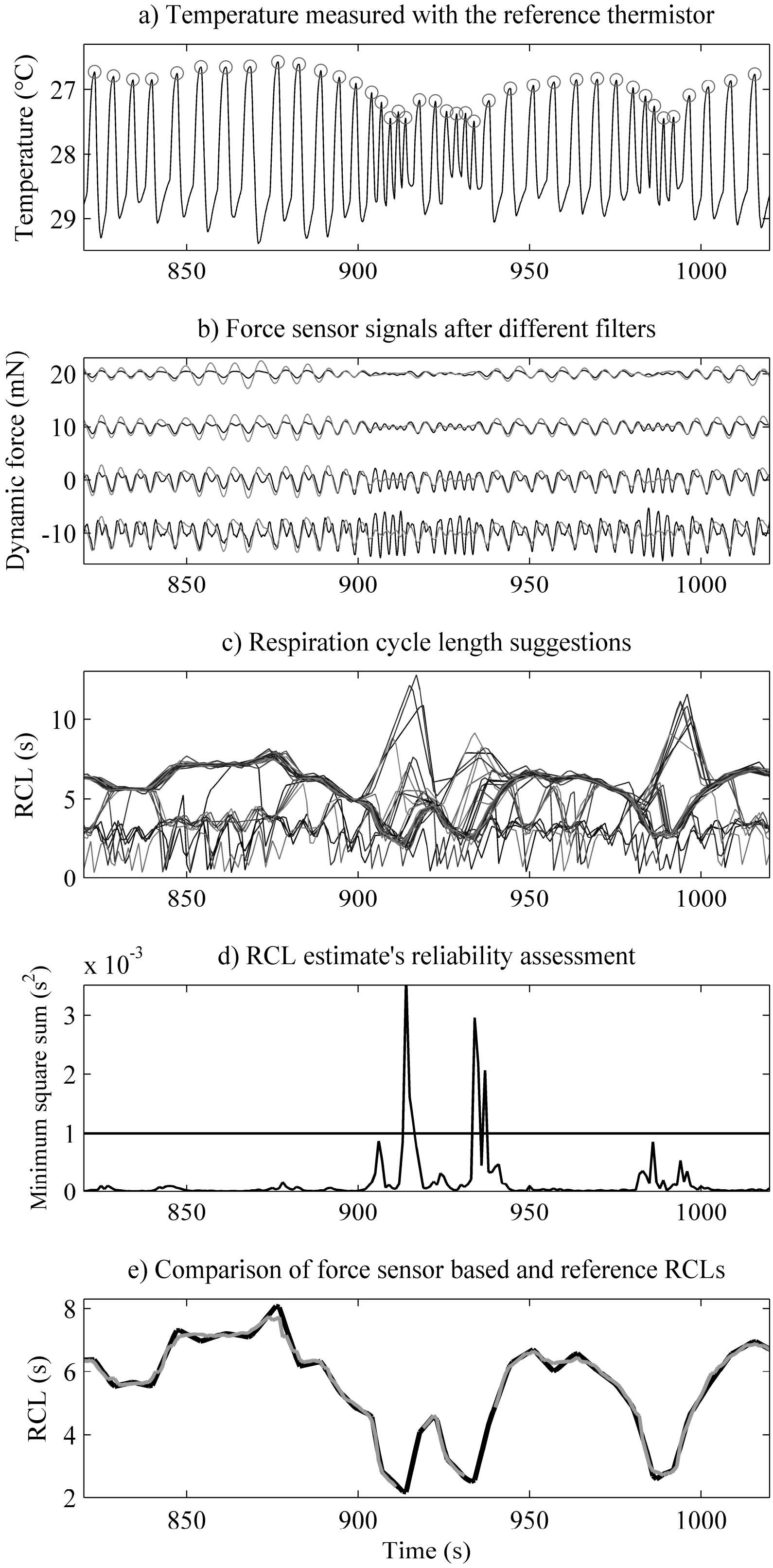

Figure 10. *A 200-second example of a force sensor based respiration detection. The reference signal recorded with a thermistor is shown in a) and the signals of the force sensors filtered with different pass bands in b) (offset for clarity). The RCL suggestions based on the signals of b) are shown in c), the square sum of the closest suggestions along with the threshold for discarding the RCL value in d), and the RCLs detected with the reference sensor (black) and the force sensors (grey) in e). The figure is adopted from Publication III.*

3.2.2 Respiration detection from the bed sheet ECG signals

As explained earlier in Section 2.3.2, the respiration is visible in the ECG signal and can be detected from several features calculated from the ECG. The R-R-interval based respiratory sinus arrhythmia and the R-peak amplitude modulation were selected as the EDR features from which the respiration was detected in Publication IV. The R-peaks were detected using the method presented in Publication II. Both of the selected features provide one sample per heartbeat. The formed EDR signals were interpolated to 0.1 s sample interval by cubic spline interpolation. Fairly short interval was used in order to increase the temporal resolution of the EDR signals.

The method used for the ECG based respiration cycle length detection follows the same principle as the detection of the RCL from the force sensor signals in Publication III. The EDR signals formed by the interpolated R-R-interval and R-peak amplitude vectors were now used instead of the two force sensor signals. Ideally, both signals would contain only the variation related to respiration but in practice they also include other, interfering, components. Again, different pass-bands were used because the RCL usually varies between 2 s and 10 s, corresponding to the frequency range of 0.1–0.5 Hz. Depending on the respective value of the RCL, different pass-band will produce the best filtering result. In this case, the best results were achieved by using three filters (0.1–0.22 Hz, 0.1–0.33 Hz, and 0.1–0.5 Hz). RCL suggestion vectors were calculated using the same simple features as earlier: peaks, troughs, and zero-crossings.

Figure 11 shows an example how the ECG signal is affected by respiration (upper panel). R-peaks recognized from the preprocessed signal are shown in the middle panel and the calculated R-R-intervals in the lower panel. The data in the example has been recorded during extensively deep breathing. Normal breathing has smaller effect on the ECG signal and the R-R-intervals.

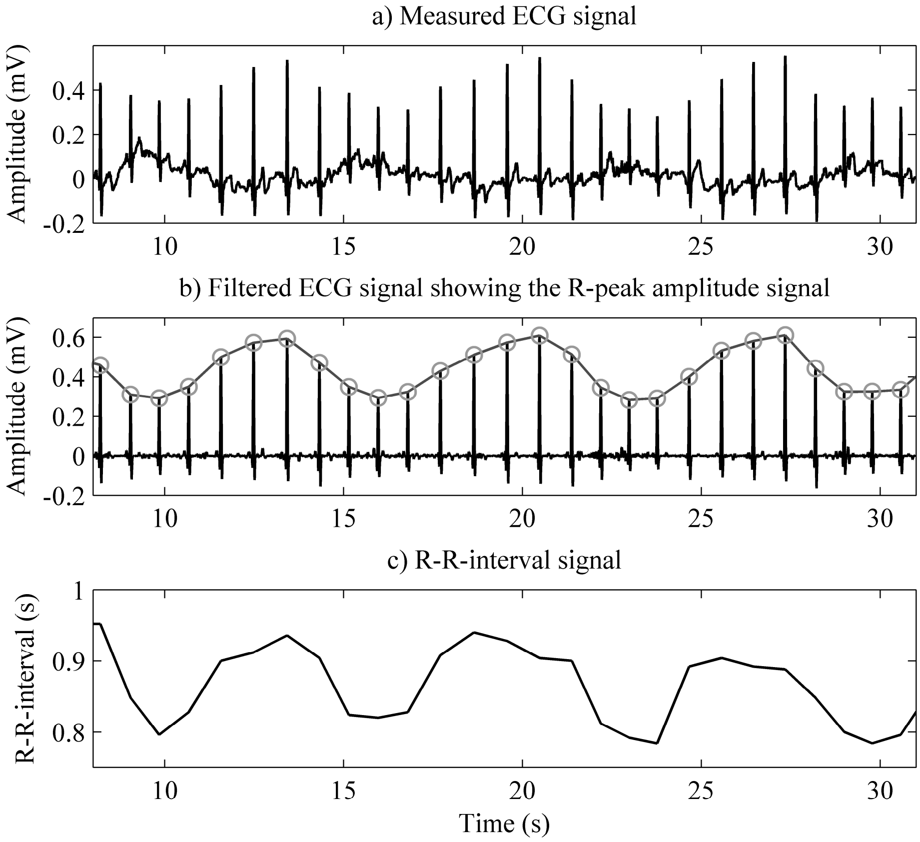

Figure 11. *The effect of respiration on the ECG signal. Raw ECG signal recorded with textile electrodes is shown in panel a, filtered signal along with detected R-peaks and R-peak amplitude signal (before interpolation) in panel b, and formed R-R-interval signal in panel c.*

The detected instantaneous RCL values were also used to calculate the mean RCL for 1 and 5 minute long epochs. If the mean RCL is calculated for all epochs that contain at least one detected instantaneous RCL, good detection coverage is achieved but the error for the epochs that contain only a few RCLs is probably higher. The error can be decreased by setting the minimum number of RCLs that must have been detected during an epoch before the mean RCL for that epoch is reported. The results were calculated using the overlaps of 50 and 240 seconds for the 60- and 300-second epoch lengths, respectively. The overlap was used in order to increase the amount of data in the test.

3.2.3 Combining the force sensor and ECG based respiration detection

Combining the force sensor and the ECG based respiration detection methods in order to increase the RCL detection coverage was also tested in Publication III. The force sensor based detection was selected as the basic method because it provided better coverage and smaller error than the ECG based method as presented in Section 4.3. The approach was simply to fill the gaps in the force sensor based RCL signal with the values provided by the ECG based detection in case the ECG based value was available. No separate post-processing was made to the combined signal because both source signals had already been post-processed and clear errors had been removed.

4 Results and discussion

This chapter presents the heart rate and respiration detection results obtained with the developed measurement systems and discusses the findings of the thesis. The error metrics used in the attached publications is introduced next.

4.1 The error metrics used in thesis

Following metrics have been used in the thesis and in the related publications to compare the measured and the reference heartbeat interval and respiration cycle length values.

The methods developed and presented in the thesis for calculating heartbeat intervals and respiration cycle lengths all include a certain kind of assessment of the reliability of the obtained BBI or RCL result. The assessment is firstly included into the BBI or RCL detection algorithm and in most cases also as a post-processing step. Those BBI or RCL values that are considered unreliable are discarded by the algorithms and are not reported in the final results. A parameter called detection coverage is used to tell which proportion of time the BBI or RCL values have been reported by the signal processing algorithms. Detection coverage is defined as:

$$\text{Coverage} = \frac{\text{The amount of time the BBI or RCL values have been reported}}{\text{Total measurement time}} 100\% \tag{4}$$

Root-mean-square error (RMSE) has been used to describe the error between heartbeat intervals or respiration cycle lengths measured with the developed systems and the references. The RMSE is defined as:

$$RMSE = \sqrt{\frac{1}{N}\sum_{i=1}^{N}(x_i - y_i)^2}\ , \tag{5}$$

where x_i are the heartbeat intervals or respiration cycle lengths measured with the evaluated method and y_i are the respective figures calculated from signals of the reference sensors. N is the number of the compared values. The same notation is used in (6) – (10).

The drawback of the RMSE is that it is strongly affected by possible occasional large errors and in such cases, does not give a representative estimate about the overall performance of the method. Mean absolute error (MAE) is not as sensitive to occasional large errors as the RMSE and it therefore suits better for comparison. MAE is defined as:

$$MAE = \frac{1}{N}\sum_{i=1}^{N}\left|x_i - y_i\right|. \tag{6}$$

Relative MAE, sometimes also called as mean absolute percentage error, is a convenient measure of error because it allows of comparison results whether they are calculated, e.g. in case of respiration detection, as breaths per minute or cycle duration in seconds. Relative mean absolute error is defined as:

$$MAE_{REL} = \frac{1}{N}\sum_{i=1}^{N}\frac{\left|x_i - y_i\right|}{y_i}100\%\ . \tag{7}$$

Pearson correlation coefficient is a commonly used figure for estimating the linear dependency of two measurement sequences or variables. It measures the deviation of the sample pairs from the best fit straight line. In the studies presented in the thesis, one of the variables has always been the reference that is considered as the true value. In such a case it is more reasonable to use concordance correlation which takes this into account and tries to evaluate the ability of the two methods to produce same results. The concordance correlation calculates the correlation of the sample pairs with respect to a 45 degree line that goes through the origin, not the best fit straight line (Lin, 1989). Concordance correlation coefficient of two variables x and y is defined as:

$$\rho_c = \frac{2s_{xy}}{s_x^2 + s_y^2 + (m_x - m_y)^2}, \tag{8}$$

where s_{xy} is the sample covariance of the sequences, s_x^2 and s_y^2 are the sample variances of the sequences, and m_x and m_y are the sample mean values of x and y. The sample covariance of two sequences is defined as:

$$s_{xy} = \frac{1}{N-1}\sum_{i=1}^{N}(x_i - m_x)(y_i - m_y), \tag{9}$$

and the sample variance of a sequence as:

$$s_x^2 = \frac{1}{N-1}\sum_{i=1}^{N}(x_i - m_x)^2. \tag{10}$$

Because of the nature of the heartbeat interval detection method presented in Publication II and the respiration cycle length detection methods presented in Publications III and IV, the reported error values have been calculated by comparing the interpolated heartbeat interval or interpolated respiration cycle length signals with the values recognized and interpolated from the reference signals. This has an effect to the value of the error when comparing with the situation where the individual heartbeat intervals are recognized and compared with the corresponding reference heartbeat intervals. Tests with simulated and bed sheet ECG data showed that the values of the RMSE and MAE can be up to approximately 30 % smaller when calculated using data values interpolated linearly between the original unequally spaced data values.

4.2 Results of the heartbeat interval detection

This section summarizes the results achieved with the systems and methods developed for ballistocardiogram, contact ECG, and capacitive ECG based heartbeat interval detection and compares the performance of the methods.

4.2.1 Ballistocardiographic heartbeat interval detection

Test measurements

The measurement system and the BBI detection method proposed in Publication II were tested with four female and five male subjects in one hour long recordings. The subjects were free to change the posture during the measurement. Reference heartbeat intervals were calculated from an ECG signals recorded with disposable Ag/AgCl electrodes. The reference R-peak detections were visually inspected, corrected, and the detected R-R-intervals interpolated to the same 0.5 s sample intervals as the force sensor based BBIs.

Results

An average of 5.4 % of the measurement data was labeled to contain large artifacts and thus removed in the preprocessing phase. From the remaining data, the algorithm was able to detect the beat-to-beat intervals for an average of 96.2 % of the time. The overall average recognition coverage was thus 91 %.

BBI detection can be defined erroneous if the detected value deviates more than a certain amount from the reference. 50 ms difference was used as the threshold in the comparison. An average of 98.6 % of reported BBI values were within 50 ms from the reference value. The relative MAE of the BBI values was 0.88 % and varied in the range 0.42 – 1.51 % between the subjects. More detailed results can be found in Publication II.

Similar or slightly better results have been reported by other authors for the BCG based monitoring systems that use multiple measurement channels. Coverages of 85.9 % and 84.4 % were reported for the methods developed by Kortelainen et al. and Brüser et al. respectively when testing with people having various sleeping disorders (Brüser et al., 2015). Two most difficult subjects were discarded from their results. The corresponding relative MAE values were 0.9 % and 0.5 %. The results achieved by Kortelainen et al. for healthy subjects were even better: the coverage was 88 % and the relative MAE 0.40 % (Kortelainen et al., 2012). The results found in literature for systems that use only one BCG channel have been slightly worse. 73 % and 54 % coverage and 0.78 % and approximately 1.3 % MAE have been reported in (Brüser et al., 2013b) and (Paalasmaa et al., 2014b) for large variety of subjects, respectively.

The accuracy of certain heart rate variability parameters that have been earlier used in sleep monitoring and classification was also evaluated. The HRV parameters were calculated for 30 second epochs. The normally used window length in HRV analysis is 5 minutes (Malik et al., 1996) but because sleep data is usually analyzed in 30 second epochs, the same length has been used in some studies also for the HRV parameter calculation (Adnane et al., 2012; Devot et al., 2007; Ebrahimi et al., 2013; Redmond and Heneghan, 2006).

Only the epochs that included all BBIs were considered in the analysis. The mean coverage of these full epochs was 61.2 % of the recording time with all subjects. One of the evaluated parameters was the standard deviation of the BBIs in an epoch, which has been found to decrease during the deep sleep phase (Kesek et al., 2009). The relative MAE of this parameter was 6.0 %. The ratio between the low frequency and the high frequency power (LF/HF-ratio) in the beat-to-beat interval signal has been found to differentiate especially in the NREM and REM sleep stages and it has been used in sleep classification in (Bušek et al., 2005; Choi et al., 2009; Choi and Jiang, 2008; Kesper et al., 2012). The LF/HF-ratio has also been studied for the detection of several medical sleep disorders (Stein and Pu, 2012). The low frequency band is commonly defined as the frequencies between 0.04 Hz and 0.15 Hz and the high frequency band between 0.15 Hz and 0.4 Hz. The average relative error in the LF/HF-ratio with all subjects was 9.4 %. Figure 12 shows an example of two 30 s BBI time series measured with the bedpost force sensors along with the reference RRI data and the respective power spectral densities (PSD). The PSDs were calculated in this study using discrete Fourier transform (Oppenheim and Schafer, 1989).

An alternative method for calculating physiological parameters when performing an epoch-wise sleep analysis is to use a longer computation window and assign the parameter values to the 30 s epoch in the middle of the window as in (Choi et al., 2009). Another possibility for calculating the HRV parameters is using a time-variant autoregressive modelling as in (Devot et al., 2007; Kortelainen et al., 2010). The accuracy of the HRV parameters calculated using these techniques was, however, not evaluated in the thesis.

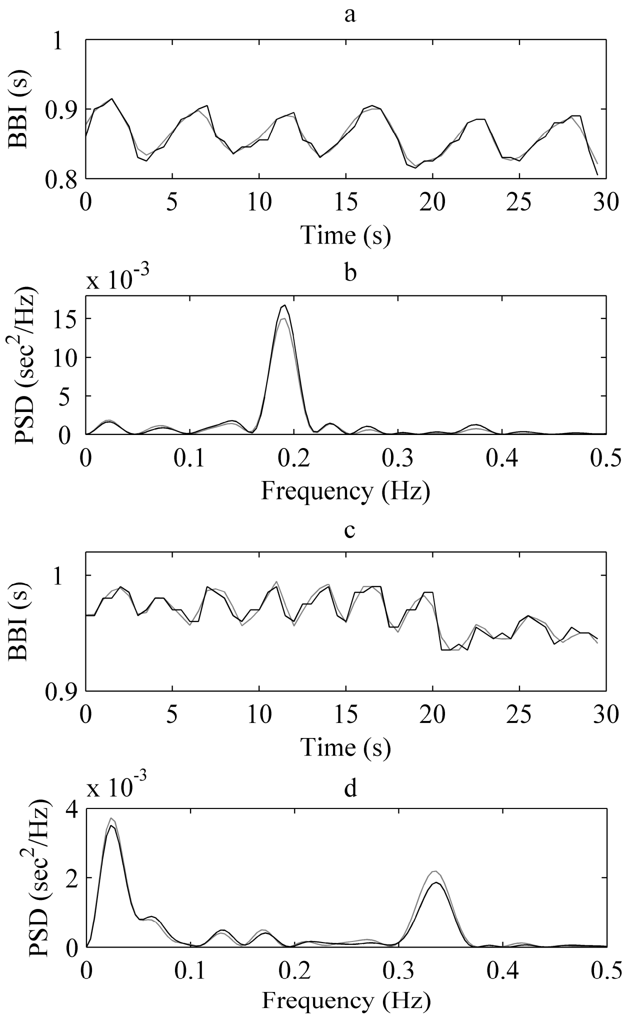

Figure 12. *Two examples of BBI signals in 30 s epochs (black) with corresponding RRI references (grey); (a) and (c), and their PSDs; (b) and (d) calculated using discrete Fourier transform. The time domain signals as well as the PSDs in these examples correspond well with each other. The figure is adopted from Publication II.*

4.2.2 Heart rate detection with bed sheet integrated textile electrodes

Test measurements

The original measurement setup and signal processing algorithm presented in Publication I were tested with five subjects in overnight measurements at home environment. One subject was later discarded due to extensive amount of disturbances, mainly of physiological origin (heartbeats appeared like premature ventricular contractions), in the acquired signals. Altogether 29 full night recordings were included in the analysis. All subjects were male, aged

23–32 years, 173–185 cm, 64–80 kg, and healthy without previously known cardiac disorders. The performance of the further developed setup presented in Publication III was tested with ten subjects (eight male, two female, 23-33 year old, normal weight) in one hour long recordings performed in laboratory conditions.

Results

The average heart rate detection coverage achieved with the original system described in Publication I in overnight measurements was 94.9 % and the average RMSE of the calculated R-R-intervals was 4.48 ms, which corresponds to 0.27 bpm.

When the inter-electrode distances were decreased to 5 cm in Publication III and the combined measurement channels were included, the RMSE was slightly higher, 5.81 ms (0.36 bpm). The reason is probably not in the different measurement setup but rather it might be the different test conditions. In the tests of Publication III, shorter one hour recordings were used and the relative amount of wake time and therefore the amount of movements were higher, possibly causing more detection errors. The average MAE in the second experiment was 1.12 ms and varied between 0.48–1.70 ms between the subjects.

The average RRI detection coverage in the second test was 91.5 % when the force sensor was not used to assist in channel reselection and when all subjects were included. One of the test subjects was removed from the calculation of average results in Publication III because in his measurements, the sheet electrodes were located poorly, which degraded the quality of the recorded signals. The average coverage reported in Publication III was 95.1 %. The detection coverage results of Publication III cannot be compared with the results of Publication I because of the different measurement conditions and different test subjects.

The effect of combined measurement channels and decreased inter-electrodes distance was therefore studied by calculating the coverage with the data of the second trial but by using only the original measurement channels with 5 cm inter-electrode distance or 10 cm inter-electrode distances that were formed by combining two adjacent measurement channels. The coverages for all subjects in these cases were 77.6 % and 82.3 %, which shows that the improvement in the coverage was significant when more channel combination options were available. Especially, for one test subject the coverage was only 0.6 % when only the original measurement channels were used but it increased to 47.5 % when using the 10 cm electrode distances, and further to 61.3 % when all channel combinations were included.

Introducing the force sensor to assist in the channel reselection decision improved the RRI detection coverage by 0.9 percentage point to 92.4 %. Even more important consequence was the decreased number of channel reselections, which lengthens the continuously detected RRI series. This facilitates especially the computation of frequency domain heat rate variability parameters.

Similarly as in Publication II, the R-R-interval signal was divided into sequential 30 second epochs and certain HRV parameters were calculated and compared with the ones calculated from the reference ECG signal. Again, only the epochs that according to the algorithm contained all the R-R-intervals were taken into account. The average coverage of these epochs was 85.6 % of the total measurement time. In Publication I, the PSDs were calculated using Welch modified periodogram method (Ifeachor and Jervis, 1993). The compared frequency domain HRV parameters were low frequency power, high frequency power, and the LF/HF-ratio. The respective relative MAE values were 0.89 %, 3.90 %, and 2.20 %.

4.2.3 Heart rate detection with capacitive electrodes

Test measurements

The capacitive system was tested with five male subjects in one hour long recording. The subjects were instructed to change their sleeping posture every 15 minutes so that all four main postures (supine, left side, prone, and right side) were tested. With this arrangement it was possible to compare whether there were differences in the performance between the postures.

Care must be taken when testing capacitively coupled ECG measurement systems, to prevent the reference measurement from affecting the capacitive measurements. For example, the reference device should not be connected in such a way that a galvanic ground current path would be provided through its electrodes. Therefore a separate wireless ECG measurement device was used for recording the reference signal. A single ECG channel was measured by using disposable Ag/AgCl electrodes that were attached below the left and the right clavicles. The used reference recording system has been presented in (Vehkaoja et al., 2012).

Results

The RR-interval detection coverage varied from 62 % to 96 % between the subjects. The average coverage was 81 %. There were significant differences in the detection coverage between the sleeping postures. The system performed well in other sleeping postures but had problems, especially with two subjects, in detecting the heart rate when lying on the right side. The coverage for one of the two was only 8.4 % and for the other one, the algorithm was not able to detect any R-peaks in this posture. A visual inspection of the latter case showed that too large artefact component (presumably resulting from the ballistocardiographic movement) was present in the signal preventing the preprocessing from providing a good enough signal for the R-peak detection algorithm. Furthermore, the ECG component was almost equal in all channels and therefore subtracting the signals did not produce good enough ECG signal either. The mean detection coverage increased to 92.4 % when the data recorded during the right side posture of the two subjects and the posture changes from all subjects were removed from the analysis. The average MAE of the detected R-R-intervals was 1.78 ms, which can be considered as a good result. Subject-wise results can be found in Publication V.

4.2.4 Comparison of the heartbeat interval monitoring methods

The presented measurement systems and signal processing methods have been developed and tested separately, which means that an accurate comparison of their performance cannot be done based on the test results. Especially the comparison of the detection coverage achieved with different technologies is difficult because the measurement conditions and subjects have not been the same. Still, based on the test results the beat-to-beat interval detection coverage seems to be the highest when using the contact electrodes with short inter-electrode distance and when including the combined measurement channels in the analysis. The coverage was further increased when the movement information from the force sensor was utilized.

The error in the detected beat-to-beat signals is more comparable even when the recording situations are different. The average mean absolute error of the measured R-R-intervals was 1.78 ms with the capacitive electrode system and 1.12 ms with the textile electrodes. The relative mean absolute error of 0.88 % achieved with the ballistocardiographic system corresponds to 8.8 ms if an average heart rate of 60 bpm is assumed. The conclusion supported by both, the presented measurements and the results reported in literature, is that the ECG measured with bed sheet textile electrodes provides more accurate heartbeat interval information than ballistocardiographic data. This naturally reflects also to the accuracy of the calculated HRV parameters. The relative mean absolute error of 2.2 % was achieved for the LF/HF-ratio with the bed sheet ECG system while the relative MAE with the ballistocardiographic method was 9.4 %. The methods used for calculating the PSDs were, however, different in the two studied. The respective full 30 s epoch detection coverages were 85.6 % and 61.2 %. Table 1 summarizes the average BBI detection results achieved with the three sensor modalities.

Table 1. *Comparison of the heartbeat interval detection performance achieved with different monitoring techniques in one hour recording.*

Measurement method	**BBI detection performance characteristics**			
	***Coverage* (%)**	***MAE* (ms)**	***LF/HF MAE* (%)**	***30 s epoch coverage* (%)**
BCG	91.0	8.8	9.4	61.2
Contact ECG	91.5[a]	1.12	2.2	85.6
Capacitive ECG	81.0[b]	1.78	-	-

a. 95.1 % if the subject who had s is discarded from the analysis

b. 92.4 % if the data of two subjects' right side posture and the posture changes of all subjects is removed.

4.3 Results of respiration cycle length detection

This section summarizes the results achieved with systems and methods developed for force sensor based and ECG based respiration cycle length detection and compares the two methods.

4.3.1 Force sensor based respiration detection

Test measurements

The data collection for testing the respiration detection algorithm was done together with the data collection for the combined ECG channels testing. The number of subjects was ten and the duration of each recording was one hour. An NTC thermistor placed inside a breathing mask was used as the reference respiration sensor. The resistance of the thermistor was measured, converted into temperature, and filtered. The respiration cycles were detected from the band-pass filtered (0.01–5 Hz) temperature signal by finding the minimum temperature of each segment below the baseline level. These points correspond to the end of the inhale phase. The signals were visually inspected and false or missing detections were corrected. Short sections were found in the recordings of four test subjects, where the amplitude of the reference breathing signal was significantly decreased and clear respiration rhythm was not visible in the signal. These sections were interpreted as apneic breathing and discarded from the analysis. The total amount of discarded data was clearly less than one percent of the recording time.

Results

The average force sensor based RCL detection coverage achieved in the test with ten subjects was 82 %. The coverage, however, varied significantly between the subjects. The minimum coverage was 61 % and the maximum was more than 97 %. On average, 95.5 % of the detected respiration cycle length valuess were within 0.25 seconds and 99.1 % within 0.5 seconds from the reference value. The average relative MAE was 2.1 %. Subject-wise concordance correlation coefficients between the reference and the force sensor based respiration cycle length values were on average 0.946. More detailed results can be found in Publication III.

4.3.2 ECG based respiration detection

The same data set as in the force sensor based RCL detection was also used to evaluate the performance of the ECG based RCL detection. The respiration cycle length detection coverage again varied significantly between the subjects. The individual coverage varied between 19.0 and 83.2 % of the whole recording time, the average being 39.6 %. The RCL detection coverage is naturally affected by the fact that R-peaks cannot be recognized from the bed sheet ECG signals all the time. When only the time the R-peaks had been detected was considered (82.0 %), the mean RCL coverage was increased to 48.3 %. The average MAE of the detected respiration cycle length signal was 0.24 s, which corresponds to 5.6 % relative mean absolute error. On average, 89.7 % of the detected RCL values were within 0.5 second from the reference values. Subject-wise concordance correlation coefficients between the reference and the ECG based respiration cycle length values were on average 0.777.

For comparison, the RCL detection algorithm was also tested with reference ECG signal that had been simultaneously measured with normal gel electrodes placed under both clavicles. The mean RCL detection coverage from the reference ECG signal was 47.8 % and the average relative MAE was 4.1 %. Surprisingly, the RCL detection coverage calculated using the good quality reference ECG signal was not better than what was obtained using the bed sheet ECG signals when the 82 % R-peak detection coverage was taken into account. There is some difference in the accuracy though, which may be due to the generally worse quality of the bed sheet ECG signal. In addition, because the electrode locations on the body vary depending on the posture in the bed, the variation in the R-peak amplitude is not seen equally well in all sleeping postures. The measurement lead selected by the algorithm also affects the inter-electrode distance which may have an effect on how well the respiration variation is seen in the R-peak amplitude. The measurement lead or the quality of the ECG signal, however, may only have a very minor effect to the RSA, the other EDR signal used in the respiration detection. It can be concluded that the quality of the bed sheet ECG signal is adequate for the RCL detection with close to the same performance as when the high quality reference ECG signal is used. This applies at least with the developed signal processing and RCL detection method.

Epoch mean RCL accuracy and coverage were also evaluated as a function of minimum number of instantaneous RCLs in an epoch required for reporting the result. Figure 13 shows the detection coverage and the MAE of the mean RCL values as a function of the minimum number of the instantaneous RCLs in an epoch. The results in Figure 13 are calculated for 1 minute epoch length using 50 seconds overlap between the epochs. 88.4 % of all epochs calculated using the bed sheet ECG data contained at least one RCL value and the average relative MAE for the mean RCL was in this case 6.6 %. Better coverage was achieved by using the reference ECG signal because the reference signal and thus R-peaks are practically always available. The average MAE is slightly smaller for the reference ECG when all possible epochs are considered. However, both signals produce similar error values when the minimum number of the required RCLs in an epoch is increased to more than 25 %.

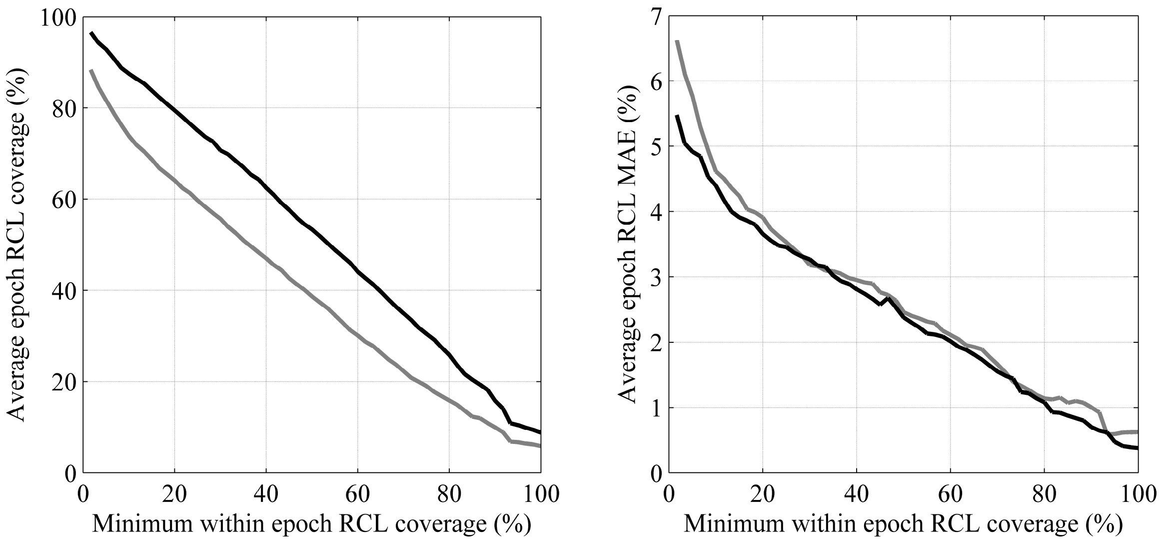

Figure 13. *The average dependency of the coverage (left panel) and the MAE of the mean RCL values (right panel) for one minute epochs for all subject. The results calculated using the reference ECG signal are shown in black and the results calculated using the bed sheet ECG signal in grey. The figure is adopted from Publication IV.*

4.3.3 Combined force sensor and ECG based respiration detection

The mean RCL coverage was increased by 3 percent units from 82.0 % to 85.0 %, when the ECG based RCL values were added to the gaps of the force sensor based RCL signal. The overall accuracy was however decreased. The relative MAE, for example, was increased from 2.09 % to 2.29 %. The reason for the relatively high increase in the error is probably that the situations where the force sensor RCL data is missing are often related to movements and therefore also the ECG based RCL information is more unreliable than on average. More advanced method for combining the RCL information from different sources should therefore be developed.

4.3.4 Comparison of the respiration cycle length monitoring methods

As seen by comparing the results of the respiration detection with force sensors and by using the ECG signal, the respiration information derived from the ECG signal has not been as reliable as the results obtained with the force sensors. The ECG-based algorithm provided a respiration result on average 39.6 % of the time, which is less than a half of the coverage obtained using the force sensors 82.0 %. Also the accuracy of the RCL detection is worse with the ECG based detection (average MAE 5.6 %) than when using the force sensors (average

MAE 2.1 %). Table 2 summarizes the average results with the two sensor modalities separately and when they are combined.

Table 2. *Comparison of RCL detection performance of different monitoring techniques.*

Sensor	**Respiration detection performance characteristics**						
	***Coverage* (%)**	***Correlation*[a]**	***RMSE* (s)**	***MAE* (%)**	***e*<0.25 s[b]**	***e*<0.5 s[b]**	***e*<1 s[b]**
Force sensor	82.0	0.946	0.179	2.09	95.5	99.1	99.6
ECG	39.6	0.777	0.378	5.60	71.2	89.7	97.0
Combined	85.0	0.925	0.216	2.29	94.6	98.7	99.5

a. Concordance correlation of the measured respiration cycle length values and the reference values.

b. Percentage of the detected respiration cycle length values whose error is smaller than 0.25 s, 0.5 s, or 1 s.

5 Conclusions

Monitoring systems that utilize different unobtrusive sensing principles for measuring physiological signals of a person in bed were developed and presented in the thesis and the appended publications. Signal analysis methods for extracting heartbeat intervals and respiration cycle lengths from the measured signals were also developed and presented.

The first research question studied in the thesis was: "*What kind of unobtrusive measurement principles and sensor setups are suitable for unobtrusive monitoring of heart rate and respiration rate and what limitations do the methods have?*"

This research objective has been discussed in Section 2.2 that presents the unobtrusive monitoring methods found in literature. Three measurement methods were realized and presented in the attached publications. Publications I and III present a monitoring system that uses textile electrodes placed transversally on the bed sheet. The ECG signal was measured between each adjacent electrode pair. This kind of electrode setup for contact electrodes has not been previously used in studies found in literature. ECG signals of adequate quality for the heart rate detection were obtained with narrow, 5 cm inter-electrode distance used in Publication III from all test subjects except one. Combining the measurement channels enabled the heart rate detection also for this person. The quality of the recorded signals was also adequate for the detection of instantaneous respiration cycle lengths as was shown in Publication IV. The proposed contact ECG monitoring system requires the user to have a naked upper body. For people who anyway sleep without wearing a shirt this does not pose a problem but for the others it might be unacceptable. Such contact ECG monitoring systems that overcome this requirement by locating the electrodes to the pillow and the foot of the bed have been studied but they may have another problems for example if the hair of the subject is preventing the galvanic contact between the body and the electrode.

Bed integrated measurement setups for recording ballistocardiographic signals have been extensively studied by several research groups and the methods found in literature were reviewed in Section 2.2.3. Publication II presents a measurement setup that uses simple force sensors made of EMFi material for recording ballistocardiographic signals. The sensors were located under the bed posts, from where they were able to record good quality BCG signals. The recorded signals also include variation caused by respiration and are therefore suitable for respiration rate detection, which was studied in Publication III. The methods based on the ballistocardiographic measurements do not set any constrains for the clothing but the limitation of these methods is that they are sensitive to any forces present. If two people are sleeping in the same bed, the force signals of the sleepers' heartbeat and respiration can mix and cause the deterioration of the accuracy and detection coverage, especially if the force sensors are placed under the bedposts as stated in (Paalasmaa, 2014a). Forces caused by other person's movements can cause problems also when using force sensors that are placed right under the person being monitored.

Publication V presents a measurement setup that contains capacitive electrodes for recording ECG signal through clothing. Similarly as in Publications I and III the electrodes were located transversally on the bed sheet but in this setup their potentials were measured against a common capacitive ground electrode. ECG signals of adequate quality were also obtained with the capacitive electrodes. The structure of the capacitive electrodes was, however, relatively complex compared with the other tested sensors. Due to the requirement of very high input impedance, well shielded active electrodes were needed. The capacitive ECG was found to be more sensitive to movement artifacts than the contact ECG. It was concluded based on the measurements that even the movements caused by the ballistocardiographic forces can sometimes create artefacts in the measured signal that have larger amplitude than the electric activity of the heart. The developed capacitive ECG monitoring system also had problems in measuring signal with detectable heartbeats from two subjects in right side sleeping posture.

The efficiency of detecting respiration cycles from the capacitive ECG signals was not evaluated in the thesis.

A common shortcoming of all studied and also other unobtrusive non-wearable monitoring methods is that they are sensitive to movements. The techniques that measure ECG signal lose the electrode contact during movements and techniques based on the measurement of force or acceleration signal cannot separate the components caused by heartbeats or respiration from much stronger movement artefact signal. The same applies also to the monitoring systems that use microwave Doppler radars, since the radar measurement is based on monitoring the movements of the chest. So far, no such unobtrusive monitoring technique has been proposed that could detect heart rate or respiration rate continuously including the time periods of changing the sleeping posture.

The second research question concerned signal processing methods that can be used for detecting the physiological parameters from the measurement signals. The question was formulated as: "*What specific requirements do the investigated sensing methods set for the signal processing algorithms used for extracting the heart rate and the respiration information from the measurement data?*"

The ECG signals recorded with the bed sheet textile electrodes usually contain at least the R-peak, which can be detected with similar signal processing methods that are used for the ECG signals recorded with conventional electrodes. However, the quality of the bed sheet ECG signals is often worse than the quality of the signals obtained with regular electrodes. The amplitude of the R-peaks vary significantly depending on the electrode location, which changes according to the sleeping posture, and also depending on the quality of the skin-electrode contact. The signal processing method should therefore be able to adapt to the changing properties of the measured signal. Even when the criteria for the R-peak detection are carefully adjusted, the varying signal properties can sometimes cause erroneous peaks being classified as R-peaks. The post-processing phase, which detects the physiological reasonability of the detected peaks, was therefore also found to have an important role in improving the specificity of the R-peak detector. The aforementioned requirements were considered when the signal processing method for the bed sheet ECG signals was designed as explained in Section 3.1.2 and in more detail in Publication I.

The effect of combining the measurement channels on the detection coverage was studied in Publication III. The detection coverage was significantly improved when also the combined measurement leads were used in the heart rate detection. It is therefore beneficial if the algorithm is able to use several ECG signals, if available, for heartbeat detection. This is necessarily not so important when using ECG signals that have been recorded with conventional gel electrodes or wearable textile electrodes as in (Vehkaoja et al., 2012).

The waveforms of the ballistocardiographic signals vary significantly between people, depending on the sleeping posture, location on the bed and the location of the sensor. The signals do not always contain any clearly distinguishable waveform such as the R-peak of the ECG signal and therefore the heart rate cannot be reliably detected by searching for such predefined waveform. Methods that try to find repeating patterns from the signals are therefore commonly used with BCG signals. The method presented in Publication II for the detection of the heartbeat interval signal uses the correlation of consecutive signal segments for finding the repeating patterns in the BCG signals. Even the method does not detect the individual heartbeats or individual heartbeat intervals, it was able to extract the equally sampled beat-to-beat interval signal with good performance.

The properties of the capacitively measured ECG signal were found to be similar to those of the ECG recorded using the textile electrodes, with the exception that the capacitive measurement was more sensitive to movement artifacts. Formation of new measurement leads by subtracting the ECG signals from each other was found to improve the detection coverage because the common component of the movement artefact was this way suppressed and because more measurement channels were available for the channel selection algorithm. In principle, the formed measurement leads correspond the original leads of the contact ECG measurement setup. The same R-peak detection method as with the textile electrodes then performed well also with the capacitive ECG signals.

While respiration related variation is seen in the signals recorded with force sensors that are placed under the bed posts, it is not as straight forward to detect instantaneous respiration cycles from these signals as it is when using traditional respiration sensors such as an airflow sensor or thermistor. There often is another signal component of higher frequency combined in the signal as was shown in Figure 10. A method for extracting the instantaneous respiration cycle lengths described in Section 3.2.1 and in Publication III was therefore developed. The method was found to perform well in the tests.

The properties of the ECG signal that can be used in deriving respiration signals were presented in Section 2.3.2. The method developed for the respiration detection from the force sensor signals was successfully used also with the EDR signals derived from the bed sheet ECG.

The third research question dealt with the evaluation of the results of the measurement system testing: "*How do the developed monitoring methods perform in the detection of the physiological parameters and are there noticeable differences in their performances?*"

The results achieved with the developed measurement systems were summarized in Sections 4.2.4 and 4.3.4 for heart rate and respiration rate, respectively. Good detection results were achieved with all methods. Although the systems developed for heartbeat interval detection have been tested separately and partially with different test subjects, some conclusions about their performance compared with each other can still be drawn. The measurement methods that use the unobtrusively measured ECG signal seem to provide clearly better heartbeat interval accuracy than the developed ballistocardiographic method or the ballistocardiographic methods found in literature. The detection coverage achieved with the contact ECG method was also better than what was achieved with the ballistocardiographic method or the capacitive ECG method in similar test conditions.

The respiration detection performance achieved with the force sensors was clearly better than when estimating the respiration cycle lengths from the EDR signals. The RCL detection coverage values were 82 % and 40 % (48 % of the time the R-peaks were found from sheet ECG signals), and relative MAEs 2.1 % and 5.6 %, respectively. Similar coverage but better RCL accuracy was achieved when the reference ECG signal measured with gel electrodes was used for the detection of instantaneous RCLs.

The aim of the fourth research question was to conclude, based on the published studies: "*What kind of a measurement system would suit best for unobtrusive respiration and heart rate detection?*"

The results of Publication I – V suggest that among the studied methods and from the data quality or accuracy point of view, an optimal system for unobtrusive night-time physiological monitoring would include an ECG measurement modality for the heartbeat interval monitoring and force sensors for the respiration monitoring. The force sensor would also be an obvious choice to be used in the detection of movements. Using more than one sensor modality in the measurement system would also enable combining their information to enhance the measurement coverage or the accuracy and thus improve the monitoring performance. The increase in the detection coverage by simple methods of combining the information of the sensor was demonstrated in Publication III but increasing the accuracy would require more advanced data processing methods to be used.

However, combining more than one sensing modality into a measurement system increases its technical complexity and inevitably also the cost level of fabrication. Furthermore, it does not necessarily matter from the application point of view if one measurement method produced better data accuracy than another, if the accuracy of both methods is adequate. It should be tested in the future if the better accuracy and heart rate detection coverage achieved with the contact ECG monitoring system would also be able to provide significantly better sleep classification accuracy than the BBI information obtained with the ballistocardiographic sensors. Currently there are no products on the market that use contact or capacitive ECG sensing principles for unobtrusive monitoring of night-time heart rate and the viability of systems of this kind in practical use should be evaluated in the future.

The tests with the developed methods have been performed with healthy young adults mainly in laboratory conditions and it is likely that the results would be different if the tests were conducted in home conditions, with subjects of wider demographic distribution or with subjects who suffer from sleep disorders. Evaluating the systems in all-night use instead of one hour recordings would probably improve the results because the subjects would be asleep a larger part of the recording, which would decrease the relative amount of movement artifacts. On the other hand, testing the methods with subjects who suffer from sleep disorders would probably decrease the performance when compared with testing with healthy subjects.

Bibliography

Abbas, A. K., Heimann, K., Jergus, K., Orlikowsky, T., and Leonhardt, S., “Neonatal non-contact respiratory monitoring based on real-time infrared thermography,” *Biomedical engineering online*, vol. 10, no. 1, pp.1–17, Oct. 2011.

Abibullaev, B., and Seo, H. D., “A new QRS detection method using wavelets and artificial neural networks,” *Journal of Medical Systems*, vol. 35, no. 4, pp. 683–691, Aug. 2011.

Adnane, M., Jiang, Z., and Yan, Z., “Sleep–wake stages classification and sleep efficiency estimation using single-lead electrocardiogram,” *Expert Systems with Applications*, vol. 39, no. 1, pp. 1401–1413, Jan. 2012.

Alametsä, J., Rauhala, E., Huupponen, E., Saastamoinen, A., Värri, A., Joutsen, A., Hasan, J., Himanen, S. L., “Automatic detection of spiking events in EMFi sheet during sleep,” *Medical Engineering & Physics*, vol. 28, no. 3, pp. 267–275, Apr. 2006.

Alhola, P. and Polo-Kantola, P., ”Sleep deprivation: Impact on cognitive performance,” *Neuropsychiatric Disease and Treatment*, vol. 3, no. 5, pp. 553–567, Oct 2007.

Alihanka, J., Vaahtoranta, K., and Saarikivi, I., “A new method for long-term monitoring of the ballistocardiogram, heart rate, and respiration,” *American Journal of Physiology*, vol. 240, no 5, pp. 384–392, May 1981.

Andreão, R.V., Dorizzi, B., and Boudy, J., "ECG signal analysis through hidden Markov models," *IEEE Transactions on Biomedical Engineering*, vol. 53, no. 8, pp. 1541–1549, Aug. 2006.

Avci, C., Besli, S., and Akbas, A., “Performance of the EDR methods: Evaluations using the mean and instantaneous respiration rates,” in *Proceeding of 5th International Conference on Bioinformatics and Biomedical Engineering (iCBBE)*, May 2011, pp.1–5.

Ayas, N., Pittman, S., MacDonald, M., and White, D., “Assessment of a wrist-worn device in the detection of obstructive sleep apnea,” *Sleep Medicine*, vol. 4, no 5, pp. 435–442, Sept. 2003.

BAM Labs Inc. www.bamlabs.com, accessed 1.5.2014.

Bartula, M., Tigges, T., and Muehlsteff, J., "Camera-based system for contactless monitoring of respiration," in *Proceedings of 35th Annual International Conference of the IEEE Engineering in Medicine and Biology Society (EMBC)*, July 2013, pp.2672–2675.

Beattie, Z. T., Hayes, T. L., Guilleminault, C., and Hagen, C. C., “Accurate scoring of the apnea-hypopnea index using a simple non-contact breathing sensor,” *Journal of Sleep Research*, vol. 22, no. 3, pp. 356–362, June 2013.

Beddit Ltd. www.beddit.com, accessed 1.5.2014.

Berntson, G. G., Cacioppo, J. T., and Quigley, K. S., “Respiratory sinus arrhythmia: autonomic origins, physiological mechanisms, and psychophysiological implications,” *Psychophysiology*, vol. 30 no. 2, pp. 183–196, Mar 1993.

Boyle, J., Bidargaddi, N., Sarela, A., and Karunanithi, M., “Automatic detection of respiration rate from ambulatory single-lead ECG,” *IEEE Transactions on Information Technology in Biomedicine*, vol. 13, no. 6, pp. 890–896, Nov. 2009.

Brink, M., Müller, C. H., and Schierz, C., “Contact-free measurement of heart rate, respiration rate, and body movements during sleep,” *Behavior Research Methods*, vol. 38, no 3, pp. 511–521, Aug. 2006.

Brüser, C., Stadlthanner, K., de Waele, S., and Leonhardt, S., "Adaptive beat-to-beat heart rate estimation in ballistocardiograms," *IEEE Transactions on Information Technology in Biomedicine,* , vol.15, no.5, pp.778–786, Sept. 2011.

Brüser, C., Diesel, J., Zink, M. D., Winter, S., Schauerte, P., and Leonhardt, S., “Automatic Detection of Atrial Fibrillation in Cardiac Vibration Signals,” *IEEE Journal of Biomedical and Health Informatics*, vol. 17, no. 1, pp. 162–171, Jan. 2013a.

Brüser, C., Winter, S., and Leonhardt, S., “Robust inter-beat interval estimation in cardiac vibration signals,” *Physiological Measurement*, vol. 34, no. 2, pp. 123–138, Feb. 2013b.

Brüser, C., Kortelainen, J., Winter, S., Tenhunen, M., Pärkkä, J., and Leonhardt, S., "Improvement of Force-sensor-based Heart Rate Estimation Using Multi-channel Data Fusion," *IEEE Journal of Biomedical and Health Informatics*, vol. 19, no. 1, pp.227–235, Jan. 2015.

Bušek, P., Vaňková, J., Opavský, J., Salinger, J., and Nevšímalová, S., “Spectral analysis of heart rate variability in sleep,” *Physiological Research*, vol. 54, no. 4, pp. 369–376, 2005.

Böhm, A., Brüser, C., and Leonhardt, S. L., “A novel BCG sensor-array for unobtrusive cardiac monitoring,” *Acta Polytechnica*, vol. 53, no. 6, pp. 862–867, 2013.

Chee, Y., Han, J., Youn, J., and Park, K., “Air mattress sensor system with balancing tube for unconstrained measurement of respiration and heart beat movement,” *Physiological Measurement*, vol. 26, no 4, pp. 413–422, Aug. 2005.

Chen, W., Zhu, X., Nemoto, T., Kitamura, K., Sugitani, K., and Wei, D., "Unconstrained monitoring of long-term heart and breath rates during sleep," *Physiological Measurement*, vol. 29, no. 2, pp. N1–N10, Feb. 2008.

Choi, B. H., Chung, G. S., Lee, J. S., Jeong, D. U., and Park, K. S., "Slow-wave sleep estimation on a load-cell-installed bed: a non-constrained method," *Physiological Measurement*, vol. 30, no. 11, pp. 1163–1170, Nov. 2009.

Choi, S. and Jiang, Z., "A wearable cardiorespiratory sensor system for analyzing the sleep condition," *Expert Systems with Applications*, vol. 35, no. 1–2, pp. 317–329, July-Aug. 2008.

Chung, G. S., Choi, B. H., Lee, J. S., Lee, J. S., Jeong, DU., and Park, K. S., "REM sleep estimation only using respiratory dynamics," *Physiological Measurement*, vol. 30, no. 12, pp. 1327–1340, Dec. 2009.

Cohen, S., Doyle, W. J., Alper, C. M., Janicki-Deverts, D., and Turner, R.B., "Sleep habits and susceptibility to the common cold," *Archives of Internal Medicine*, vol. 169, no. 1, pp. 62–67, Jan. 2009.

Collop, N. A., Anderson, W. M., Boehlecke, B., Claman, D., Goldberg, R., Gottlieb, D. J., Hudgel, D., Sateia, M., and Schwab, R., "Clinical guidelines for the use of unattended portable monitors in the diagnosis of obstructive sleep apnea in adult patients," *Journal of Clinical Sleep Medicine*, vol. 3, no. 7, pp. 737–747, Dec. 2007.

Cysarz, D., Zerm, R., Bettermann, H., Frühwirth, M., Moser, M., and Kröz, M., "Comparison of Respiratory Rates Derived from Heart Rate Variability, ECG Amplitude, and Nasal/Oral Airflow," *Annals of Biomedical Engineering*, vol. 36, no. 12, pp. 2085–2094, Dec. 2008.

Darrington, J., "Towards real time QRS detection: A fast method using minimal pre-processing," *Biomedical Signal Processing and Control*, vol. 1, no 2, pp. 169–176, Apr. 2006.

Devot, S., Bianchi, A., Naujokat, E., Mendez, M., Brauers, A., and Cerutti, S., "Sleep monitoring through a textile recording system," in *Proceedings of 29th Annual International Conference of the IEEE Engineering in Medicine and Biology Society (EMBC)*, Aug. 2007, pp. 2560–2563.

Ding, S., Zhu, X., Chen, W., and Wei, D., "Derivation of respiratory signal from single-channel ECGs based on source statistics," *International Journal of Bioelectromagnetism*, vol. 6, 2004.

Dinges, D. F., Pack, F., Williams, K., Gillen, K. A., Powell, J. W., Ott, G. E., Aptowicz, C., and Pack, A.I., "Cumulative sleepiness, mood disturbance, and psychomotor vigilance performance decrements during a week of sleep restricted to 4-5 hours per night," *Sleep*, vol. 20, no. 4 pp. 267–277, Apr. 1997.

Droitcour A, Non-contact measurement of heart and respiration rates with a single-chip microwave Doppler radar, Doctoral dissertation, Stanford University, Stanford, CA, USA, 2006.

Ebrahimi, F., Setarehdan, S. K., Ayala-Moyeda, J., and Nazeran, H., "Automatic sleep staging using empirical mode decomposition, discrete wavelet transform, time-domain, and nonlinear dynamics features of heart rate variability signals," *Computer methods and programs in biomedicine*, vol. 112, no. 1, pp. 47–57, Oct. 2013.

Elgendi, M., “Fast QRS detection with an optimized knowledge-based method: Evaluation on 11 standard ECG databases,” *PLoS ONE*, vol. 8, no. 9, pp. 1–18, Sept. 2013.

Elgendi, M., Eskofier, B., Dokos, S., and Abbott, D., “Revisiting QRS detection methodologies for portable, wearable, battery-operated, and wireless ECG systems.” *PLoS ONE*, vol. 9, no. 1, pp. 1–18, Jan. 2014.

Emfit IP-9150 vital signs monitor: http://www.emfit.com/en/care/products_care/vitals-monitor-and-nurse-call/, accessed 1.5.2014.

Friedrich, D., Aubert, X. L., Fuhr, H., and Brauers, A., "Heart rate estimation on a beat-to-beat basis via ballistocardiography - a hybrid approach," in *Proceedings of 32nd Annual International Conference of the IEEE Engineering in Medicine and Biology Society (EMBC),* Aug.-Sept. 2010, pp.4048–4051.

Gagnadoux, F., Pelletier-Fleury, N., Philippe, C., Rakotonanahary, D., and Fleury, B., “Home unattended vs hospital telemonitored polysomnography in suspected obstructive sleep apnea syndrome: a randomized crossover trial,” *Chest*, vol. 121, no. 3, pp. 753–758, Mar. 2002.

Giovangrandi, L., Inan, O. T., Wiard, R. M., Etemadi, M., and Kovacs, G. T. A., “Ballistocardiography—A method worth revisiting,” in *Proceedings of 33rd Annual International Conference of the IEEE Engineering in Medicine and Biology Society (EMBC)*, Aug. – Sept. 2011, pp. 4279–4282.

Goldberger, A. L., Amaral, L. A. N., Glass, L., Hausdorff, J. M., Ivanov, P. Ch., Mark, R.G., Mietus, J. E., Moody, G. B., Peng, C. K., and Stanley, H. E., “PhysioBank, PhysioToolkit, and PhysioNet: Components of a New Research Resource for Complex Physiologic Signals,” *Circulation*, vol. 101, no. 23, pp. 215–220, June 2000.

Hall, M., Vasko, R., Buysse, D., Ombao, H., Chen, Q., Cashmere, J. D., Kupfer, D., and Thayer J. F., “Acute stress affects heart rate variability during sleep,” *Psychosomatic Medicine*, vol. 66, no 1, pp. 56–62, Jan.-Feb. 2004.

Hao, T., Xing, G., and Zhou, G., “iSleep: unobtrusive sleep quality monitoring using smartphones,” in *Proceedings of the 11th ACM Conference on Embedded Networked Sensor Systems, SenSys '13*, Nov. 2013, 14 pages.

Harrison, Y. and Horne, J. A., “The Impact of Sleep Deprivation on Decision Making: A Review,” *Journal of Experimental Psychology: Applied*, vol. 6, no. 3, pp. 236–249, Sept. 2000.

Hill, S., Tononi, G., and Ghilardi, M. F., “Sleep improves the variability of motor performance,” *Brain Research Bulletin*, vol 76, no. 6, pp. 605–611, Aug. 2008.

Iber, C., Ancoli-Israel, S., Chesson, A., and Quan, S. F., “The AASM manual for the scoring of sleep and associated events: rules, terminology and technical specifications,” *American Academy of Sleep Medicine*, Westchester, IL, USA, 2007.

Ifeachor, E. C. and Jervis, B. W., *Digital Signal Processing: A Practical Approach*, Boston, Massachusetts, USA: Addison-Wesley, 1993.

Irwin, M., McClintick, J., Costlow, C., Fortner, M., White, J., and Gillin, J.C., “Partial night sleep deprivation reduces natural killer and cellular immune responses in humans,“ *The Journal of Federation of American Societies for Experimental Biology*, vol. 10, no 5, pp. 643–653, Apr. 1996.

Ishida, S., Shiozawa, N., Fujiwara, Y., and Makikawa, M., “Electrocardiogram measurement during sleep with wearing clothes using capacitively coupled electrodes,” in *Proceedings of 29th Annual International Conference of the IEEE Engineering in Medicine and Biology Society (EMBC)*, Aug. 2007, pp. 2647–2650.

Ishijima, M., “Cardiopulmonary monitoring by textile electrodes without subject-awareness of being monitored,” *Medical & Biological Engineering & Computing*, vol. 35, no. 6, pp. 685–690, Nov. 1997.

Jacobs, J. L., Embree, P., Glei, M., Christensen, S., and Sullivan, P.K., “Characterization of a novel heart and respiratory rate sensor,” in *Proceedings of 26th Annual International Conference of the IEEE Engineering in Medicine and Biology Society (EMBC)*, Sept. 2004, pp. 2223–2226.

Jansen, B. H., Larson, B. H., and Shankar, K., “Monitoring of the ballistocardiogram with the static charge sensitive bed,” *IEEE Transactions on Biomedical Engineering*, vol. 38, no 8, pp.748–751, Aug. 1991.

Jin, J., Wang, X., Li, S., and Wu, Y., "A novel heart rate detection algorithm in ballistocardiogram based on wavelet transform," in *Proceedings of Second International Workshop on Knowledge Discovery and Data Mining (WKDD)*, Jan. 2009, pp.76–79.

Jung, W. G., *Op Amp Applications Handbook*, Burlington, Massachusetts, USA: Elsevier, 2004.

Kahn-Greene, E. T., Lipizzi, E. L., Conrad, A. K., Kamimori, G. H., and Killgore, W. D. S., “Sleep deprivation adversely affects interpersonal responses to frustration,” *Personality and Individual Differences*, vol. 41, no. 8, pp. 1433–1443, Dec. 2006.

Kamphuis, J., Meerlo, P., Koolhaas, J. M., and Lancel, M., “Poor sleep as a potential causal factor in aggression and violence,” *Sleep Medicine*, vol. 13, no. 4, pp. 327–334, Apr. 2012.

Kelly, J., Strecker, R., and Bianchi, M., “Recent Developments in Home Sleep-Monitoring Devices,” *ISRN Neurology*, vol. 2012, 10 pages, 2012.

Kesek, M., Franklin, K. A., Sahlin, C., and Lindberg, E., “Heart rate variability during sleep and sleep apnoea in a population based study of 387 women,” *Clinical physiology and functional imaging*, vol. 29, no. 4, pp. 309–315, July 2009.

Keselbrener, L., Keselbrener, M., and Akselrod, S., “Nonlinear high pass filter for R-wave detection in ECG signal,” *Medical Engineering & Physics*, vol. 19, no. 5, pp. 481–484, July 1997.

Kesper, K., Canisius, S., Penzel, T., Ploch, T., and Cassel, W., “ECG signal analysis for the assessment of sleep-disordered breathing and sleep pattern,” *Medical & Biological Engineering & Computing*, vol. 50, no. 2, pp. 135–144, Feb. 2012.

Knutson, K. L. and Van Cauter E., “Associations between sleep loss and increased risk of obesity and diabetes,” *Annals of the New York Academy of Science*, vol. 1129, pp. 287–304, 2008.

Kohler, B. U., Hennig, C., and Orglmeister, R., "The principles of software QRS detection," *IEEE Engineering in Medicine and Biology Magazine*, vol. 21, no. 1, pp. 42–57, Jan.-Feb. 2002.

Kortelainen, J. and Virkkala, J., "FFT averaging of multichannel BCG signals from bed mattress sensor to improve estimation of heart beat interval," in *Proceeding of 29th Annual International Conference of the IEEE Engineering in Medicine and Biology Society (EMBC)*, Aug. 2007, pp. 6685–6688.

Kortelainen, J., Mendez, M., Bianchi, A., Matteucci, M., and Cerutti, S., "Sleep staging based on signals acquired through bed sensor," *IEEE Transactions on Information Technology in Biomedicine*, vol. 14, no 3, pp.776–785, May 2010.

Kortelainen, J., van Gils, M., Pärkkä, J., "Multichannel bed pressure sensor for sleep monitoring," *Computing in Cardiology (CinC)*, Sept. 2012, pp.313–316.

Krejcar, O., Jirka, J., and Janckulik, D., "Use of mobile phones as intelligent sensors for sound input analysis and sleep state detection," *Sensors*, vol. 11, no.6, pp. 6037–6055, June 2011.

Kushida, C. A., Littner, M. R., Morgenthaler, T., Alessi, C. A., Bailey, D., Coleman, J. Jr, Friedman, L., Hirshkowitz, M., Kapen, S., Kramer, M., Lee-Chiong, T., Loube, D. L., Owens, J., Pancer, J. P., and Wise, M., "Practice parameters for the indications for polysomnography and related procedures: An update for 2005," *Sleep*, vol. 28, no. 4, pp. 499–521, Apr. 2005.

Kwon, S., Lee, J., Chung, G. S., and Park K. S., "Validation of heart rate extraction through an iPhone accelerometer," in *Proceedings of 33rd Annual International Conference of the IEEE Engineering in Medicine and Biology Society (EMBC)*, Aug.-Sept. 2011, pp.5260–5263.

Kärki, S. and Lekkala, J., "A new method to measure heart rate with EMFi and PVDF materials," *Journal of Medical Engineering & Technology*, vol. 33, no. 7, pp. 551–558, Oct. 2009.

Lee, H. J., Hwang, S. H., Lee, S. M., Lim, Y. G., and Park, K.S., "Estimation of body postures on bed using unconstrained ECG measurements," *IEEE Journal of Biomedical and Health Informatics*, vol.17, no. 6, pp.985–993, Nov. 2013

Leivo, S., "Quality control of ambulatory polysomnography for the diagnosis of sleep apnea Syndrome," *American Journal of Electroneurodiagnostic Technology*, vol. 47, no. 4, p. 307, Dec. 2007.

Lim, J. and Dinges, D. F., "Sleep deprivation and vigilant attention," *Annals of the New York Academy of Sciences*, vol. 1129, pp. 305–322, 2008.

Lim, Y. G., Kim, K. K., and Park, K. S., "ECG recording on a bed during sleep without direct skin-contact," *IEEE Transactions on Biomedical Engineering*, vol. 54, no. 4, pp. 718–725, Apr. 2007.

Lin, L. I., "A concordance correlation coefficient to evaluate reproducibility," *Biometrics*, vol. 45, no. 1, pp. 255–268, Mar. 1989.

Mack, D. C., Patrie, J. T., Suratt, P. M., Felder, R. A., and Alwan, M., "Development and preliminary validation of heart rate and breathing rate detection using a passive, ballistocardiography-based sleep monitoring system," *IEEE Transactions on Information Technology in Biomedicine*, vol.13, no 1, pp.111–120, Jan. 2009a.

Mack, D. C., Patrie, J. T., Felder, R. A., Suratt, P. M., and Alwan, M., "Sleep assessment using a passive ballistocardiography-based system: preliminary validation", in *Proceedings of 31st Annual International Conference of the IEEE Engineering in Medicine and Biology Society (EMBC)*, Sept. 2009b, pp. 4319–4322.

Maglaveras, N., Stamkopoulos, T., Diamantaras, K., Pappas, C., and Strintzis, M., "ECG pattern recognition and classification using non-linear transformations and neural networks: A review," *International Journal of Medical Informatics*, vol. 52, no. 1–3, pp. 191–208, Oct. 1998.

Malik, M., Bigger, J. T., Camm, A. J., Kleiger, R. E., Malliani, A., Moss, A. J., and Schwartz, P. J., "Heart rate variability standards of measurement, physiological interpretation, and clinical use," *European heart journal*, vol. 17, no. 3, pp. 354–381, Mar. 1996.

Malmivuo, J. and Plonsey, R., *Bioelectromagnetism*, New York, New York, USA: Oxford University Press, 1995. Electronically available: http://www.bem.fi/book, accessed 25.7.2014.

Martin, J. and Hakim, A., "Wrist actigraphy," *Chest*, vol. 139, no. 6, pp. 1514–1527, June 2011.

Mignot, E., "Why we sleep: The temporal organization of recovery," *PLoS Biology*, vol. 6, no. 4, pp. 661–669, Apr. 2008.

Moody, G. B. and Mark, R.G., "The impact of the MIT-BIH Arrhythmia Database," *IEEE Engineering in Medicine and Biology Magazine*, vol. 20, no. 3, pp. 45–50, May-June 2001.

Moody, G. B., Mark, R. G., Zoccola, A., and Mantero, S., "Derivation of respiratory signals from multi-lead ECGs," *Computers in Cardiology*, vol. 12, 1985, pp. 113–116.

Morgenthaler, T., Alessi, C., Friedman, L., Owens, J., Kapur, V., Boehlecke, B., Brown, Chesson, A. Jr., Coleman, J., Lee-Chiong, T., Pancer, J., and Swick, T. J., "Practice parameters for the use of actigraphy in the assessment of sleep and sleep disorders: An update for 2007," *Sleep*, vol. 30, no. 4, pp. 519–529, Apr. 2007.

Mukai, K., Yonezawa, Y., Ogawa, H., Maki, H., and Caldwell, W. M., "A remote monitor of bed patient cardiac vibration, respiration and movement," in *Proceedings of 31st Annual International Conference of the IEEE Engineering in Medicine and Biology Society (EMBC)*, Sept. 2009, pp. 5191–5194.

Murata, MEMS accelerometer based heart & respiration rate detection module: http://www.murata.eu/healthcare_applications/BCG_Flyer_Compamed.pdf, accessed 1.4.2014.

Murthy, R., Pavlidis, I., Tsiamyrtzis, P., "Touchless monitoring of breathing function," in *Proceedings of 26th Annual International Conference of the IEEE Engineering in Medicine and Biology Society (EMBC)*, Sept. 2004, pp. 1196–1199.

Niizeki, K., Nishidate, I., Uchida, K., and Kuwahara, M., "Unconstrained cardiorespiratory and body movement monitoring system for home care," *Medical & Biological Engineering & Computing*, vol. 43, no 6, pp. 716–724, Nov. 2005.

O'Brien, C. and Heneghan, C., "A comparison of algorithms for estimation of a respiratory signal from the surface electrocardiogram," *Computers in Biology and Medicine*, vol. 37, no. 3, pp. 305–314, Mar. 2007.

Ohayon, M. M. and Bader, G., "Prevalence and correlates of insomnia in the Swedish population aged 19–75 years," *Sleep Medicine*, vol. 11, no. 10, pp. 980–986, Dec. 2010a.

Ohayon, M. M. and Sagales, T., "Prevalence of insomnia and sleep characteristics in the general population of Spain," *Sleep Medicine*, vol. 11, no. 10, pp. 1010–1018, Dec. 2010b.

Okada, S., Fujiwara, Y., Yasuda, M., Ohno, Y., Makikawa, M., "Non-restrictive Heart Rate Monitoring Using an Acceleration Sensor," in *Proceedings of 28th Annual International Conference of the IEEE Engineering in Medicine and Biology Society (EMBC)*, Aug.-Sept. 2006, pp. 5093–5096.

Oppenheim, A, V. and Schafer, R. W., *Discrete-Time Signal Processing*, Englewood Cliffs, New Jersey, USA: Prentice-Hall, 1989.

Orphanidou, C., Fleming, S., Shah, S. A., and Tarassenko, L., "Data fusion for estimating respiratory rate from a single-lead ECG," *Biomedical Signal Processing and Control*, vol. 8, no. 1, pp. 98–105, Jan. 2013.

Paajanen, M., Lekkala, J., and Kirjavainen, K., "ElectroMechanical Film (EMFi) — a new multipurpose electret material," *Sensors and Actuators A: Physical*, vol. 84, no. 1–2, pp. 95–102, Aug. 2000.

Paalasmaa, J. and Ranta, M., "Detecting heartbeats in the ballistocardiogram with clustering," in *Proceedings of the ICML/UAI/COLT 2008 Workshop on Machine Learning for Health-Care Applications*, July 2008.

Paalasmaa, J., Leppäkorpi, L., and Partinen, M., "Quantifying respiratory variation with force sensor measurements," in *Proceedings of 33rd Annual International Conference of the IEEE Engineering in Medicine and Biology Society (EMBC)*, Aug. 2011, pp. 3812–3815.

Paalasmaa, J., Waris, M., Toivonen, H., Leppäkorpi, L., and Partinen, M., "Unobtrusive online monitoring of sleep at home," in *Proceedings of 34th Annual International Conference of the IEEE Engineering in Medicine and Biology Society (EMBC)*, Aug.-Sept. 2012, pp. 3784–3788.

Paalasmaa, J., "Monitoring sleep with force sensor measurement," Doctoral dissertation, University of Helsinki, Helsinki, Finland, 2014a, 59 pages.

Paalasmaa, J., Toivonen, H., and Partinen, M., "Adaptive Heartbeat Modelling for Beat-to-beat Heart Rate Measurement in Ballistocardiograms," *IEEE Journal of Biomedical and Health Informatics*, accepted for publication, 2014b.

Pan, J. and Tompkins, W.J., "A real-time QRS detection algorithm," *IEEE Transactions on Biomedical Engineering*, vol. 32, no. 3, pp. 230-236, Mar. 1985.

Park, S. B., Noh, Y. S., Park, S. J., and Yoon, H. R., "An improved algorithm for respiration signal extraction from electrocardiogram measured by conductive textile electrodes using instantaneous frequency estimation," *Medical & Biological Engineering & Computing*, vol. 46, no. 2, pp. 147–158, Feb. 2008.

Patel, S. R., Malhotra, A., Gao, X., Hu, F. B., Neuman, M. I., Fawzi, W. W., "A prospective study of sleep duration and pneumonia risk in women," *Sleep*, vol. 35, no. 1, pp. 97–101, Jan. 2012.

Peltokangas, M., Verho, J., and Vehkaoja, A., "Unobtrusive night-time EKG and HRV monitoring system," in *Proceeding of 10th International Workshop on Biomedical Engineering,* Oct. 2011, pp. 1–5.

Phan, D. H., Bonnet, S., Guillemaud, R., Castelli, E., and Pham Thi, N.Y., "Estimation of respiratory waveform and heart rate using an accelerometer," in *Proceedings of 30th Annual International Conference of the IEEE Engineering in Medicine and Biology Society (EMBC)*, Aug. 2008, pp. 4916–4919.

Physionet, cited 15.1.2015, http://physionet.org/physiobank/database/#ecg

Pinheiro, E., Postolache, O., and Girão, P., "Theory and Developments in an Unobtrusive Cardiovascular System Representation: Ballistocardiography," *The Open Biomedical Engineering Journal*, vol. 4, pp. 201–216, Oct. 2010.

Pollak, C. P., Tryon, W. W., Nagaraja, H., and Dzwonczyk, R., "How Accurately Does Wrist Actigraphy Identify the States of Sleep and Wakefulness?," *Sleep*, vol. 24, no. 8, pp. 957–965, Dec. 2001.

Portier, F., Portmann, A., Czernichow, P., Vascaut, L., Devin, E., Benhamou, D., Cuvelier, A., and Muir, J. F., "Evaluation of Home versus Laboratory Polysomnography in the Diagnosis of Sleep Apnea Syndrome," *American Journal of Respiratory and Critical Care Medicine*, vol. 162, no. 3, pp. 814–818, Sept. 2000.

Puurtinen, M., "Precordial bipolar leads for mobile ECG applications," Doctoral dissertation, Tampere University of Technology, Tampere, Finland, 2012, 69 pages.

Rauhala, E. "Performance of non-invasive devices in evaluation of periodic limb movements and sleep-disordered breathing," Doctoral dissertation, University of Tampere, Tampere, Finland, 2009, 98 pages.

Redmond, S. J. and Heneghan, C., "Cardiorespiratory-based sleep staging in subjects with obstructive sleep apnea," *IEEE Transactions on Biomedical Engineering*, vol. 53, no. 3, pp. 485–496, Mar. 2006.

Roche, F., Gaspoz, J.-M., Court-Fortune, I., Pascal, M., Pichot, V., Duverney, D., Costes, F., Lacour, J.-R., and Barthélémy, J.-C., "Screening of obstructive sleep apnea syndrome by heart rate variability analysis," *Circulation*, vol. 100, no. 3, pp. 1411–1415, Sept. 1999.

Romeijn, N., Verweij, I. M., Koeleman, A., Mooij, A., Steimke, R., Virkkala, J., van der Werf, Y., and Van Someren, E. J. W., "Cold hands, warm feet: sleep deprivation disrupts thermoregulation and its association with vigilance," *Sleep*, vol. 35, no. 12, pp. 1673–1683, Dec. 2012.

Rosales, L., Skubic, M., Heise, D., Devaney, M. J., and Schaumburg, M., "Heartbeat detection from a hydraulic bed sensor using a clustering approach," in *Proceedings of 34th Annual International*

Conference of the IEEE Engineering in Medicine and Biology Society (EMBC), Aug.-Sept. 2012, pp. 2383–2387.

Scarborough, W. R., Talbot, S. A., Braunstein, J. R., Rappaport, M. B., Dock, W., Hamilton, W. F., Smith, J. E., Nickerson, J. L., and Starr, I., “Proposals for ballistocardiographic nomenclature and conventions: revised and extended report of Committee on Ballistocardiographic Terminology,” *Circulation*, vol. 14, no. 3, pp. 435–450, Sept. 1956.

Scharf, M. T., Naidoo, N., Zimmerman, J. E., and Pack, A. I., “The energy hypothesis of sleep revisited,” *Progress in Neurobiology*, vol. 86, no. 3, pp. 264–280, Nov. 2008.

Shannon, C. E. "Communication in the presence of noise," *Proceeding of the Institute of Radio Engineers*, vol. 37, no. 1, pp. 10–21, Jan. 1949.

Shin, J. H., Chee, Y. J., Jeong, D. U., Park, K. S., "Nonconstrained Sleep Monitoring System and Algorithms Using Air-Mattress With Balancing Tube Method," *IEEE Transactions on Information Technology in* Biomedicine, vol. 14, no. 1, pp. 147–156, Jan. 2010.

Siivola, J., “New noninvasive piezoelectric transducer for recording of respiration, heart rate and body movements,” *Medical & Biological Engineering & Computing*, vol. 27, no. 4, pp. 423–424, July 1989.

Sleep as Android, cited 10.5.2014: https://sites.google.com/site/sleepasandroid/

Sleep Cycle Alarm Clock, cited 10.5.2014: http://www.sleepcycle.com/

Stein, P. K. and Pu, Y., “Heart rate variability, sleep and sleep disorders,” *Sleep Medicine Reviews*, vol. 16, no. 1, pp. 47–66, Feb. 2012.

Stickgold, R., “Sleep-dependent memory consolidation,” *Nature*, vo. 437, no. 7063, pp. 1272–1278, Oct. 2005.

Tanaka, S., Matsumoto, Y., and Wakimoto, K., “Unconstrained and non-invasive measurement of heart-beat and respiration periods using a phonocardiographic sensor,” *Medical & Biological Engineering & Computing*, vol. 40, pp. 246–252, Mar. 2002.

Tenhunen, M., Rauhala, E., Virkkala, J., Polo, O., Saastamoinen, A., and Himanen, S. L., “Increased respiratory effort during sleep is non-invasively detected with movement sensor,” *Sleep and Breathing*, vol. 15, no. 4, pp. 737–746, Dec. 2011.

Thomas, R .J., Mietus, J. E., Peng, C. K., and Goldberger, A. L., “An electrocardiogram-based technique to assess cardiopulmonary coupling during sleep,” *Sleep*, vol. 28, no. 9, pp. 1151–1161, Sept. 2005.

Vehkaoja, A., Verho, J., Cömert, A., Honkala, M., and Lekkala, J., “Wearable system for EKG monitoring - evaluation of night-time performance,” Revised Selected Papers of *Second International ICST Conference on Wireless Mobile Communication and Healthcare, MobiHealth, Oct. 2011, Lecture Notes of the Institute for Computer Sciences, Social Informatics and Telecommunications Engineering*, vol. 83, pp. 119–126, 2012.

Wang, F., Tanaka, M., and Chonan, S., “Development of a PVDF piezopolymer sensor for unconstrained in-sleep cardiorespiratory,” *Journal of Intelligent Material Systems and Structures*, vol. 14, no. 3, pp. 185–190, Mar. 2003.

Wartzek, T., Eilebrecht, B., Lem, J., Lindner, H. J., Leonhardt, S., and Walter, M., "ECG on the Road: Robust and Unobtrusive Estimation of Heart Rate," *IEEE Transactions on Biomedical Engineering*, vol. 58, no. 11, pp. 3112–3120, Nov. 2011.

WatchPAT, cited 15.1.2015, http://www.itamar-medical.com

Widjaja, D., Taelman, J., Vandeput, S., Braeken, M. A. K. A., Otte, R. A., Van den Bergh, B. R. H., and Van Huffel, S., "ECG-derived respiration: Comparison and new measures for respiratory variability," *Computing in Cardiology (CinC),* Sept. 2010, pp. 149–152.

Woodward, S. H., Arsenault, N. J., Voelker, K., Nguyen, T., Lynch, J., Leskin, G., and Sheikh, J., “Estimating heart rate and RSA from the mattress-recorded kinetocardiogram,” *Psychophysiology*, vol. 44, no. 4, pp. 635–638, July 2007.

Wu, K.-F. and Zhang, Y.-T., “Contactless and continuous monitoring of heart electric activities through clothes on a sleeping bed,” in *Proceedings of International Conference on Information Technology and Applications in Biomedicine (ITAB)*, May 2008, pp. 282–285.

Xiaomeng, G., Singh, A., Yavari, E., Lubecke, V., and Boric-Lubecke, O., "Non-contact displacement estimation using Doppler radar," in *Proceedings of 34th Annual International Conference of the IEEE Engineering in Medicine and Biology Society (EMBC)*, Aug.-Sept. 2012, pp. 1602–1605.

Yang, C. M., Chou, C. M., Chen, S. G., Li, B. J., Hung, S. H., Yang, C. H., Wu, C. C., Hsieh, M .C., and Yang, T. L., "Sleeping ECG and body position monitoring system," in *Proceedings of the 31st Annual International Conference of the IEEE Engineering in Medicine and Biology Society (EMBC)*, Sept. 2009, pp.1856–1859.

Yeh, Y. C. and Wang, W. J., “QRS complexes detection for ECG signal: the difference operation method,” *Computer Methods and Programs in Biomedicine*, vol. 91, no. 3, pp. 245–254, Sept. 2008.

Zaffaroni, A., Kent, B., O'Hare, E., Heneghan, C., Boyle, P., O'Connell, G., Pallin, M., de Chazal, P., and McNicholas, W. T., “Assessment of sleep-disordered breathing using a non-contact bio-motion sensor,” *Journal of Sleep Research*, vol. 22, no. 2, pp. 231–236, Apr. 2013.

Zakrzewski, M., Raittinen, H., and Vanhala, J., "Comparison of center estimation algorithms for heart and respiration monitoring with microwave doppler radar," *IEEE Sensors Journal*, vol.12, no.3, pp. 627–634, Mar. 2012

Zhengzhong, G., Fanxue, K., and Xu, Z., “Accurate and rapid QRS detection for intelligent ECG monitor,” in *Proceedings of Third International Conference on Measuring Technology and Mechatronics Automation (ICMTMA)*, Jan. 2011, pp. 298–301.

Zhu, X., Chen, W., Tetsu, N., Kanemitsu, Y.; Kitamura, Kei-ichiro; Yamakoshi, K.; Daming Wei, "Real-Time Monitoring of Respiration Rhythm and Pulse Rate During Sleep," *IEEE Transactions on Biomedical Engineering*, vol. 53, no. 12, pp. 2553–2563, Dec. 2006.

Zidelmal, Z., Amirou, A., Adnane, M., and Belouchrani, A., “QRS detection based on wavelet coefficients,” *Computer Methods and Programs in Biomedicine*, vol. 107, no. 3, pp. 490–496, Sept. 2012.

Original publications

Publication I

Peltokangas, M., Verho, J., and Vehkaoja, A., “Night-time EKG and HRV monitoring with bed sheet integrated textile electrodes," *IEEE Transactions on Information Technology in Biomedicine*, vol. 16, no. 5, pp. 935–942, Sept.2012.

Night-Time EKG and HRV Monitoring with Bed Sheet Integrated Textile Electrodes

Mikko Peltokangas, Jarmo Verho, and Antti Vehkaoja

***Abstract*—A system for unobtrusive night-time EKG and HRV monitoring as well as data analysis methods are presented, comparing bed sheet HR and HRV values with corresponding parameters obtained by a reference measurement. Our system uses 8 embroidered textile electrodes attached laterally to a bed sheet for measuring bipolar contact EKG from multiple channels. The electrodes are arranged as a line so that at least two adjacent electrodes make sufficient skin contact. The focus of the signal processing development has been in selecting the best measurement channel for further analysis and minimizing the amount of incorrectly detected R-peaks.**

The test measurements were performed with four healthy men without previously known cardiac disorders and one who frequently had premature ventricular contractions (ectopic beats). For healthy test subjects, an average of 94.9 % heartbeat detection coverage was achieved with the system during 29 measurement nights (in total 213.8 hours of data).

In most cases, the quality of the signal obtained from bed sheet electrodes is good enough for the computer-assisted cardiac arrhythmia detection. Applications for EKG derived RR-interval data include the calculation of HRV parameters that can be utilized in sleep quality analysis and other wellness-related topics as well as sleep apnoea detection.

***Index Terms*—Night-time electrocardiogram (EKG, ECG), night-time heart rate variability (HRV), physiological monitoring, textile electrode**

I. Introduction and Motivation

Increasing interest in wellness applications has expanded the will to measure the information on cardiac activity from sports to other domains of living. Measuring EKG and especially heart rate (HR) and heart rate variability (HRV) during sleep provides valuable information about sleep quality and other wellbeing and health related indicators. HR based awakening detection for sleep quality monitoring has been studied e.g. by Bulckaert *et al.* in [1]. Applications for night time HR and HRV measurements also include detection of acute mental stress [2] and sleep apnoea [3]. Obviously, many kinds of cardiac arrhythmias can be detected and analyzed when HR or EKG data is available.

The system we are proposing consists of eight embroidered fabric electrodes that are sewn on the bed sheet, forming seven bipolar EKG channels. Compared with traditional long term EKG recordings, (Holter devices), our approach is more user-friendly: the measurement of bed sheet EKG is unobtrusive, without electrodes to be worn or a data acquisition device to be carried. It is also possible to automate it so that it does not require any attention from the user. The aforementioned benefits make using such system continuously in everyday life possible.

In this study, we compared both HR values and HRV frequency domain parameters obtained by bed sheet electrodes to corresponding reference values obtained by disposable Ag/AgCl electrodes. In addition, we developed an automatic ectopic beat (EB) detector in order to show that the computer-assisted ectopic beat detection is possible even though the signal quality is not always good and the measurement lead varies.

II. Related Work

A. Methods for HR and HRV Detection

The night-time cardiac activity monitoring has been studied by measuring the electrical as well as mechanical activity of the heart. The most traditional method for long-term EKG recording is Holter-type measurement device, which records EKG data from 2–12 standardized measurement channels (EKG leads). In our system, the measurement leads are not standardized and they are changed during night when person changes his sleeping posture. Thus, some of the EKG information provided by the Holter type devices is not available from our system. Another limitation is the requirement of galvanic skin contact, which means that the user cannot wear a shirt or pyjamas while being monitored.

Ishijima [4] and Devot *et al.* [5] have studied unobtrusive non-wearable night-time EKG measurements based on direct skin contact by using large textile electrodes located on a pillow and on the foot of the bed. An advantage of their methods is that wearing a pyjama is allowed. On the other hand, their system requires the pillow with connecting wires located under the head. They also do not discuss whether thick or long hair possibly affects the measurement. According to the results reported by Ishijima [4], night-time HR can be recorded 83%–93% of sleeping time. Devot *et al.* reported the coverage percent ranging from 47.9% to 95.8% with an average of 81.8%.

Lim *et al.* [6] have developed multichannel EKG measurement system by using capacitive electrodes. In their work, the measurement electrodes were assembled into line onto the mattress as in our system (Fig. 1), but a common reference electrode was located in the foot of the bed. Despite the multichannel measurement setup, they did not specify how the channels were selected for the analysis. Most other capacitive electrode configurations utilize wide electrode stripes spanning

Manuscript received January 22, 2012; revised May 11, 2012; accepted July 7, 2012.

M. Peltokangas, J. Verho and A. Vehkaoja are with the Department of Automation Science and Engineering, Tampere University of Technology, P.O. Box 692, FI-33101 Tampere, Finland. E-mail for everyone: firstname.lastname@tut.fi.

from bed side to bed side [7], [8]. Although capacitive EKG measurements are absolutely unobtrusive, a drawback is that they are extremely sensitive against artefacts and electromagnetic interferences. Wu *et al.* [7] reached a coverage factor of 98% in one night measurement performed in an RF-shielded room. As a contrary, in measurements performed by Ishida *et al.* [8] with a quite similar electrode configuration in a real world environment, only 27% of the entire sleeping time was covered.

Methods for night-time HR measurement based on the non-electrical events of the cardiovascular system may utilize the mechanical movement of the body caused by the heart beat or the blood pressure wave signal. Like electrodes, also pressure and force sensors can be used in HR measurement by attaching them to the bed. In addition, the pulsatile blood flow can be detected with a photoplethysmograph (PPG) sensor under the bed sheet as Wong *et al.* have presented in [9].

Kortelainen *et al.* [10] used a pressure sensitive mattress manufactured from EMFi (Electro Mechanical Film), that included as many as 160 sensor elements. Their research focused on detecting different sleep stages. Paalasmaa [11] used a piezo-electric bedpost vibration sensor developed by Finsor Ltd. [12] in his work, where he developed signal processing methods for enhancing the heartbeat detection accuracy by compensating the effects of respiration on the waveform of the heartbeats. Zhu *et al.* [13] studied HR and respiration by using a pillow that had pockets filled with water and measuring the pressure variations in the water. They used approximately two-hour data periods from 13 different test subjects' sleep and the method gave 99.17 % average HR detection sensitivity. Mechanical movements caused by the heart have also been measured by Okada *et al.* by placing an accelerometer in the bedding [14]. They noticed a large variation in the reliability of the method for HR detection.

All the methods that are based on the measurement of mechanical signals are very sensitive to movement artefacts. This applies also to the movements of the other person or persons sleeping in the same bed. In addition, the waveforms recorded with non-electrical methods are not as clear and sharp as R-peaks in EKG which may affect the accuracy of the HR detection. Also ectopic beats (EB) are often missed with non-electrical activity based methods because EBs do not influence the pumping mechanism of the heart [10].

B. HRV Applications

In HRV analysis, we are usually interested in normal sinus rhythm which is regulated by the autonomous nervous system and thus gives valuable information on the stress state of the body. For that reason, all ectopic beats (EB) originated from somewhere else than the sinus node should be identified and corrected since they skew the results. Correction is important since e.g. according to Simpson Jr. *et al.* [15], more than 6% of the American middle-aged adults suffer from premature ventricular contractions.

An interesting application for HRV data is sleep staging. Nowadays, most clinical sleep studies are performed in specialized sleep labs by using polysomnographic (PSG) devices measuring e.g. EEG, EMG, EOG and EKG. The PSG measurement is however expensive and extremely obtrusive for the patient.

The frequency domain properties of HRV are commonly used in sleep analysis. Generally, the HRV spectrum is divided into very low frequency (VLF, $\leq$0.04 Hz), low frequency (LF, 0.04 Hz–0.15 Hz), and high frequency (HF, 0.15 Hz–0.4 Hz) bands whose spectral powers vary in different sleep stages. The change in the spectral powers is a result of the changes in sympathetic and parasympathetic activity of the autonomous nervous system: increased sympathetic activity indicates REM sleep whereas the situation is contrary during non-REM sleep [5], [16]. For instance, Devot *et al.* in [5] have studied textile electrode EKG in REM/non-REM sleep classification reaching good results. They detected REM sleep stages by using a hidden Markov model classifier and utilized a decrease in HF power and increase in VLF power during REM sleep. Kesper *et al.* [17] have developed HRV-based sleep stage classifier which is able to discriminate also non-REM stages 1–4 by using the normalized LF/HF ratio, the relative HF peak power and the variability of HF peak frequency. PDFA (Progressive Detrended Fluctuation Analysis) is another kind of method for sleep staging presented by Telser *et al.* in [18]. They utilized different correlations in the RR series during REM and non-REM sleep as well as uncorrelated heart beats during transitions between different sleep stages.

The detection of sleep apnoea, which is a common sleep disorder with incidence of 4% in adult men and 2% in adult women, is another useful application of HRV [3], [19]. In many cases, the spectral properties or periodic variations of RR-series are utilized in sleep apnoea detection [3], [17].

Our current work focuses on validating the accuracy of the HRV parameters recorded with the system. Sleep classification and apnoea detection will be studied later.

III. Materials and Methods

A. The Bed Sheet Electrodes

The electrodes we are using are manufactured by embroidering silver coated polyamide yarn. The size of the oval shaped electrodes is 32 mm $\times$ 22 mm. An insulating layer is used under the electrodes in order to prevent the electrodes from drying (after first moistened by the moisture of the skin). Wires are connected to the electrodes by sewing them with silver coated yarn and they are located between the mattress and the bed sheet. The EKG signals in each seven channels are formed by amplifying the potential difference between two adjacent electrodes.

Since people are of different sizes and sleep in different postures, a compromise was made with the electrode setup. If the inter-electrode distance in bipolar HR measurement is too wide, there would be cases where only one electrode has a proper contact with the skin whereas too small inter-electrode distance would narrow the measurement area and decrease the magnitude of the EKG signal. Due to the limited number of available measurement channels, we optimized the inter-electrode distance so that the electrodes cover the bed sheet (Fig. 1) as widely as possible, but at the same time are close

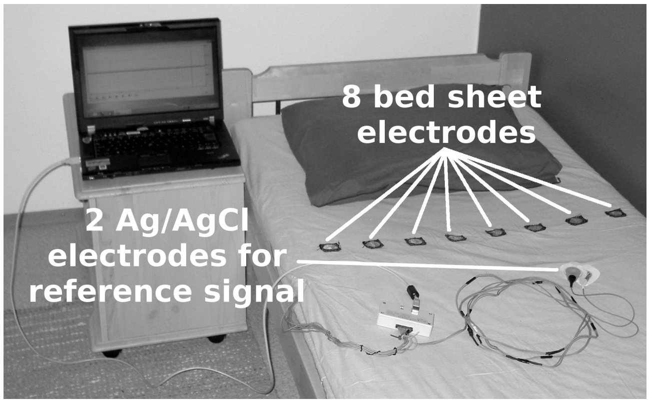

Fig. 1. The EKG recording sheet and the measurement hardware used in the test measurements.

enough to each other so that at least two electrodes make contact even when the person is sleeping in a lateral position. Eight electrodes were sewn into a line onto the bed sheet, forming seven EKG channels, so that electrodes are 9.8 cm apart and cover a width of 69 cm (Fig. 1). We also made additional test measurements with inter-electrode distance of 5 cm to verify that the distance could be further decreased if the system would be used by a smaller person.

B. *Measurement Hardware*

Our measurement hardware consists of an EKG amplifier circuit board and a data acquisition circuit board that communicates with a PC via USB. The amplifier board contains eight EKG amplifiers, seven of them for the bed sheet EKG channels and the remaining one for the reference EKG signal recorded with conventional disposable Ag/AgCl electrodes. All channels are identical, having two amplifier stages. The first stage is an instrumentation amplifier and the second is a non-inverting gain stage. Between the amplifiers there is a first order high-pass filter and after the second stage a second order 40 Hz Butterworth low-pass filter.

The data acquisition board has a 16-bit successive approximation type eight channel analog-to-digital converter (ADC). A microcontroller handles the controlling of the ADC and relays the measurement data to the PC via a serial-to-USB converter.

According to Rosell *et al.* [20], skin impedance varies between 10 kΩ and 1 MΩ at frequency range of 10 Hz–100 Hz when an electrolyte gel is used without any other preparation. To estimate amplifier noise during EKG recording, we connected a 47 kΩ resistor between two adjacent electrodes. The unprocessed noise voltage corresponds to the input noise of 6.47 $\mu\mathrm{V}_{\mathrm{rms}}$ when the measured pass-band gain (102) is considered. After pre-processing the signal as described in Section IV-A, the corresponding input noise voltage reduces to 0.61 $\mu\mathrm{V}_{\mathrm{rms}}$.

C. *Test Measurements*

We tested our system with four subjects, denoted with person A, B, C and D, in their homes for a total of 29 nights or 213.8 hours. All subjects were male, aged 23–32 years, 173–185 cm, 64–80 kg and healthy without previously known cardiac disorders. We also had a fifth test subject, person E, but measurements performed by him are left outside the analysis since his EKG contained a large number of premature ventricular contractions (PVC) and was extremely distorted by artefacts. However, PVCs were detected in his EKG in most cases correctly by the automatic EB detector.

During the test measurements, the reference EKG signal was recorded with conventional disposable Ag/AgCl electrodes. The sampling frequency was 250 Hz. We did all the signal processing off-line using Matlab and the periods of 5 minutes were removed from the beginning and the end of each signal before any signal processing.

IV. Channel Selection and Heart Rate Detection

Compared with standard EKG processing, the biggest challenges that are encountered in R-peak detection are unknown polarity and posture-dependent amplitude of R-peaks as well as significantly increased signal artefacts and overall worse signal-to-noise ratio. In our test measurements, the amplitude of R-peak varied almost two orders of magnitude, which occasionally causes difficulties in the separation of artefact-related signal peaks from actual R-peaks. Similarly, the noise amplitude of the pre-processed signal can be even higher than R-peak amplitude in some other case. Since motion artefacts and poor electrode contact disturb the signal heavily in some cases, our aim was that the system would not produce any HR output values when the signal quality does not allow R-peak detection with sufficient confidence.

The R-peaks from the reference EKG signal were detected with the same method as from the bed sheet EKG signal. To get more reliable values, misdetected beats in the reference EKG signal were corrected manually.

A. *Signal Pre-Processing*

Besides the analog filtering and gain in the measurement electronics, we synthesized a 10^{th} order Butterworth low-pass filter with a cut-off frequency of 30 Hz to remove the 50 Hz power line interference and other higher frequency interferences. The low-pass filter is implemented with forward-backward filtering, so the actual filter order is 20. Wandering baseline is efficiently removed with a non-linear high-pass filtering using 100 ms moving median, suggested by Keselbrener *et al.* in [21].

B. *Channel Selection*

To select the best EKG channel for HR detection from the seven recorded channels, a 10-second period is extracted from all pre-processed signals. In these signals, all possible R-peaks (Fig. 2) whether they have positive or negative polarity, are pre-detected based on a method proposed by Zhengzhong *et al.* in [22].

To get threshold values for R-peak pre-detection, a 10-second window is divided into five sections and the local maximum and minimum as well as the steepest slopes (the

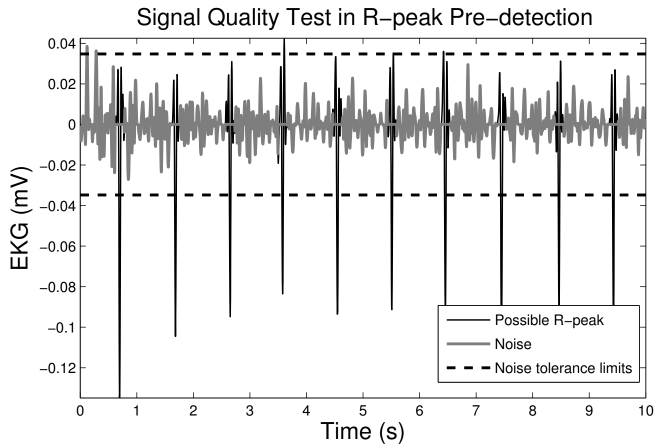

Fig. 2. Pre-processed EKG is composed of a noise (solid grey) and possible R-peaks (solid black). Noise tolerance limits are shown as dashed black lines.

highest differences between consecutive samples) of each section are detected. The extreme values and the steepest slopes of each section are investigated in order to find the tip of an R-peak as well as the rising and the falling edges of a QRS complex. These quantities from the five sections are averaged in order to find the initial values for thresholds applied in R-peak pre-detection.

An amplitude threshold is set to 60% of the mean value of maxima (or minima, if negative R-peak) in the 10-second window and slope thresholds are set to 20% of the mean values of maximum and minimum differences in the 10-second window. Differing from Zhengzhong's method, absolute lower and upper limits for acceptable R-peak amplitudes were set exploiting the magnitude of observed extreme values in test measurements. In addition, we used an upper relative amplitude limit in R-peak detection: A peak is considered as a noise peak if its amplitude is more than 2 times the amplitude mean value in the 10-second window.

After pre-detecting R-peaks, the first quality assessment is done on the signal by examining the noise level of the pre-processed signal. In the first step, the noise (solid grey line in Fig. 2) is separated from possible R-peaks by excluding all R-peak-centered 0.16 s long intervals (solid black line in Fig. 2) from pre-processed EKG signal. Then, noise tolerance limits are defined with expression $\pm 0.35 \times \max(A_p, |A_n|)$, where A_p and A_n denote the mean value of detected positive and negative R-peak amplitudes, respectively. A channel may contain useful EKG if the noise stays either below the upper noise tolerance limit or above the lower noise tolerance limit. The noise tolerance limits are set so that signal with definitely too high noise level fails the test, but potentially useful signal always passes it. An example of a signal that passes the test is shown in Fig. 2.

On the second stage of the channel selection, a channel is discarded if the signal is physiologically unreasonable, which means that any of the following conditions is true:

- the mean value of the RR-intervals is less than 0.27 s (corresponds a heart rate of 222 bpm),
- any of the RR-intervals is less than 0.2 s,
- any of the RR-intervals is longer than 2.5 s,
- there is more than 2 s signal, which does not contain any R-peaks in the beginning or at the end of the 10-second period.
- the longest RR-interval is more than 166% of the average of the RR-intervals in the 10 second window,
- the standard deviation of the RR-intervals is more than 35% of their average value.

These conditions are not set to be strict since the heart rate may change widely between people.

If a useful signal is found in more than one channel, the best channel is chosen by calculating the ratio between the average of the R-peak amplitudes and the variance of the noise level (R-peakless grey curve in Fig. 2) and selecting the channel having the highest ratio. If no channel contains the signal of sufficient quality, the 10-second window is moved one second forward and the process is repeated.

C. Channel Re-selection Conditions

If the quality of the signal on the selected channel drops too much or if there is not found any R-peak, the channel has to be re-selected. When a channel change occurs, it is always marked as a break in the RR-series.

In a good-quality pre-processed signal, the noise level is small and relatively constant since the baseline is forced efficiently near zero by removing the median as described earlier while noisy signals have more variation due to incomplete removal of the wandering baseline. Thus, the increased signal variance in the interval between R-peaks in the pre-processed EKG is used as an indicator for channel, re-selection which is done if:

- the signal variance of the newest RR-interval (excluding the R-peaks) is more than 50% of the variance of the accepted signal (including the R-peaks) of the latest 4 seconds, or
- the same signal variance is more than 25% of the variance of the accepted signal (including R-peaks) during the latest 4 seconds and 4 times higher than the variance of the 4 most recent accepted RR-intervals (excluding R-peaks)

In addition, if the heart rate is significantly higher or lower than normally, stricter noise thresholds than aforementioned will be used to minimize the number of falsely detected R-peaks. In this case significantly lower or higher heart rate means that the RR-interval between the last accepted R-peak and R-peak candidate is shorter than 0.5 s or longer than 1.8 s. In such cases, the mean absolute difference of the pre-processed signal in that RR-interval will be also checked and compared with the maximum slope of the rising and falling edges of the QRS complex. This is done because the signal with poor quality varies a lot between successive R-peaks.

D. Heart Beat Detection

The R-peaks are detected for HR determination using Zhengzhong's method [22] as described shortly in section IV-B. The initial values of the positive and negative slope as well as the amplitude thresholds are inherited from the channel selection process. During the HR detection process, thresholds are continuously updated by averaging the eight newest values.

Due to short-term HRV and breathing, the duration of successive RR-intervals may vary significantly. If the period where the next R-peak is searched is too long, it would frequently cause cases in which R-peaks are skipped. On the other hand, if the interval for the next R-peak search is too short, a break would be caused to the RR-series since no R-peak is found within a given interval. For these reasons, the R-peak must be found within the window of 166% of the average of the 10 newest RR-intervals. The use of several previous RR-intervals instead of the single previous one prevents the effects of deviant RR-intervals but ensures still fast adaptivity. The window width is two seconds if less than five R-peaks have been found after the last channel re-selection since HR might have been significantly higher before than after channel re-selection.

Secondary amplitude thresholds are tried if the R-peak is not found within the given time interval. In such cases, 40% (instead of 60%) of the aforementioned amplitude mean value is used as a lower limit and 300% of the amplitude mean value is used as an upper limit. If successive R-peaks are found within short interval (smaller than 40% of the mean value of the 10 newest RR-intervals), another R-peak is tried to find before the end of the window under processing. If another R-peak is found, the first one is discarded as a noise peak, otherwise the process continues normally.

One problem is that we do not know if the R-peaks are negative or positive. If the absolute value of the negative threshold is at least 90% of the positive threshold and vice versa, peaks with both polarities are searched. If peaks with opposing polarities are detected within 200 ms, the first one is selected for HR calculation.

In R-peak detection, a fiducial point of each R-peak is marked where the pre-processed EKG curve reaches its local extremum. In order to obtain better temporal accuracy in R-peak detection [23], the 2^{nd} order polynomial is fitted to the set consisting of 3 points: the fiducial point and its two nearest sample points. After a 2^{nd} order polynomial interpolation, the location of the fitted curve peak value is saved as a refined R-peak location.

E. Heart Rate Post-Processing

A special post-processing method was implemented to decrease especially the false-positive (FP) R-peak detection rate and to distinguish ectopic beats from normal sinus beats. Since the channel re-selection always causes a break in the RR-series, there may be breaks in the RR-series although no heart beat is missed. During post-processing, also these unnecessary breaks in the RR-series are removed and two piecewise periods are combined.

1) Ectopic Beat Detection: Automatic EB detection could be done e.g. by examining the EKG morphology: QRS complex duration, R-peak amplitude, P-wave morphology, intervals between different EKG waveforms and utilizing the redundancy of different EKG leads. The utilization of P-wave morphology and intervals between different waveforms except

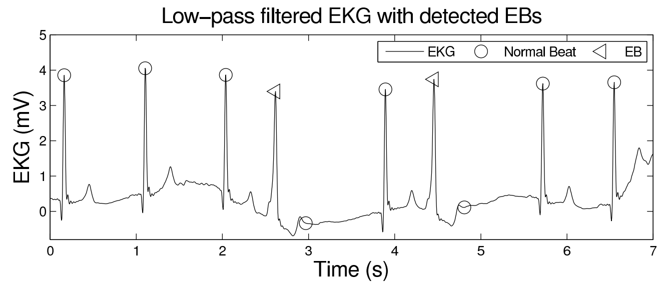

Fig. 3. An example of correctly detected ectopic beats (EBs) in low-pass filtered bed sheet EKG. Detected EBs are marked with a triangle. Circles on the baseline are the locations of corrected interpolated heart beats.

R-peaks are not suitable with the proposed system since the signal quality is not always good enough to detect these features.

Our EB detector prototype is based on the longer duration, different amplitude and abnormal temporal location of a QRS complex compared with the normal sinus rhythm. The QRS duration and R-peak amplitude are obtained during R-peak detection process whereas the locations of R-peaks are investigated during the post-processing stage. Since we have not had enough test subjects with cardiac arrhythmias, we are not able to claim that fully automatized EB detection is always possible for the signal obtained with textile electrodes. For that reason, we can only state that computer assisted EB detection would help the data analysis. An example of correctly detected EBs is seen in Fig. 3.

2) RR-series Correction: After EB detection, continuous RR series with less than 4 RR-intervals are discarded, since the quality of the signal is checked first time after five detected R-peaks. Next, the unnecessary breaks caused by channel re-selections are removed and the RR-series separated by such break are combined (Fig. 4) if

- the time difference between two R-peaks surrounding the break is less than 166% of mean value of all RR-intervals,
- the minimum interval between the three closest R-peaks on both sides of the break location is more than 0.27 s and
- the mean absolute deviation (MAD) of totally seven RR-intervals (three RR-intervals before and after the break and one is formed by removing the break) is less than 15% of the mean value of all RR-intervals.

With regard to the last-mentioned condition, the break will be removed also if the MAD of the RR-intervals between the last R-peak before the break location and first three R-peaks after the break location is less than 15% of the mean value of all RR-intervals. The limits above are set so that if noise peaks are detected as R-peaks just after or before channel re-selection, the break is not removed.

Since incorrectly detected extra R-peaks might appear especially before or after channel changes, the next step is to focus on a few nearest R-peaks surrounding the breaks in the R-peak sequence. If the MAD of the 2–7 successive RR-intervals is more than 20% of their local mean value or the minimum of those RR-intervals is less than 0.27 s, those peaks are deleted. In some cases, this operation removes correctly detected R-

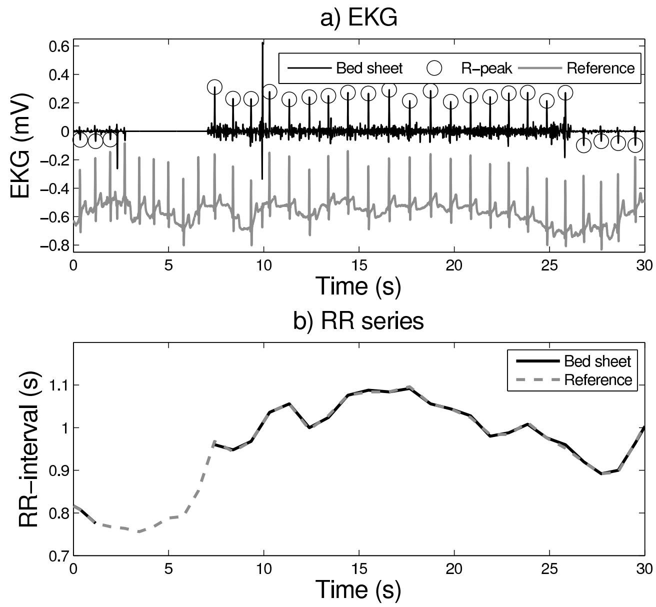

Fig. 4. (a) Bed sheet EKG and reference signal (offset by -0.5 mV) and (b) corresponding RR-series. Channel reselection process has been initiated at around 2 s and again at 26 s because of significant artefacts in the signal, causing two breaks to the RR-series. Between 2 s–7 s, the signal quality has been too low in all channels and a new channel has not been found immediately and missed R-peaks result an unremovable break in the RR-series between 2 s–7 s. At 26 s, a new channel with sufficient signal quality is found immediately and the break has been removed during HR post-processing.

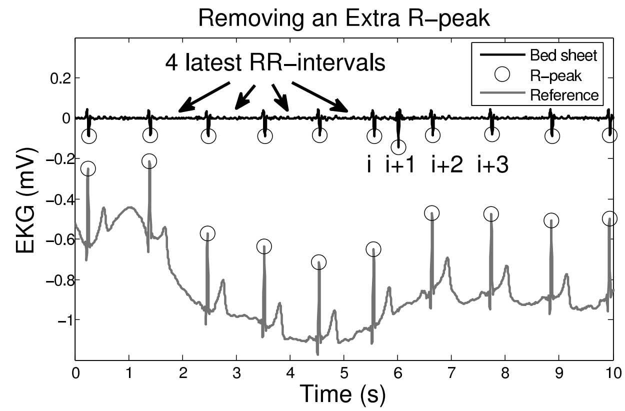

Fig. 5. Noise peak detection: The peak at index $i+1$ is determined to be a noise peak and will be removed.

peaks, but its benefits in decreasing the number of erroneously detected R-peaks are bigger than its disadvantages. Despite this operation, the HR detection coverages presented in Table I are still high.

In our tests, particular electrical devices caused waveforms resembling R-peaks. These RF interference (RFI) spikes might get detected as R-peaks as in Fig. 5. To reduce the false detections caused by the RFI transients, the average of the three smallest RR-intervals of R-peaks in the peak sequence at $[i-4, i]$ is calculated. If all the R-peaks in the peak sequence at $i, i+1$ and $i+2$ are found to be within 1.3 times the aforementioned average and the RR-interval between the R-peaks at $i+2$ and $i+3$ is more than 0.7 times that self-same average, the R-peak at $i{+}1$ or $i{+}2$ may be incorrectly detected (Fig. 5). An extra peak at $i+1$ or $i+2$ is removed so that the MAD of the RR-intervals between the R-peaks at $[i-4, i+2]$ minimizes. If the MAD of the RR-intervals between the R-peaks at $[i-4, i+2]$ is smaller without deleting one peak, then the peak is not discarded.

Next, two adjacent RR-intervals are compared with each other and if their length deviates too much (e.g. their MAD is more than 40% of their mean), those RR-intervals are discarded. This is done in order to find skipped heart beats and noise peaks that were not removed previously. For instance, if there were 2 adjacent RR-intervals whose MAD is 35% of their mean, there is one RR-interval which is over 2 times longer than the other one. Final step is to remove too short continuous RR-series and corresponding R-peaks because they are often from an erroneously selected channels.

F. HRV Frequency Domain Parameter Calculation

The standard HRV frequency domain analysis can be divided into two classes: the analysis of entire 24 h recordings and the analysis of short-term (5 min) recordings measured in physiologically stable conditions [23]. However, it is more practical in studies on HRV based sleep staging — like Devot *et al.* in [5] — to use 30-second epochs so that the results would be comparable with values obtained by traditional analysis of PSG. We computed frequency domain parameters with Welch's method using 30-second epochs, first removing the mean and interpolating RR-series with spline interpolation at the sampling frequency of 4 Hz [24].

V. Results and Discussion

The results of HR recognition performance are presented in Table I. The root mean square error (RMSE) for the RR-intervals has been calculated by comparing the values obtained by the bed sheet electrodes and the reference electrodes at those sections where both signals have been acquired.

The majority of the cases where the HR detection failed (heart beats were missed or detected wrongly), occur during the sleeping posture changes or during smaller movements. This information can however, be used in sleep quality analysis: a large amount of breaks in the EKG and RR-series may indicate nervous sleep.

As in [25], the time domain parameters of short time HRV, such as RMSSD (the square root of the mean squared differences of successive RR-intervals) and SDSD (the standard deviation of differences of successive RR-intervals) obtained from bed sheet electrodes are very close to the corresponding reference values. As a contrast, the standard deviation of all RR-intervals (SDRR) computed from the signal of the bed sheet electrodes differs more from the reference values. This is because of the movements cause an increase of HR and these parts are missed with the bed sheet because of the movement artefact.

The HR detection coverage for a single night was in most of our measurements significantly over 90%, with a range of 85.05%–98.98% and the average being an excellent 94.90%. Table I shows the average values for each test subject. The straightforward comparison between our results and some

TABLE I
THE RESULTS OF HR MEASUREMENTS FOR HEALTHY SUBJECTS.

Test Subject	Nights	Total length (h)	RMSE (ms)	HR Coverage (%)
A	10	72.39	2.52	97.05
B	8	58.08	5.31	96.55
C	4	26.98	3.80	97.02
D	6	56.37	6.46	89.43
Weighted average			4.48	94.90

TABLE II
THE RESULTS OF HRV MEASUREMENTS FOR HEALTHY SUBJECTS.

Test Subject	HRV Coverage (%)	Relative Mean Absolute Error (%)		
		LF	HF	LF/HF
A	91.90	0.76	4.78	3.23
B	88.32	0.89	2.56	1.66
C	89.42	0.71	1.24	0.90
D	72.80	1.15	5.44	2.06
Weighted average	85.59	0.89	3.90	2.20

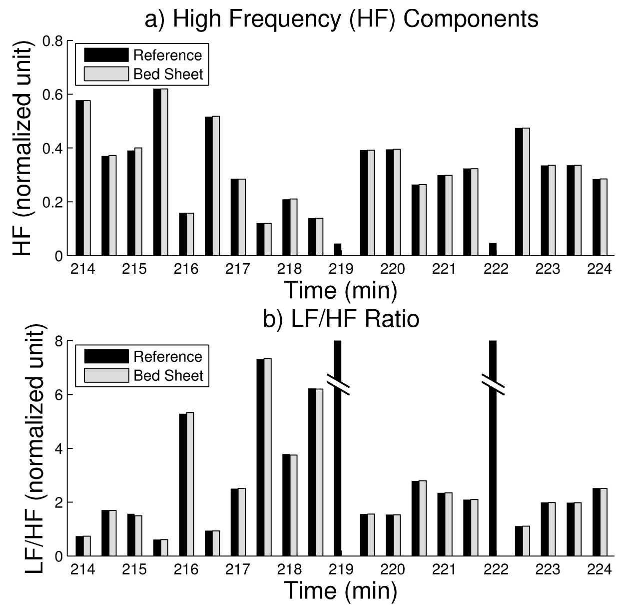

Fig. 6. (a) The magnitude of high frequency (HF) components in normalized units. (b) LF/HF ratio over a 10-minute period. The bed sheet EKG contains artefacts at 219 min and 222 min, resulting missing values.

other studies is not possible since error rates are expressed differently or the results are reported for shorter, non-over-night recordings. The HR detection coverage values we achieved are significantly higher than what has been reported by Devot *et al.* [5] (81.89%) and Ishijima *et al.* [4] (83%–93%). In addition to high coverages, the RMSE of RR-series was in low level varying 0.94 ms–10.57 ms with the weighted average of 4.48 ms. Corresponding RMSE in beat-to-beat HR signal varied between 0.10 bpm–0.58 bpm with the weighted average of 0.27 bpm.

While HR detection coverage is high, the single night coverage for HRV frequency domain parameters varies between 61.9%–96.6% with weighted average over all the nights of 85.6% (Table II) when 30-second windowing is used. The difference is explained by different initial requirements: In order to calculate HRV frequency domain parameters, a fixed-length (in this case 30 s) continuous RR-series is required whereas beat-to-beat HR can be obtained also for shorter continuous RR-series. Generally, the coverage percent is strongly dependent on the incidence of breaks in the EKG signal: if the signal of the whole night recording is heavily distorted, channel reselections and breaks in RR-series exist frequently. One method to improve these percent is the interpolation of RR-series when a short break occurs, but the reliability of the result with such method is not necessarily sufficient. Although, when the system is able to calculate frequency domain parameters of HRV, they are very often nearly identical compared to the reference signal as can be seen as small relative mean absolute errors in Table II and in Fig. 6.

As the error rates in Tables I and II show, higher error rate in HR detection does not necessary cause bigger error in HRV parameters. Because of noise peaks detected as extra R-peaks, in many cases the error in HF power is clearly more significant than the error in LF power.

In many cases, it is challenging to distinguish whether an abnormal peak is caused by interferences or an ectopic beat. In some cases the error rate is also slightly increased by EB detector since the marginal amount of false positive EBs occurred mostly when a noise spike was marked as EB and corrected wrongly instead of removing such one. Thus, the results can be improved by disabling the EB detector if it is known that the person does not suffer from these.

An example of the high frequency (HF) power and LF/HF ratios, calculated by using a 30-second windowing, are presented in Fig. 6 over a 10-minute period. In order to make the figure more readable, the magnitude of HF components has been normalized by calculating the ratio between the HF power and the remainder of total power and VLF power [23].

As can be seen from Figs. 2, 3, 4 and 5, the bed sheet EKG signal amplitude and quality vary widely depending on the sleeping posture and the electrode humidity level. As contrast to low signal levels shown on these plots, the R-peak amplitude may be also as high as 5 mV. The effect of dry electrodes can be seen as poor signal-to-noise ratio in Fig. 2: the test subject has just changed his position causing channel re-selection. We also observed that the location of the electrodes in the axial direction of the body may affect the quality of the signal, but this never caused problems if the bed sheet was set so that electrodes were initially at the correct location.

We have developed a novel unobtrusive night-time cardiac monitoring system consisting of small textile electrodes that are unnoticeable when lying on a bed. Despite the promising results, further development is required. For instance, the use of an additional mechanical movement sensor would help to distinguish artefact signal peaks from the actual R-peaks and help us to reduce the need for signal post-processing. The information on test subject's movements could prevent unnecessary breaks in such cases where the noise level is slightly too high, causing a channel re-selection although R-peak detection would still be possible. Additionally, this would provide information on the subject's respiration rate.

Acknowledgment

The authors would like to thank all voluntary test subjects for their contribution.

References

[1] A. Bulckaert, V. Exadaktylos, G. De Bruyne, B. Haex, E. De Valck, J. Wuyts, J. Verbraecken, and D. Berckmans, "Heart rate-based nighttime awakening detection," *European Journal of Applied Physiology*, vol. 109, no. 2, pp. 317–322, May 2010.

[2] M. Hall, R. Vasko, D. Buysse, H. Ombao, Q. Chen, J. D. Cashmere, D. Kupfer, and J. F. Thayer, "Acute stress affects heart rate variability during sleep," *Psychosomatic Medicine*, vol. 66, no. 1, pp. 56–62, Jan. 2004.

[3] T. Penzel, J. McNames, P. de Chazal, B. Raymond, A. Murray, and G. Moody, "Systematic comparison of different algorithms for apnoea detection based on electrocardiogram recordings," *Medical and Biological Engineering and Computing*, vol. 40, pp. 402–407, 2002.

[4] M. Ishijima, "Cardiopulmonary monitoring by textile electrodes without subject-awareness of being monitored," *Medical and Biological Engineering and Computing*, vol. 35, no. 6, pp. 685–690, Nov. 1997.

[5] S. Devot, A. Bianchi, E. Naujokat, M. Mendez, A. Brauers, and S. Cerutti, "Sleep monitoring through a textile recording system," in *Engineering in Medicine and Biology Society, 2007. EMBS 2007. 29th Annual International Conference of the IEEE*, Aug. 2007, pp. 2560 – 2563.

[6] Y. G. Lim, K. K. Kim, and K. S. Park, "Ecg recording on a bed during sleep without direct skin-contact," *Biomedical Engineering, IEEE Transactions on*, vol. 54, no. 4, pp. 718–725, Apr. 2007.

[7] K.-f. Wu and Y.-t. Zhang, "Contactless and continuous monitoring of heart electric activities through clothes on a sleeping bed," in *Information Technology and Applications in Biomedicine, 2008. ITAB 2008. International Conference on*, May 2008, pp. 282–285.

[8] S. Ishida, N. Shiozawa, Y. Fujiwara, and M. Makikawa, "Electrocardiogram measurement during sleep with wearing clothes using capacitively-coupled electrodes," in *Engineering in Medicine and Biology Society, 2007. EMBS 2007. 29th Annual International Conference of the IEEE*, Aug. 2007, pp. 2647 –2650.

[9] M. Wong, H. Leung, E. Pickwell-MacPherson, W. Gu, and Y. Zhang, "Contactless recording of photoplethysmogram on a sleeping bed," in *Engineering in Medicine and Biology Society, 2009. EMBC 2009. Annual International Conference of the IEEE*, sept. 2009, pp. 907–910.

[10] J. Kortelainen, M. Mendez, A. Bianchi, M. Matteucci, and S. Cerutti, "Sleep staging based on signals acquired through bed sensor," *Information Technology in Biomedicine, IEEE Transactions on*, vol. 14, no. 3, pp. 776 –785, May 2010.

[11] J. Paalasmaa, "A respiratory latent variable model for mechanically measured heartbeats," *Physiological Measurement*, vol. 31, no. 10, pp. 1331–1344, Oct. 2010.

[12] Finsor, dynamic force sensor, http://www.finsor.com/en_US/, cited 14.6.2011.

[13] X. Zhu, W. Chen, T. Nemoto, Y. Kanemitsu, K. Kitamura, and K. Yamakoshi, "Accurate determination of respiratory rhythm and pulse rate using an under-pillow sensor based on wavelet transformation," in *Engineering in Medicine and Biology Society, 2005. IEEE-EMBS 2005. 27th Annual International Conference of the*, Jan. 2005, pp. 5869 –5872.

[14] S. Okada, Y. Fujiwara, M. Yasuda, Y. Ohno, and M. Makikawa, "Non-restrictive heart rate monitoring using an acceleration sensor," in *Engineering in Medicine and Biology Society, 2006. EMBS '06. 28th Annual International Conference of the IEEE*, Aug.–Sep. 2006, pp. 5093 –5096.

[15] R. J. Simpson Jr, W. E. Cascio, P. J. Schreiner, R. S. Crow, P. M. Rautaharju, and G. Heiss, "Prevalence of premature ventricular contractions in a population of african american and white men and women: The atherosclerosis risk in communities (aric) study," *American Heart Journal*, vol. 143, no. 3, pp. 535 – 540, 2002.

[16] S. Elsenbruch, M. J. Harnish, and W. C. Orr, "Heart rate variability during waking and sleep in healthy males and females." *Sleep (Rochester)*, vol. 22, pp. 1067–1071, 1999.

[17] K. Kesper, S. Canisius, T. Penzel, T. Ploch, and W. Cassel, "Ecg signal analysis for the assessment of sleep-disordered breathing and sleep pattern," *Medical and Biological Engineering and Computing*, pp. 1–10, 2012.

[18] S. Telser, M. Staudacher, B. Hennig, Y. Ploner, A. Amann, H. Hinterhuber, and M. Ritsch-Marte, "Temporally resolved fluctuation analysis of sleep ecg," *Journal of Biological Physics*, vol. 33, pp. 19–33, 2007.

[19] T. Young, P. Peppard, M. Palta, K. M. Hla, L. Finn, B. Morgan, and J. Skatrud, "Population-based study of sleep-disordered breathing as a risk factor for hypertension," *Arch Intern Med*, vol. 157, no. 15, pp. 1746–1752, 1997.

[20] J. Rosell, J. Colominas, P. Riu, R. Pallas-Areny, and J. Webster, "Skin impedance from 1 hz to 1 mhz," *Biomedical Engineering, IEEE Transactions on*, vol. 35, no. 8, pp. 649 –651, aug. 1988.

[21] L. Keselbrener, M. Keselbrener, and S. Akselrod, "Nonlinear high pass filter for r-wave detection in ecg signal," *Medical Engineering & Physics*, vol. 19, no. 5, pp. 481 – 484, Jul. 1997.

[22] G. Zhengzhong, K. Fanxue, and Z. Xu, "Accurate and rapid qrs detection for intelligent ecg monitor," in *Measuring Technology and Mechatronics Automation (ICMTMA), 2011 Third International Conference on*, Jan. 2011, pp. 298 –301.

[23] Task Force of the European Society of Cardiology the North American Society of Pacing Electrophysiology, "Heart rate variability : Standards of measurement, physiological interpretation, and clinical use," *Circulation*, vol. 93, no. 5, pp. 1043–1065, 1996.

[24] D. Singh, K. Vinod, and S. Saxena, "Sampling frequency of the rr interval time series for spectral analysis of heart rate variability," *Journal of Medical Engineering & Technology*, vol. 28, no. 6, pp. 263–272, 2004.

[25] M. Peltokangas, J. Verho, and A. Vehkaoja, "Unobtrusive night-time ekg and hrv monitoring system," in *Biomedical Engineering, 2011 10th International Workshop on*, Oct. 2011, pp. 1–5.

Mikko Peltokangas received his B.Sc. degree in biotechnology program from Tampere University of Technology (TUT), Tampere, Finland, in 2011. His research interests lie in biomeasurements, human measurements and microsystem technology. He is currently working as a research assistant at the Department of Automation Science and Engineering, TUT.

Antti Vehkaoja received his M.Sc. degree in electrical engineering from Tampere University of Technology (TUT), Tampere, Finland, in 2004. He is currently working as a teaching associate in the Department of Automation Science and Engineering, TUT and working toward the Ph.D. degree as a member of the Sensor Technology Research Group. His current research interests include sensors and measurement systems for physiological monitoring and processing of physiological signals.

Jarmo Verho is working as a research assistant at the Department of Automation Science and Engineering, Tampere University of Technology. He is specialized in low-noise electronics design and embedded systems. His other research interests include sensor networks, radio networks, short range inductive links and capacitive sensing techniques.

Publication II

Vehkaoja, A., Rajala, S., Kumpulainen, P., and Lekkala, J., “Correlation approach for the detection of the heart beat intervals by using bed integrated force sensors,” *Journal of Medical Engineering & Technology*, vol. 37, no. 5, pp. 327–333, July 2013.

JOURNAL OF
Medical Engineering &Technology

http://informahealthcare.com/jmt
ISSN: 0309-1902 (print), 1464-522X (electronic)

J Med Eng Technol, 2013; 37(5): 327–333
 DOI: 10.3109/03091902.2013.807523

informa healthcare

INNOVATION

Correlation approach for the detection of the heartbeat intervals using force sensors placed under the bed posts

Antti Vehkaoja*, Satu Rajala, Pekka Kumpulainen, and Jukka Lekkala

Department of Automation Science and Engineering, Tampere University of Technology, Korkeakoulunkatu 3, 33720, Tampere, Finland

Abstract

This study proposes a method for detecting the heartbeat intervals of a person lying on a bed from ballistocardiographic signals recorded unobtrusively with four dynamic force sensors located under the bed posts. The method does not recognize individual heartbeats, but the intervals where the correlation between two consecutive signal segments maximizes. This study evaluated the performance of the method with nine subjects in 1-h long recordings and achieved 91% beat-to-beat interval (BBI) recognition coverage; 98.6% of the detected BBIs differed less than 50 ms from the values calculated from a reference electrocardiogram signal. This study also evaluated the reliability of two parameters of heart rate variability that have been used in sleep quality assessment in several studies and are usually calculated for 30 s epochs. The results suggest that the method is able to provide sufficient reliability for using the data in evaluation of sleep quality.

Keywords

Ballistocardiogram, night-time physiological monitoring, Unobtrusive heart rate

History

Received 14 January 2013
Revised 14 May 2013
Accepted 14 May 2013

1. Introduction and motivation

Night-time physiological signals have traditionally been measured and used only for medical purposes in diagnosing sleep-related disorders like sleep apnoea or insomnia. An obvious reason behind this has been the lack of methods for collecting the information unobtrusively and that the value of the information has not been found high enough compared with the added discomfort of using wearable sensors. Therefore, the unobtrusive and continuous acquisition of night-time physiological parameters is an enabler for interesting and useful applications for different situations of life. Applications for the night time heart rate (HR) and the heart rate variability (HRV) information are found in a purely medical domain, e.g. sleep research [1] and sleep apnoea monitoring [2,3], and wellness domain, e.g. monitoring of sleep quality [4] and psychophysiological stress monitoring [5]. The use of the HRV information, for example in sleep staging, is based on the autonomous nervous system's (ANS) regulation of heart rate. Decreased parasympathetic activity of the ANS has been shown to indicate rapid eye movement (REM) sleep state [6] and it can be seen in HRV as the decreased relative power of the higher frequency components of the power density spectrum.

In medical applications, polysomnography is used as the golden standard for collecting data and evaluating the medical condition of the patient because it is considered to produce the most reliable analysis results. Its drawback is that it is normally recorded only during a single night; thus, not providing longitudinal data. Furthermore, the multiple sensors installed all over the body may affect the sleep. Actigraphy measured using wrist mounted accelerometers has been used as a standard method for collecting sleep-related longitudinal data for medical assessment. The information and its reliability is, however, limited [7].

Unobtrusive methods for monitoring physiological information with sensors installed into the bed make the wellness-related applications viable in practice and potentially improve the reliability and information content of the longitudinal data used in medical assessment compared to the currently used actigraphy method. For example, people with diseases like sleep apnoea or arrhythmias could monitor their health status more accurately than currently by using the new technology.

2. Related work

2.1. Methods for unobtrusive night-time physiological monitoring

Several methods have been developed and published for unobtrusive night-time monitoring of physiological parameters that rely on piezoelectric force sensors installed on top of or into the mattress of the bed. These methods measure the HR through a ballistocardiogram (BCG), which is the mechanical signal caused by the movement of blood due to the heart contraction. In the early 1980s, Alihanka *et al*. [8] published a method of using a static charge-sensitive-bed (SCSB) for measuring the physiological parameters of a person during sleep. More recently, piezoelectric polymer

Corresponding author. Email: antti.vehkaoja@tut.fi

polyvinylidenefluoride (PVDF) has been widely used as a sensor material in applications of this kind. For instance, Niizeki *et al*. [9] utilized a PVDF cable sensor to detect the respiratory activity and the ballistic movement of the body due to the heartbeat. The cable sensors were located horizontally along the bed surface covering the upper half of the subject's body. Jacobs *et al*. [10] developed a PVDF sensor array to extract heart and respiratory rates. Their sensor was placed under the sheets of a hospital bed. When a patient lies on the bed, the sensor detects the pressure waves generated by heart beating and breathing. A similar method but only one PVDF sensor element was also used by Wang *et al*. [11]. Kortelainen *et al*. [12] used a pressure sensitive mattress that included as much as 160 sensor elements in their research that focused on sleep staging based on physiological parameters. The sensing elements of their mattress were fabricated from permanently charged electret polymer material called EMFi (Electro Mechanical Film) [13].

Other sensor types besides the piezoelectric and electret mattress sensors have also been developed for monitoring the ballistographic forces. Brüser *et al*. [13] used strain gauges in a Wheatstone bridge configuration attached to the slat under the mattress of a hospital bed. Chee *et al*. [14] developed an air mattress system for the unconstrained measurement of respiration and heartbeat movement. Tanaka *et al.* [15] proposed a home healthcare system that utilizes a phonocardiographic sensor installed on an air-mat or water-mat for measuring heartbeat and respiration periods. An unconstrained method for long-term monitoring of heart and breathing rates during sleep was proposed also by Chen *et al*. [16]. Their sensor unit that consisted of two waterfilled tubes and pressure sensors was installed underneath a pillow to pick up the pressure variations from the head induced by inhalation/exhalation and heart pulsation during sleep. Brink *et al*. [17] developed a method for tracing body movements, respiration and heart action of a person at rest or asleep on a bed using four high-resolution force sensors installed under the bedposts. The sensors were based on the optical detection of beam deflection. The strength of their method is the measurement of static force in addition to the dynamic force, which enables also tracking of body position in the bed. We are also using force sensors installed under the bed posts, but the sensors we are using are significantly simpler and they measure only the dynamic component of the force.

2.2. Algorithms for heartbeat detection

Various signal processing techniques have been developed to detect beat-to-beat intervals from BCG signals.

The method developed by Paalasmaa and Ranta [18] is based on forming morphological feature vectors starting at the locations of every possible heartbeat, i.e. from the local maxima in the BCG signal. The 30 sample long feature vectors are formed by down-sampling the original signal to 25 ms sample intervals. Beat-to-beat intervals are then found by forming clusters of similar vectors and selecting the densest cluster whose members are the most similar to represent the heart beats. The assumption is that the best matching feature vectors correspond to heartbeats. The strength of their method is the really high specificity. Only 0.09% of the detected heartbeats were more than 50 ms apart from the actual heartbeat in the study reported by Paalasmaa and Ranta [18].

Another interesting method for heartbeat detection from the BCG signal has been developed by Kortelainen *et al*. [12]. Their method is based on using cepstra, which are the inverse Fourier transforms of the logarithm of spectra. Heartbeat frequency and its harmonics form a peak into the cepstrum at the time point that corresponds to the time interval of two heartbeats. They used averaging of multiple measurement channels in order to reduce the variance of cepstra and improve the accuracy of the method. Their Matsense sensor includes 160 channels in total, but they were able to achieve 1.1% relative heartbeat interval error when only eight measurement channels were used [12].

Wang *et al*. [11] used wavelet decomposition in pre-processing the BCG signal and a smoothed square of a certain wavelet component to highlight the heartbeat complexes, which were then recognized by adaptive thresholding. Mack *et al*. [19] used an adaptive threshold and varying search window length in the detection of the HIJK complexes of the BCG produced by each heartbeat. Their focus was on finding representative heart rate values for 30-s epochs and, therefore, did not report the accuracy of finding individual heartbeat intervals.

Jansen *et al*. [20] used the cross-correlation of the hand-selected BCG sample and the signal recorded with Static Charge Sensitive Bed (SCSB) in heart rate detection already in 1991. Using a single template, however, does not provide good results at least with our sensor set-up due to the large variation in the signal waveforms, as seen in Figure 1.

Our approach is based on the calculation of the correlation as well but we do not use a static template. We calculate the correlation between two consecutive signal segments. Thus, our method does not try to find out any particular waveform in the signal, but the maximum similarity in the signal that

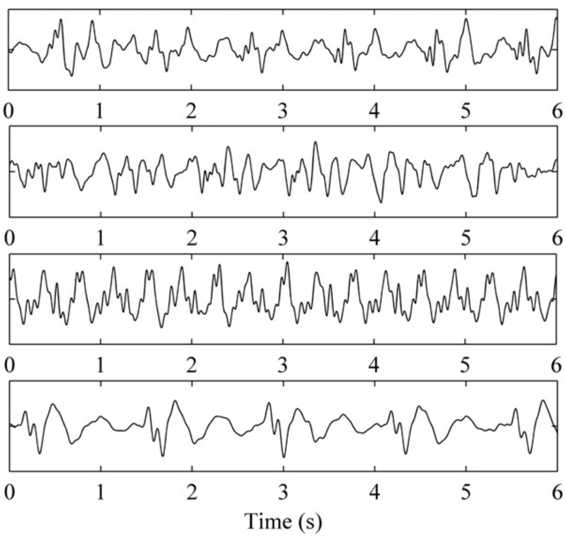

Figure 1. Examples of different BCG signal waveforms acquired with our bed post sensor system. Due to large variation in signal shape, methods that make assumptions about the waveform do not necessarily perform well.

repeats with the same rate as the normal heartbeat at rest. The aim of our study is to show that the parameters used for the evaluation of sleep, which are normally derived by first finding the individual heartbeat locations and then calculating the BBI signal, can be calculated with similar accuracy also from the heartbeat interval signal where the single heartbeats are not detected.

3. Materials and methods

3.1. Test subjects

We tested our heart rate measurement method with nine subjects (four females and five males). The subjects were healthy adults with no history of cardiac or sleep-related problems. The data were collected during 1 h from each subject. Most subjects fell asleep during the measurement. Characteristics of the subjects are shown in Table 1.

3.2. Measurement set-up

Our measurement system consists of a bed with four force sensitive film sensors located under the bed posts, signal conditioning and data acquisition hardware and a computer for the data collection and analysis. The reference heart rate is calculated from the electrocardiogram (ECG) signal recorded using disposable Ag/AgCl gel electrodes attached on the chest and a custom-made ECG amplifier.

We used sensors made of EMFi material for measuring the ballistographic forces exerted by heartbeat and breathing functions to the bed. EMFi is a thin polypropylene (PP) film having a special cellular structure. The internal cellular structure is made by stretching the PP film preform during manufacturing both in longitudinal and transversal directions. The film is charged permanently with a corona discharge method and metalized on both sides to provide electrodes. EMFi is sensitive to dynamic forces exerted in perpendicular direction to its surface. The sensitivity of the sensors used in the study is 20 pC/N in perpendicular direction, but only ~1% of that in the lateral direction. The charge generation results from the change of the internal electric field due to change of the thickness of the sensor, as force is applied to it. The sensors used were made by Emfit Ltd. (Vaajakoski, Finland) [21,22].

The main component of the ballistocardiographic signal is the recoil force that results when the left ventricle of the heart presses the blood into the aorta. The direction of this force component is approximately the same as the longitudinal direction of the torso. The mechanics of the bed, however, translate the direction of the force so that it can be detected as a vertical force with sensors placed under the bed posts.

Table 1. Characteristics of the test subjects.

	Male	Female
No. of subjects	5	4
Age (years)	33.2 (24–44)	30.2 (25–40)
Height (cm)	178.0 (173–183)	167.4 (159–177)
Body mass (kg)	82.4 (69–91)	64.6 (57–76)
BMI (kg/m^2)	26.0 (21.8–28.4)	23.2 (19.5–30.1)

Values are presented as mean with the range in parentheses.
BMI: Body Mass Index.

We used a non-inverting voltage amplifier connection in conditioning the force sensor signals. The high-pass cut-off frequency was set to 0.15 Hz by placing a 100 MΩ resistor and a 10 nF capacitor in parallel with the sensing element, whose internal capacitance was measured to be slightly less than 1 nF. The low cut-off frequency guarantees that the essential components of the BCG and breathing signals are in the pass band. The amplifier has a voltage gain of 100, which, together with the overall 11 nF capacitance, set the voltage sensitivity to ~180 mV/N. First-order low-pass filter with 30 Hz cut-off was used to supress the high frequency noise and prevent aliasing.

A 16-bit custom made data acquisition card connected to PC through a USB was used for collecting the data. The card is able to measure a maximum of eight single-ended channels with adjustable sample frequency; 200 Hz sampling frequency was used in the measurements. Three minutes of data were removed from the beginning and the end of the recordings before further signal processing in order to remove the data recorded when the person who was using the measurement equipment was present in the room, possibly disturbing the test person.

3.3. Reference RRI detection

For calculating the reference HR values from the ECG signal we first used a simple descending slope detector with an adaptive threshold to find the rough R-peak locations. The simple slope detector offered 100% sensitivity and selectivity in most recordings and the errors were manually corrected. In order to gain more accurate R–R-intervals to be used as a reference we used polynomial fitting for finding sub-sample interval peak locations.

4. Signal processing

Most of the methods developed earlier for heart rate detection from BCG signals recognize the temporal locations of the heartbeats and are, therefore, able to report the individual heartbeats along with the beat-to-beat intervals. Reliable recognition of individual heartbeats from the signals recorded with our system is difficult because the signal waveforms vary very much between subjects, sleeping posture, the exact position in the bed, bed type and the sensor location, as shown in Figure 1. Our approach does not try to find individual heartbeats but produces an equally spaced signal containing the intervals of repetitive components in the signal. Our assumption is that the dominant component that repeats in 0.5–1.5 s time intervals originates from the heartbeat.

The applications where night-time BBI information is exploited do not generally require exact information of the beat location. The frequency domain parameters of HRV, for example, are commonly used in sleep staging [12,23]. In order to calculate the power density spectrum, also signals that originally contain the temporal information of heartbeat location need to be interpolated into a constant sample interval.

4.1. Force signal pre-processing

Because the measurement method is sensitive to the force variations it equally measures signals caused by breathing, heartbeat and movements of the person. The signal caused by the movement is often dominant and over-runs the BCG and breathing-related components and even saturates the amplifier that is adjusted for the low amplitude BCG signal. Therefore, the BCG and breathing signals are often temporarily lost during movements. However, the amount and magnitude of the movements can be used in monitoring of the sleep-related restlessness and sleep rhythm similarly as in wrist actigraphy monitoring.

We distinguish the larger movements simply by applying a threshold value to the edges of the linear region of the amplifier, i.e. close to the minimum and maximum values of the analogue-to-digital converter. When the signal of any channel exceeds the threshold, 2 s of data is removed from all channels around it in order to let the amplifier recover from the saturation and to remove the ringing caused by the low-pass filter after the step-like change in the input.

Because the information content of the BCG signal lies on the low frequencies, the signal is digitally low-pass filtered from 20 Hz to minimize the disturbance caused, e.g. by the power line interference. Discrete difference is then taken from the signal. This brings out the higher frequency BCG waveforms and suppresses slowly varying components. Because of the discrete difference, a separate high-pass filtering is not needed.

4.2. BBI detection algorithm

Our BBI detection algorithm is based on finding repetitive signal waveforms by forming a correlation function (Equation 1) of two consecutive signal segments and finding the delay that produces maximum correlation:

$$\rho_{xy}(\tau) = \frac{\frac{1}{N}\sum_{t=1}^{N}(x_t - \mu_x)(y_{t+\tau} - \mu_y)}{\sigma_x \sigma_y}, \qquad (1)$$

where x and y are the two consecutive signal segments of length N, μ_x and μ_y are the mean values of the segments and σ_x and σ_y are the corresponding standard deviations. Correlation ρ_{xy} is calculated for delay values τ. Figure 2 shows an example of a high quality BCG signal's discrete difference and the correlation function calculated from the two signal segments separated with vertical dash lines.

In the ideal case, the lengths of the segments are equal to the beat-to-beat interval and, therefore, the correlation is calculated with different segment lengths. We have used segment lengths of 0.5–1.5 s with steps of 0.1 s, which correspond to heart rates between 40 beats per minute (bpm)–120 bpm. The maximum is searched from the delay interval that corresponds to the aforementioned heart rate values. The maximum value of the correlation function, max(ρ_{xy}), as well as its temporal location τ, which corresponds to the beat-to-beat interval is then stored.

The correlation maximums are calculated in steps of 0.5 s producing an equally spaced beat-to-beat interval vector and the same procedure is repeated for all four sensors. This results in an array consisting of four times eleven (four sensors, 11 segment lengths) correlation values for each step value. Finally, the median of the five highest correlation values is selected as the BBI. A hard limit is set empirically to

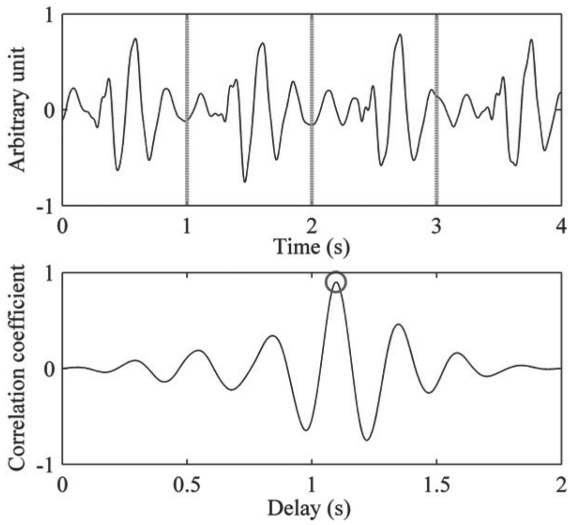

Figure 2. Upper figure shows an example of the discrete difference of a good quality BCG signal from one force sensor. The signal is cut from the vertical lines into two one second segments (1–2 s and 2–3 s) and correlation function is calculated between them. Lower figure shows the resulting correlation function. Maximum correlation is searched from the region that corresponds with physiologically reasonable beat-to-beat interval values.

0.75 for the correlation coefficients taken into account when calculating the median BBI. This prevents random BBI values from the sections, where the actual BCG signal is not present in the signal (strong movements or absence of the test subject).

4.3. BBI signal post-processing

After calculating the BBI signal it is further processed in order to minimize the number of false detections and increase the length of continuously detected BBI sequences. The latter is important, especially when calculating HRV power density spectra. For this reason we chose to allow single values being missed in the BBI detection. The single missing BBI values are filled with the mean value of the preceding and following BBIs.

There are also cases where only one or two consecutive BBI values have been detected. In these cases, the values are discarded because the missing BBIs indicate that the BCG signal is not stable and the sparse values are more likely to be incorrect than values in continuously detected BBI signal.

The third case in post-processing is when there exists a single spike in continuous BBI signal that differs more than 100 ms from the values around it and is clearly an outlier. In these cases the value is replaced with the average of the two surrounding BBI values.

5. Results and discussion

5.1. Beat-to-beat interval detection

Table 2 shows the HR and HRV detection performance characteristics of our correlation based BBI detection algorithm with nine test subjects.

The average BBI recognition coverage is 96.2%, when an average of 5.4% of the signal was first removed due to

Table 2. BBI recognition performance characteristics.

Subject number	Recognition coverage (%)	<50 ms error (%)	RRI-BBI RMSE (ms)	RRI-BBI MAE (%)	Epoch median HR error (bpm)	Distorted signal (%)
1	97.3	99.8	8.0	0.52	0.27	2.1
2	96.6	94.2	31.8	1.51	0.85	3.6
3	86.4	99.9	7.1	0.42	0.32	4.4
4	93.9	97.9	20.3	1.08	0.71	10.8
5	95.4	99.0	14.0	0.90	0.65	8.1
6	98.2	97.8	25.6	1.03	0.84	10.4
7	99.2	99.5	10.6	0.80	0.32	1.9
8	99.5	99.2	19.3	0.77	0.40	3.0
9	99.2	99.8	11.1	0.85	0.33	3.8
Average	96.2	98.6	16.4	0.88	0.52	5.4

<50 ms error, relative share of the detected BBI values that differ less than 50 ms from the corresponding reference RRI values; RRI-BBI RMSE, root-mean-square error of the RRI and BBI signals calculated from the reference ECG and BCG; RRI-BBI MAE, relative mean absolute error of the RRI and BBI signals calculated from the reference ECG and BCG; Epoch median HR error, average absolute error of median heart rates calculated for 30 s epochs.

extensive movements. Altogether 91.0% of the time in bed was, thus, covered by the algorithm. An average of 98.5% of the detected BBI values are within 50 ms of the corresponding RRI values calculated from the reference ECG signal and interpolated into 0.5 s sample intervals. Fifty millisecond differences were used by Paalasmaa and Ranta [18] for evaluating the correctness of the BBI detection and it gives a good estimate on the amount of coarse detection errors. The RRIs used in the comparison are interpolated into the same 0.5 s sample interval as BBIs from the original RRI signal.

The average root mean square error of the detected BBIs varies between 7.1–31.8 ms between the subjects, the average being 16.5 ms. The relative mean absolute error (MAE) varies between 0.42–1.51%, the average being at 0.90%, which is slightly smaller than the 1.1% error achieved by Kortelainen *et al*. [12]. They had achieved MAE as low as 0.4% when using all sensors of their system [24], but they stated that the 1.1% error was still at an acceptable level for sleep stage classification. In their measurements the average heartbeat detection coverage was 88%. The method developed by Brüser *et al*. [13] gave 1.79% MAE.

We also evaluated the accuracy of the algorithm in reporting heart rate related parameters in 30 se epochs. A 30 s median heart rate was successfully used by Mack *et al*. [25] for sleep staging. Our algorithm showed 0.52 bpm mean absolute error for median epoch HR when only epochs with at least 2/3 of successfully detected BBI values were taken into consideration. This rule excluded an average of 6.7% of the epochs from the whole measurement time. A median per-epoch BBI signal from one recording is shown as an example in Figure 3, together with the median of the reference RRI. As seen from the figure, median BBIs are missing from those epochs where the median RRI is low. The reason is that there has been movement present during those epochs, which increased the HR. Otherwise the median BBIs follow the reference median RRI values well. Epoch-wise standard deviation of BBI values (STDBBI) is another possible parameter for sleep assessment. The average error of STDBBI varied between 2.8–11.5% between the subjects. STDBBI was calculated only for those epochs, which contained all BBI values.

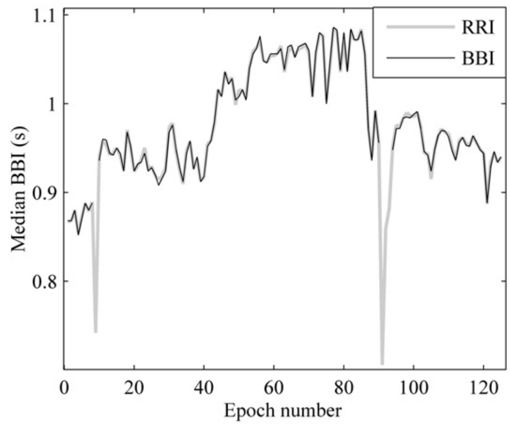

Figure 3. Median BBI and RRI calculated for 30 s epochs. Median BBI is calculated only if less than 1/3 of the BBI values are missing from that epoch. Epochs with lower median BBI usually include movements and are, therefore, more likely to be missed by the BCG-based monitoring system.

5.2. Frequency domain HRV parameters

Some authors have used the distribution of the HRV spectral power into different frequency bands in detecting sleep stages, e.g. Busek *et al*. [23]. Generally, the HRV spectrum is divided into very low frequency (VLF, <0.04 Hz), low frequency (LF, 0.04–0.15 Hz), and high frequency (HF, 0.15–0.4 Hz) bands whose spectral powers vary in different sleep stages.

BBI signals' power density spectra estimates were calculated using the fast Fourier transform method for those 30 s epochs, which did not contain missing BBI values. On average, 61.2% of all epochs in the nine measurements included all BBI values. The BBI signal of subject number 4 included a lot of short sections of missing BBIs, which caused the full epoch recognition coverage to drop to 24.3%. Figure 4 shows two examples of the BBI time series in 30 s epochs along with their power density spectra and corresponding RRI references.

The relation between power in the LF band and HF band was computed and compared with the reference value calculated from the corresponding RRI signal. An example of low and high frequency power relation calculated from

J Med Eng Technol, 2013; 37(5): 327–333

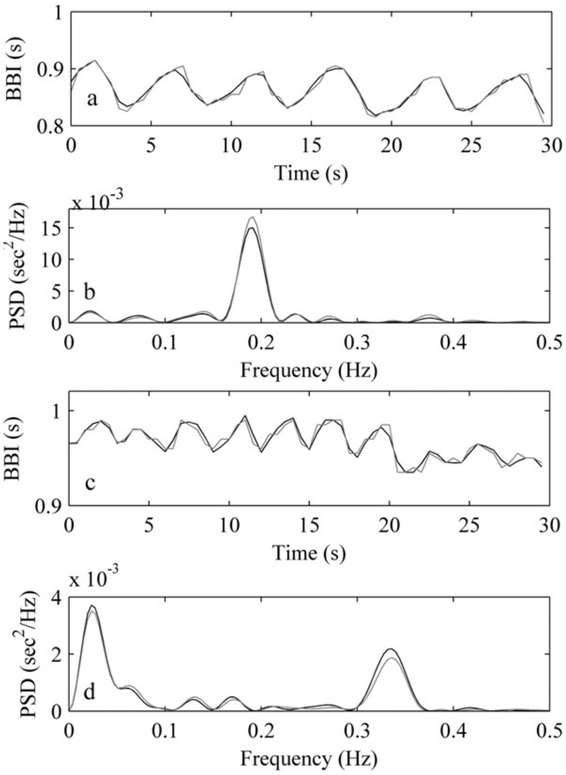

Figure 4. Two examples of BBI signals in 30 s epochs (grey) with corresponding RRI references (black); (a) and (c), and their PSDs calculated using FFT; (b) and (d). The time domain signals as well as the PSDs in these examples correspond well with each other.

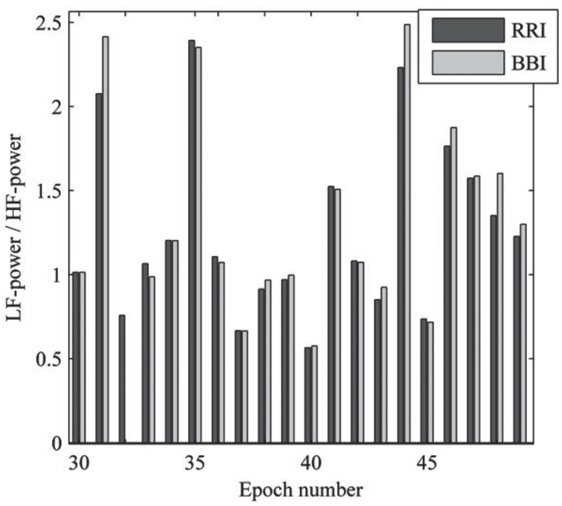

Figure 5. An example of LF/HF power ratio of BBI signal calculated for 30-s epochs compared with the reference value received from ECG-based RRI signal. The LF/HF-ratio is calculated only for the epochs that contain all BBI values.

RRI and BBI signals in 30 s epochs is shown in Figure 5. The LF/HF value calculated from the BBI signal complies with the reference fairly well most of the time, but in some cases the difference is significant because even only one erroneously detected BBI value can change the power spectrum and LF/HF-ratio dramatically. The average relative error of LF/HF-ratio varied between 5.4–14.7% between subjects, as seen in Table 3.

Table 3. Error of commonly used HRV parameters.

Subject number	Epoch total power error (%)	Epoch LF/HF power error (%)	Epoch STDBBI error (%)	Full epoch recognition (%)
1	3.7	6.6	5.1	66.7
2	5.4	7.9	7.2	57.3
3	6.7	10.6	9.2	55.9
4	3.8	8.2	3.2	24.3
5	3.0	6.4	2.8	50.8
6	7.1	13.6	5.4	52.6
7	3.6	5.4	3.9	81.1
8	7.3	11.0	5.7	81.2
9	14.2	14.7	11.5	80.8
Average	6.1	9.4	6.0	61.2

Epoch total power error, average absolute error of total power (0.04–0.4 Hz) of BBI signal calculated for 30 s epochs; Epoch LF/HF power error, average absolute error of low frequency/high frequency power ratios calculated for 30 s epochs; Epoch STDBBI error, average absolute error of beat-to-beat intervals standard deviation calculated for 30 s epochs.

6. Conclusions

We have presented a method for recognizing the heartbeat intervals of a person lying on a bed from signals recorded unobtrusively using dynamic force sensors under four bed posts. Even though our algorithm does not find the exact locations of individual heartbeats, the information it produces, an equally spaced BBI signal, can be used for example in calculating frequency domain HRV parameters that are most frequently used in the evaluation of the sleep quality. The BBI recognition coverage achieved with our method is similar to what is achieved in other studies. In addition, the accuracy of the detected BBI values is better than in some studies where the BBI information has been successfully used in sleep staging.

Acknowledgements

The authors would like to thank the volunteers participated in the test measurements. The work was partially funded by the Finnish Funding Agency for Technology and Innovation (TEKES) as a part of the project Monitoring and treatment of obesity-related sleeping disorders.

Declaration of interest

The authors report no conflicts of interest. The authors alone are responsible for the content and writing of the paper.

References

1. Burr, R.L., 2007, Interpretation of normalized spectral heart rate variability indices in sleep research: A critical review. *Sleep*, **30**, 913–919.
2. Roche, F., Gaspoz, J.-M., Court-Fortune, I., Pascal, M., Pichot, V., Duverney, D., Costes, F., Lacour, J.-R., and Barthélémy, J.-C., 1999, Screening of obstructive sleep apnea syndrome by heart rate variability analysis. *Circulation*, **100**, 1411–1415.
3. Ayas, N., Pittman, S., MacDonald, M., and White, D., 2003, Assessment of a wrist-worn device in the detection of obstructive sleep apnea. *Sleep Medicine*, **4**, 435–442.
4. Bulckaert, A., Exadaktylos, V., De Bruyne, G., Haex, B., De Valck, E., Wuyts, J., Verbraecken, J., and Berckmans, D., 2010, Heart rate-based nighttime awakening detection. *European Journal of Applied Physiology*, **109**, 317–322.

5. Hall, M., Vasko, R., Buysse, D., Ombao, H., Chen, Q., Cashmere, J.D., Kupfer, D., and Thayer, J.F., 2004, Acute stress affects heart rate variability during sleep. *Psychosomatic Medicine*, **66**, 56–62.
6. Elsenbruch, S., Harnish, M.J., and Orr, WC., 1999, Heart rate variability during waking and sleep in healthy males and females. *Sleep (Rochester)*, **22**, 1067–1071.
7. Pollak, C.P., Tryon, W.W., Nagaraja, H., and Dzwonczyk, R., 2001, How accurately does wrist actigraphy identify the states of sleep and wakefulness? *Sleep*, **24**, 957–965.
8. Alihanka, J., Vaahtoranta, K., and Saarikivi, I., 1981, A new method for long-term monitoring of the ballistocardiogram, heart rate, and respiration. *American Journal of Physiology*, **240**, 384–392.
9. Niizeki, K., Nishidate, I., Uchida, K., and Kuwahara, M., 2005, Unconstrained cardiorespiratory and body movement monitoring system for home care. *Medical & Biological Engineering & Computing*, **43**, 716–724.
10. Jacobs, J.L., Embree, P., Glei, M., Christensen, S., and Sullivan, P.K., 2004, Characterization of a novel heart and respiratory rate sensor. *Conference Proceedings IEEE Engineering in Medicine and Biology Society*, San Francisco, CA, USA, 1–5 September, pp. 2223–2226.
11. Wang, F., Tanaka, M., and Chonan, S., 2003, Development of a PVDF piezopolymer sensor for unconstrained in-sleep cardio-respiratory monitoring. *Journal of Intelligent Material Systems & Stuctures*, **14**, 185–190.
12. Kortelainen, J., Mendez, M., Bianchi, A., Matteucci, M., and Cerutti, S., 2010, Sleep staging based on signals acquired through bed sensor. *IEEE Transactions on Information Technology in Biomedicine*, **14**, 776–785.
13. Brüser, C., Stadlthanner, K., de Waele, S., and Leonhardt, S., 2011, Adaptive beat-to-beat heart rate estimation in ballistocardiograms. *Information Technology in Biomedicine, IEEE Transactions on*, **15**, 778–786.
14. Chee, Y., Han, J., Youn, J., and Park, K., 2005, Air mattress sensor system with balancing tube for unconstrained measurement of respiration and heart beat movement. *Physiological Measurement*, **26**, 413–422.
15. Tanaka, S., Matsumoto, Y., and Wakimoto, K., 2002, Unconstrained and non-invasive measurement of heart-beat and respiration periods using a phonocardiographic sensor. *Medical & Biological Engineering & Computing*, **40**, 246–252.
16. Chen, W., Zhu, X., Nemoto, T., Kitamura, K., Sugitani, K., and Wei, D., 2008, Unconstrained monitoring of long-term heart and breath rates during sleep. *Physiological Measurement*, **29**, 1–10.
17. Brink, M., Müller, C.H., and Schierz, C., 2006, Contact-free measurement of heart rate, respiration rate, and body movements during sleep. *Behavior Research Methods*, **38**, 511–521.
18. Paalasmaa, J., and Ranta, M., 2008, Detecting heartbeats in the ballistocardiogram with clustering. Proceedings of the ICML/UAI/COLT 2008 Workshop on Machine Learning for Health-Care Applications, Helsinki, Finland, 9 July.
19. Mack, D.C., Patrie, J.T., Suratt, P.M., Felder, R.A., and Alwan, M., 2009, Development and preliminary validation of heart rate and breathing rate detection using a passive, ballistocardiography-based sleep monitoring system. *IEEE Transactions on Information Technology in Biomedicine*, **13**, 111–120.
20. Jansen, B.H., Larson, B.H., and Shankar, K., 1991, Monitoring of the ballistocardiogram with the static charge sensitive bed. *IEEE Transactions on Biomedical Engineering*, **38**, 748–751.
21. Kirjavainen, K., 1987, Electromechanical film and procedure for manufacturing same. U.S. Patent No. 4654546.
22. Paajanen, M., Lekkala, J., and Kirjavainen, K., 2000, Electromechanical film (EMFi) – a new multipurpose electret material. *Sensors & Actuators A-Physical*, **84**, 95–102.
23. Busek, P., Vanková, J., Opavský, J., Salinger, J., and Nevsímalová, S., 2005, Spectral analysis of the heart rate variability in sleep. *Physiological Research*, **54**, 369–376.
24. Kortelainen, J.M., and Virkkala, J., 2007, FFT averaging of multichannel BCG signals from bed mattress sensor to improve estimation of heart beat interval. *Conference Proceedings IEEE Engineering in Medicine and Biology Society*, Lyon, France, 22–26 August, pp. 6685–6688.
25. Mack, D.C., Patrie, J.T., Felder, R.A., Suratt, P.M., and Alwan, M., 2009, Sleep assessment using a passive ballistocardiography-based system: preliminary validation. *Conference Proceedings IEEE Engineering in Medicine and Biology Society*, Minneapolis, MN, USA, 3–6 September, pp. 4319–4322.

Publication III

Vehkaoja, A., Peltokangas, M., Verho, J., and Lekkala, J., “Combining the information of unconstrained electrocardiography and ballistography in the detection of night-time heart rate and respiration rate,” *International Journal of Monitoring and Surveillance Technologies Research (IJMSTR), Special Issue on Biomedical Monitoring Technologies*, vol. 1, no. 3, pp. 52–67, July-Sept. 2013.

Combining the Information of Unconstrained Electrocardiography and Ballistography in the Detection of Night-Time Heart Rate and Respiration Rate

Antti Vehkaoja, Department of Automation Science and Engineering, Tampere University of Technology (TUT), Tampere, Finland

Mikko Peltokangas, Department of Automation Science and Engineering, Tampere University of Technology (TUT), Tampere, Finland

Jarmo Verho, Department of Automation Science and Engineering, Tampere University of Technology (TUT), Tampere, Finland

Jukka Lekkala, Department of Automation Science and Engineering, Tampere University of Technology (TUT), Tampere, Finland

ABSTRACT

An unobtrusive bed integrated system for monitoring physiological parameters during sleep is presented and evaluated. The system uses textile electrodes attached to a bed sheet for measuring multiple channels of electrocardiogram. The channels are also combined in order to form several additional ECG leads. One lead at a time is selected for beat-to-beat-interval detection. The system also includes force sensors located under a bed post for detecting respiration and movements. The movement information is also used to assist in heart rate detection and combining the ECG derived respiration information with respiration information derived from force sensors, is investigated. The authors tested the system with ten subjects in one hour recordings and achieved an average of 95.9% detection coverage and 99 percentile absolute error of 3.47 ms for the BB-interval signal. The relative mean absolute error of the detected respiration cycle lengths was 2.1%.

Keywords: *Bed Integrated Electrocardiogram (ECG/EKG), Heart Rate, Night-Time Monitoring, Respiration Rate, Unobtrusive Physiological Measurement*

DOI: 10.4018/ijmstr.2013070104

INTRODUCTION AND RELATED WORK

Automatic monitoring of night-time physiological information, especially the heart rate, the respiration rate and the movements can be used in various applications. Examples include the screening of medical disorders like sleep apnoea (Ayas *et al.,* 2003; Roche *et al.,* 1999) and monitoring of sleeping quality (Bulckaert *et al.,* 2010) or psychophysiological stress (Hall *et al.,* 2004). Polysomnography is currently used as the standard method for collecting reliable and multiparametric data from a sleeping person. Its biggest drawback is the high cost, which is the result of the requirement of specialized medical personnel and dedicated examination facilities. As a result, all the potential sleep disorder patients cannot be examined and the monitoring is usually done during one night only. The discomfort caused by wearing the measurement equipment may also affect the sleep and skew the results.

Wrist actigraphy is another examination technique increasingly used for sleep analysis. It can be used in a variety of sleep studies including longitudinal monitoring of night-time sleep patterns and circadian rhythm in the natural sleeping environment of the patient (Martin & Hakim, 2011). As the name implies, wrist actigraphy monitors patient's activity through a wrist-worn device using accelerometers or other motion sensors. The benefit is that the device is relatively unobtrusive and the data can therefore be collected for extended periods of time. On the other hand, the device only offers one modality of information, activity, which limits its usability and the achievable accuracy.

In recent years, researchers have started to investigate technologies that combine the positive features of the aforementioned monitoring methods. This means technologies that are unobtrusive like the wrist actigraphy, but would still be able to provide more detailed physiological information about the state of the person being monitored. Heart rate (HR) and respiration rate (RR) or respiration cycle length (RCL) are other interesting parameters besides the activity. These technologies can also be realized so that they do not require any effort from the user, which enables the collection of longitudinal data and consequently a more comprehensive view of the person's sleeping behavior being formed. In the future, these kinds of monitoring systems can also be integrated as a part of a wider eHealth system to provide nocturnal physiological information for supporting the decision making.

Ballistography (BG), which means the measurement of the mechanical signal produced by the heart beat or pulsatile blood movement and breathing is able to provide all the desired physiological parameters; HR, RR, and activity (movements). Recent studies that have focused on the night-time HR detection based on the ballistocardiographic (BCG) signal have reported average HR errors between 0.34% (Kortelainen *et al.,* 2010) and 1.79% (Brüser *et al.,* 2011). We obtained an average error of 0.45% in an earlier yet unpublished study by using force sensors under all four bed posts. Also the detection coverage of the HR is important for reliable sleep analysis. Long continuous beat-to-beat-interval (BBI) series enable a more reliable calculation of heart rate variability (HRV) parameters, which are commonly used in sleep staging and sleep quality evaluation. We achieved approximately 91% average recognition coverage with the ballistographic method in unsupervised recordings while Kortelainen *et al.* (2010) reported 88% coverage. Brüser *et al.* (2011) reported 95% coverage but they had instructed the test subjects to stay still during the measurements.

Even though the fairly good accuracy and high recognition coverage of the BBI data can be achieved with ballistographic sensors, it still may not be the optimal method for gathering the heart rate information. We achieved 95% recognition coverage and an average of 0.27 beats per minute (bpm) or 4.48 ms root-mean-square error with a system that measures contact ECG using textile electrodes sewn on a bed sheet (Peltokangas *et al.,* 2012). Other studies have reported detection coverages between 82% and 93% with large textile electrodes that have been located on a pillow and to the foot of the bed (Devot *et al.,* 2007; Ishijima, 1997). These electrode locations allow the user to wear pajamas as long as the electrodes are in contact with the skin. In our system, the electrodes are attached to the bed sheet in the transversal direction approximately to the height of the chest, thus requiring naked upper body. The accuracy of the detected BBI data was not defined by Devot *et al.* (2007) or Ishijima (1997) but the probability of erroneously detected R-peaks is obviously higher than when using regular ECG electrodes. Also bed integrated non-contact capacitive ECG monitoring has been studied (Ishida *et al.,* 2007; Lim *et al.,* 2007; Wu & Zhang, 2008). The benefit of these systems is that the user is allowed to wear pajamas, but they are much more prone to movement artifacts and electrical interferences and therefore do not necessarily provide benefits when compared with the ballistographic technique.

Besides the heart rate, also the respiration rate or respiration cycle length is an important and widely used physiological parameter in sleep analysis. Many authors who have developed ballistographic methods for the detection of night-time physiological parameters have developed (besides HR detection) methods for RR or RCL detection. Paalasmaa *et al.* (2011) used multiple low-pass filters suited for different RCLs for filtering the original ballistographic signal and then selected the output of the filter that produced the most consistent breathing amplitudes for RCL calculation. Wang *et al.* (2003) used a single component of the wavelet transformed BG signal and an adaptive threshold to count the breathing cycles. The breathing rate can also be detected from the ECG signal. Orphanidou *et al.* (2013) used the power density spectrum of the R-R-interval signal to find the frequency of the respiratory sinus arrhythmia (RSA) and combined that with the spectrum of the R-peak amplitude signal. They used the method for estimating the average respiration rate in one minute time windows. Avci *et al.* (2011) evaluated the performance of six different ECG based respiration detection methods in average and instantaneous RR interval detection. From the evaluated methods, a combination of the RSA signal and a band-pass filtered (0.2 – 0.8 Hz) ECG signal performed the best and gave 0.45 as the correlation coefficient with the reference instantaneous respiration rate.

In this paper, we are combining these two measurement modalities; unconstrained contact ECG and ballistography in monitoring of night-time heart rate and respiration cycle lengths and investigate whether combining their information could improve the detection performance of the physiological parameters.

MATERIALS AND METHODS

Measurement System

Our measurement system consists of eight textile electrodes placed transversally on the bed sheet, their amplifier electronic, two force sensors placed under a bed post, data acquisition (DAQ) device for sampling the signals, and a PC computer for storing the data.

We used a custom made 16-channel DAQ for sampling the sensor signals. The input voltage range of the device is ± 2.18 V with a resolution of 67 μV. The RMS noise level of the DAQ is less than 0.5 quantization units. The DAQ is capable of transmitting the measurement data either through USB or by a wireless Bluetooth link. We used the USB mode in these tests because the application at hand does not require mobility. The maximum sampling rate with the wired connection is 1 kHz per channel but 250 Hz was found high enough for the ECG and BG recording.

Bed Sheet ECG Measurement Electronics

The electrodes we are using are manufactured from silver coated polyamide yarn by embroidering. The size of the oval shaped electrodes is 3.2 cm × 2.2 cm. A moisture barrier layer is used under the electrodes in order to slow down the drying of the electrodes after they are first moistened by the moisture of the skin. Earlier we used 9.8 cm inter-electrode distance (Peltokangas *et al.,* 2012), but in the current setup we decreased the distance to 5 cm. Shorter inter-electrode distance enables combining several ECG channels, which increases the signal-to-noise ratio (SNR) of the ECG as well as gives more choices for channel selection.

Our ECG amplifier contains eight measurement channels. Seven channels are used for the bed sheet ECG measurement and the remaining one for the reference ECG recorded with conventional disposable Ag/AgCl electrodes (Blue sensor L-OO-S) manufactured by Ambu. All the channels are identical, having two amplifier stages. The first stage is an instrumentation amplifier and the second is a non-inverting gain stage. Between the amplifier stages there is a first order high pass filter and after the second stage a second order 40 Hz Butterworth low-pass filter. The amplifiers used for the sheet ECG measurement are arranged so that each of them amplifies the potential difference between two adjacent electrodes.

Eight electrodes placed 5 cm apart cover a 38 cm wide area in the middle of the bed. In order to maximize the ECG signal quality, the pillow should be located so that the electrodes are approximately 10 – 25 cm from the edge of the pillow. Even larger variation in the axial electrode location is tolerable in most cases but we have noticed that especially when sleeping on the right side, the ECG signal quality usually starts to decrease when the electrodes are located more than 20 cm down from the arm pit.

Ballistography

We use two force sensitive electret film sensors made of Electro Mechanical film (EMFi) material to measure ballistography and movement signals. Both sensors are located under the top left bed post. The size of the sensors is 1 cm x 2 cm and their approximate sensitivity is 1 V/N. The high input resistance of the DAQ device (10 GΩ) allowed us to connect the sensors directly to the device. 10 GΩ resistance in parallel with the capacitance of the sensor, the measurement cable, and the DAQ's input (together approximately 300 pF), forms a high-pass cut-off frequency of approximately 0.05 Hz. Our signal processing algorithm uses the information acquired with the ballistographic sensors for two purposes: firstly, for measuring the respiratory information and secondly, for assisting in ECG signal processing by providing movement information.

Signal Processing

The signals of the two sensor modalities, bed sheet ECG sensors and bed post force sensors, are basically processed separately but the movement information provided by the force sensor is used to assist in processing the sheet ECG signals. We did all the digital signal processing offline using MATLAB®.

Combining and Selecting the Bed Sheet ECG Channels

Before combining the bed sheet ECG signals, they are first low-pass filtered digitally using a 10^{th} order filter having Butterworth-type response and 30 Hz cut-off. The ECG signals are then combined in order to form new ECG measurement leads. This is done simply by adding the signals of adjacent channels together. Combining the signals of adjacent bed sheet ECG channels increases the signal quality in two ways. Firstly, the noise caused by the measurement electronics and the interferences in the skin-electrode interfaces is independent between the channels whereas the ECG signal is not independent. This increases the SNR by the square root of the number of combined channels. The more important source of improvement is the increased distance between the measuring electrodes, which according to the lead field theory, increases the measurement sensitivity deeper in the torso where the signal source, heart, is located (Puurtinen, 2012). Figure 1 shows an example of the improvement of the sheet ECG quality when the signals of three channels are combined.

As seen in Figure 1, the channels can be combined simply by adding the signals of adjacent bed sheet channels together. All pos-

Figure 1. An example of low quality bed sheet ECG signals from three measurement channels (upper traces). The R-peaks become more distinguishable when the signals are combined (bottom trace). Traces are offset for the sake of clarity.

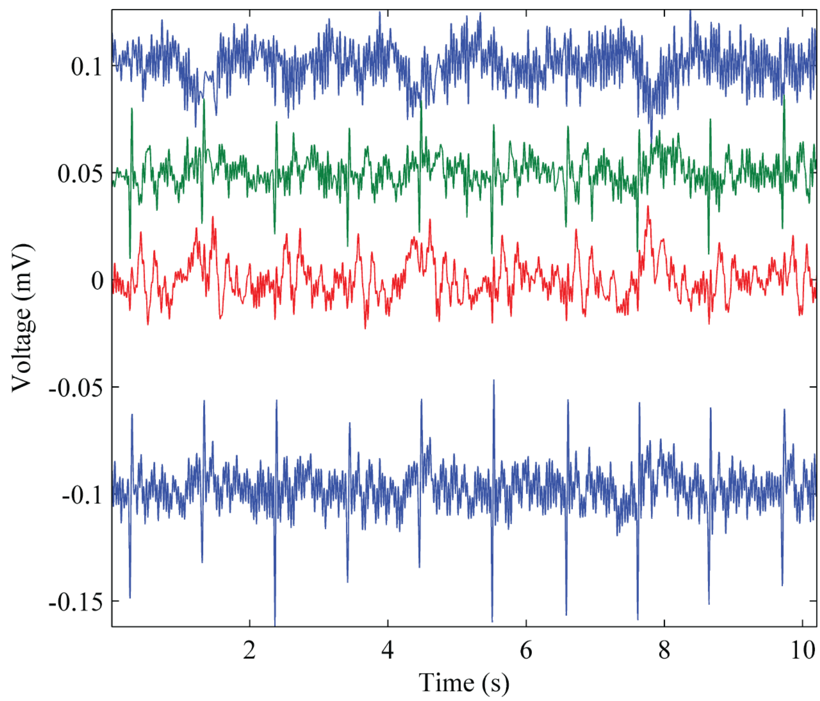

sible combinations of one to seven bed sheet channels, altogether 28 channel combinations are thus formed. The final pre-processing step is the high-pass filtering of the signal with the non-linear method proposed by Keselbrener *et al.* (1997): 100 ms sliding median is subtracted from the signal, removing efficiently low frequency components but leaving the R-peaks untouched.

The signals are then fed to the channel selection algorithm, which chooses the channel with the best signal quality to be used in BB-interval detection. The best channel is selected by taking a 10-second sample of all the channels, then detecting the R-peaks (all peaks with distinctive amplitude and steep enough rising and falling edges), and finally selecting the channel with the highest ratio between the average peak amplitude and the variance of the remaining baseline signal (power of the noise signal). It is important to notice that the preprocessing, removing the 100 ms median, suppresses all low frequency components e.g. T-wave from the signal and the remaining part essentially consists of higher frequency noise.

If none of the signals fulfill the minimum requirements of the signal quality, then no channel is analyzed and the channel selection is tried again after one second. The minimum requirements are that the found R-peak candidates or BB- intervals should be physiologically reasonable and their amplitude as well as the SNR should be within predefined limits. Depending on the sleeping posture, R-peaks may be negative or positive and both cases need to be considered. A detailed description of the algorithm can be found in (Peltokangas *et al.,* 2012). The channel selection procedure is repeated if the quality of the ECG on the currently used channel decreases too much.

Heart Beat Detection and BBI Post-Processing

After the best channel is selected, R-peaks are searched from it. The R-peak detection algorithm is based on finding all the distinctive peaks similarly as in the channel selection phase. The algorithm is based on the method published by Zhengzhong *et al.* (2011) with some modifications. After finding the R-peaks, a second order polynomial fitting is used to find the exact peak location with sub-sample interval accuracy. The polynomial is fitted to three data points by taking one sample from both sides of the original R-peak sample.

After the whole recording has been analyzed and potential R-peaks have been found, the resulting BBI series is processed in order to find possible false positive detections caused e.g. by electrical interference by investigating the peak interval signal. Earlier we have also developed an ectopic peak detector that finds and removes possible "not sinus node"-originated peaks based on their different morphology (Peltokangas *et al.,* 2012). These ectopic peaks should be removed before using the BBI signal in the HRV analysis because they are not controlled by the autonomous nervous system. The BBI post processing algorithm also combines the BBI segments computed before and after the channel reselections if it concludes that no R-peaks have been missed during the reselection.

Movement Detection with Force Sensor

We have used a variance of a four second sliding window for monitoring the amplitude level of the force signals and detecting excessive movements. These sections are excluded from the force sensor based RCL detection because the weak respiration signal is buried under the movement signal, which usually is several orders of magnitude stronger. The threshold level for the movement detection is determined empirically and is twenty times the median variance of the whole recording, calculated in four second windows. Additional five seconds of data is also discarded before and after the detected movements.

The output of the movement detector should not be used directly to exclude the sheet ECG data because in most cases the sheet ECG quality is adequate for the HR detection also during small movements. We have used the movement detector to assist in the decision of launching the channel reselection process. When the SNR of the sheet ECG is so small that the channel reselection would normally be initiated, the movement detector is used for checking whether the small SNR is a result of increased movement artifacts. We have noticed that a smaller SNR can be tolerated if no movement is present without compromising the HR detection accuracy. Therefore the HR detection can be continued without reselecting the channel if the deterioration of the SNR is caused by something else than movements. In this case a lower limit for the minimum allowable SNR is used.

Respiration Cycle Length Detection with Force Sensors

The respiration rate is normally defined from signals recorded with respiration inductance plethysmography (RIP) sensors that measure the changes in the circumference of the chest and abdomen, or signals of temperature sensors measuring the air temperature in front of the mouth and nostrils. These sensors produce fairly consistent sinusoidal like waveform during normal breathing as can be seen from the Figure 2a and respiration cycles can be detected e.g. by finding the time differences of local maxima in the signal. Waveform produced by BG sensor on the other hand is not always this consistent and the detection of the RCL is not as straightforward as with the RIP and temperature sensors. As can be seen from the Figure 2b, the signal of the force sensors sometimes includes a certain kind of a dent or a deflection at the location of the signal peak, which is physiologically at the end of the inhaling phase. The frequency of these dents is around 1.5 – 2 times higher than the actual respiration frequency and the signal

Figure 2. A 200-second example of a force sensor based respiration recording. The reference signal recorded with a thermistor is shown in a) and the signals of the force sensors filtered with different pass bands in b) (offset for clarity). The respiration cycle length suggestions based on the signals of b) are shown in c), the square sum of the closest suggestions along with the threshold for discarding the RCL value in d), and the RCLs detected with the reference sensor and force sensors in e).

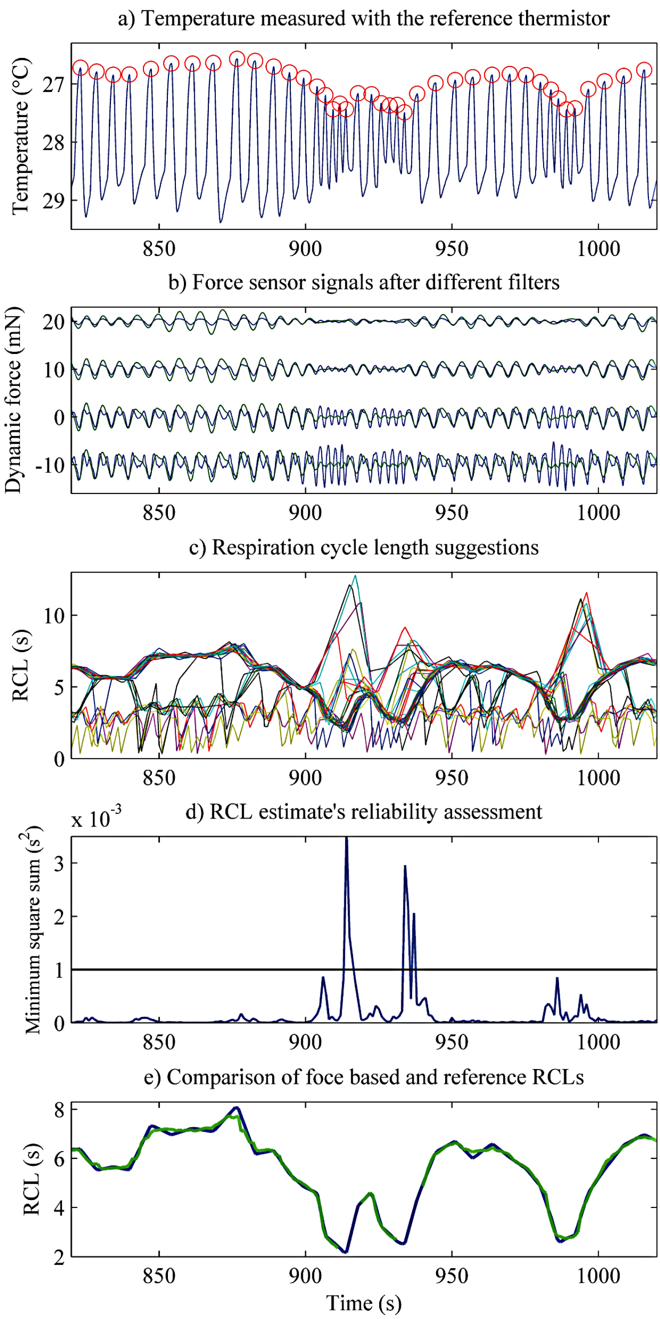

should be filtered with a cut-off that is between these two. The respiration cycle lengths usually vary between 2 s and 10 s (0.1 – 0.5 Hz), which means that one single filter does not suit all respiration rates.

Our breathing rate detection is based on filtering the ballistographic signals with four different band-pass filters and then finding the rising and falling zero crossings as well as the local maxima and minima for all the filter outputs. After this, the repetition intervals of each parameter are calculated and used as possible respiration cycle lengths. Filtering the ballistogram signal with different pass-bands for respiration detection was earlier used by Paalasmaa *et al.* (2011).

The low-pass cut-off frequencies of four filters were 0.154, 0.22, 0.433, and 0.5 Hz and the high-pass cut-offs were 0.1 Hz in all filters except the first one that had 0.05 Hz cut-off. The filter order has to be high enough so that the undesired part of the signal is attenuated without too much affecting the amplitude of the basic sinusoidal component. On the other hand, the order should not be too high so that it does not distort the shape of the signal when the basic frequency is close to the cut-off. The same applies if the filter (e.g. elliptic) is otherwise designed so that its transition band is very narrow. Fourth order filters with Butterworth response gave the best results in our tests.

The respiration cycle length suggestions are further processed by interpolating them into 1 second sample interval. The respiration cycle length is then determined by finding the densest cluster formed by at least 20% of the RCL suggestions. Figure 2 c shows an example of the distribution of the suggestion and a clear cluster formed by them. We also set a minimum limit for the cluster density meaning that if the square distance of the closest suggestions (20% of all) is too high, no RCL value is selected for that time instance. As seen from the Figure 2 e, also correct values will sometimes get discarded but on the other hand loosening the limit would increase the amount of incorrect results. Introducing this RCL discard criterion allowed us to shorten the time around the movements when the RCL values are always abandoned as unreliable from previously used 15 seconds to 5 seconds, which led to an increase in the coverage of the detected RCL.

The final step in the RCL detection is post processing. Sometimes the RCL suggestions show two apparent clusters and it may happen that the wrong cluster has smaller square distance in certain time instances. In order to detect these, we check if each RCL value is less than 1 s apart from the median of three consecutive RCLs, where the one that is being checked is in the middle. This way single peaks that deviate more than 1 s from the surrounding values are detected and replaced with the mean of surrounding values.

Data Fusion in the RCL Detection

We also tested if the respiration information obtained from the bed sheet ECG signal could be combined with the RCL calculated from the force sensor signals. The performance of the ECG based RR or RCL detection presented in the earlier studies (Orphanidou *et al.,* 2013; Avci *et al.,* 2011) has not been as good as what we obtained earlier by using the force sensors, so our basic approach was to use the force sensors as the primary RCL detection modality and then use the ECG based respiration to complement the gaps left in the force sensor RCL time series (if possible). The possible benefit of using the ECG in addition to the force sensors is that it is not so sensitive to the movement artifacts. For example, small movements of limbs do not interfere the sheet ECG signal as long as the electrode contact remains good.

We used two signals calculated from the bed sheet ECG and recognized R-peaks to determine the RCL: the RSA and the modulation of the R-peak amplitude caused by the variation in the lead field and the heart orientation due to the breathing movement. We call this as RPA. The same signals have been earlier used e.g. by Cysarz *et al.* (2008) and Orphanidou *et al.* (2013) for calculating the respiration rate from ECG that is recorded with conventional electrodes in fixed locations. The RSA and

RPA signals are interpolated to 0.1 s sample interval using cubic spline interpolation. Then both signals are processed in a similar way as the force sensor signals (filter with different pass bands, find RCL suggestions and select the clusters dense enough) in order to find the respiration cycle lengths. Finally, the gaps left to the force sensor based RCL signal are filled with the ECG based RCL values in cases where they are available.

Reference Sensors

The reference ECG signal was recorded using regular disposable electrodes attached to the chest. The electrode locations were selected so that they did not interfere with the sheet electrodes. The heart rate was calculated using the same algorithm as with the sheet ECG signals.

The reference breathing rate was measured using an NTC thermistor placed inside a breathing mask. The resistance of the thermistor was measured, converted into the temperature, and filtered. The respiration rate was calculated from the band pass filtered temperature signal by finding the maximum of each signal segment on the positive side. These points correspond to the end of the inhale phase. Finally, the signals were visually inspected and false or missing detections were corrected. We also found short sections from the recordings of four test subjects, where the amplitude of the reference breathing signal was significantly decreased. We interpreted these sections as breathing obstructions and discarded them from the analysis. In overall, the amount of discarded data was much less than one percent of the total recording time.

Test Measurements and Subjects

We made test measurements with eight male and two female subjects (subjects number 6 and 10). The subjects were 23-33 year old, normal weight and had no history of cardiovascular problems or sleeping related breathing disorders. The measurements were made in a laboratory setting using an 80 cm wide spring mattress bed. The subjects were allowed to change their sleeping posture freely. The length of the recordings was approximately one hour and most of the subjects fell asleep during this time.

RESULTS AND DISCUSSION

BBI Detection Coverage

Table 1 shows the heart rate detection coverage for each test subject with different electrode configurations as well as the effect of using the force sensor for assisting in the decision of initiating the channel reselection. The ECG signal of the subject 7 was so weak that the algorithm was not able to detect the HR from the raw ECG signals recorded with 5 cm electrode distanced and we therefore excluded the subject from the calculation of the average results.

The first and the third column in the Table 1 show the BBI detection coverage when the force sensor is used and is not used in assisting the channel reselection, respectively. As seen in the table, using the force sensor information improved the average BBI detection coverage by 0.8 percentage points from 95.06% to 95.85%. We can also say that the amount of undetected BBI signal was decreased by 16%. Using the force sensor can only have an effect when channel reselections occur. The subject 10, for example, stayed in the same position during the whole measurement and the channel was reselected only once. Therefore the use of the force sensor does not bring any advantage in this case. While the improvement in the coverage provided by the force sensor is fairly small, a more important aspect is that because the channel is not changed so easily, there are overall less channel changes and the segments of continuously detected BBI data are thus longer. This benefits especially the calculation of frequency domain HRV parameters, which are usually calculated in sleep analysis from 30 or 60 second long data segments.

Earlier we achieved 95.1% average recognition coverage in overnight measurements by using 9.8 cm inter-electrode distance and not combining the channels (Peltokangas *et al.,*

Table 1. The effect of the force sensor and the channel combination on the BBI detection coverage and the uncertainty of the BBI detection

Subject Number	Heart Rate Detection Performance					
	Cov. Force[a]	*99 per*[b]	*Cov. no Force*[a]	*99 per*[b]	*Cov. 10 cm*[a]	*Cov 5 cm*[a]
1	97.19	1.71	97.16	1.64	96.93	96.72
2	97.31	2.75	97.37	3.25	96.77	96.33
3	92.94	4.88	91.30	3.57	87.77	85.74
4	88.96	3.87	86.74	3.80	71.78	84.18
5	97.10	2.53	96.93	2.65	95.74	78.14
6	92.42	3.29	89.31	3.12	67.17	39.08
7	61.25	4.12	59.84	3.69	47.45	0.56
8	99.36	5.62	99.17	5.75	98.26	98.39
9	97.69	3.08	97.89	3.07	88.36	97.28
10	99.71	3.49	99.71	3.49	72.35	99.71
Average[c]	95.85	3.47	95.06	3.37	86.13	86.17

a. BBI detection coverage when the force sensor information is applied (column 2), not applied (column 4), and when using only 10 cm or 5 cm inter-electrode distances (column 6 and 7).
b. 99 percentile of the absolute error in milliseconds with and without the force sensor.
c. The results of subject 7 are discarded from the calculation of the average results.

2012). Because the measurement conditions in the current study are different (the measurement time is shorter and the portion of the time spent awake is longer), we also calculated the coverage with the current data by using only the 10 cm inter-electrode distances that were simulated by combining two adjacent measurement channels. The coverage achieved was 86.1%. The improvement achieved by using also the channel combination is, according to the paired T-test, statistically significant ($p = 0.028$). The difference between this and the earlier 9.8 cm setup is that the combinations of two adjacent channels also provide interleaved 10 cm ECG leads in addition to the 10 cm leads, which are next to each other. The rightmost column in Table 1 shows the recognition coverage when only the data recorded with 5 cm electrode distances is used. The average detection coverage was almost the same with 5 cm and 10 cm electrode distances.

We also investigated if including an additional ECG channel combination would further improve the coverage. For example summing up measurement channels 2 and 5 and not considering channels 3 and 4 would work in a case where the electrode that is common to channels 3 and 4 has a bad skin contact. These combinations were selected as the best channel quite often by the algorithm and they were also sometimes able to measure ECG of sufficient quality when other channels were not. However, their signal usually did not stay stable for a long time, which caused more channels reselections to happen and therefore the overall detection coverage was not improved. We therefore did not use them in the final setup.

Figure 3 shows the BBI detection result from the recording of subject 5 along with the information about the selected ECG lead. ECG leads numbered as 1 – 7 in the vertical axis of the subfigure a, are the original ECG channels measured between two adjacent electrodes. Leads 8 – 13 are formed by summing up the signals from two adjacent channels. Similarly, leads 14 – 18 are formed by summing up three

Figure 3. A one hour recording showing the measurement leads used for sheet BBI calculation in a). Leads 1 – 7 below the lowest horizontal line are the single measurements channels, leads 8 – 13 between the two lowest horizontal lines are augmented ECG leads formed by two adjacent channels etc. Subfigure b) shows the BBI signals calculated from the sheet ECG signals and from the reference ECG. The sections of shorter BB-interval are results of larger movements and sleeping posture changes and are therefore not detected from the sheet ECG. Subfigure c) shows the error of the detected BB-intervals. The maximum error has been less than 5 ms in this recording.

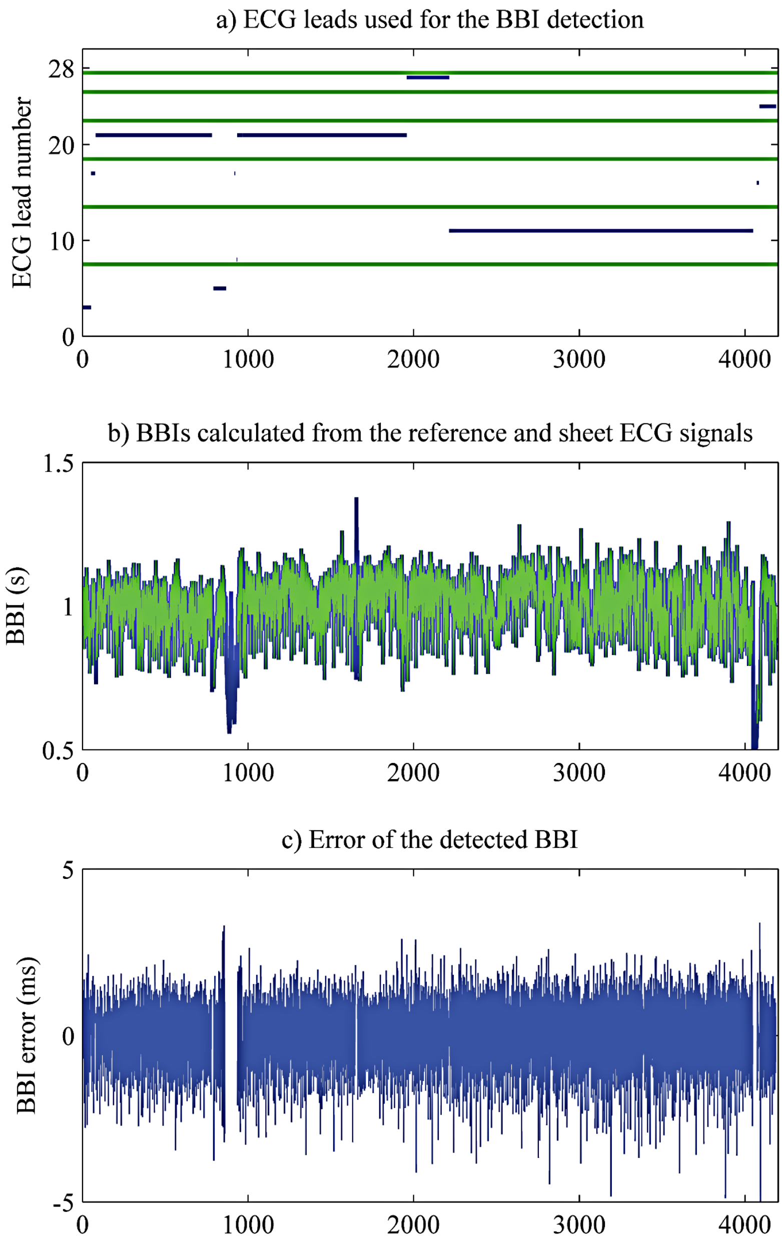

channels, and so on. The channels formed by different number of electrodes are separated by the continuous horizontal lines. The shorter horizontal line pieces in the subfigure a shows, which ECG lead has been selected and used at a certain time for BBI detection. 44.7% of the total measurement time of all subjects, the channel selection algorithm had selected a measurement lead formed by one channel as the best. A lead formed by two channels was used 20.7% of the time, three channels 13.0%, four channels 16.8%, five channels 1.2%, and six channels 3.4% of the time. The measurement lead formed by all seven channels was not selected in any of the recordings.

BBI Accuracy

Authors have used a lot of different metrics to describe the performance of their measurement systems and the uncertainty of the results. Commonly used values are mean absolute error (MAE) as in (Kortelainen *et al.,* 2010; Brüser *et al.,* 2011) or RMS error (RMSE) as in (Wu & Zhang, 2008):

$$MAE\left(ms\right) = \frac{1}{N}\sum_{i=1}^{N}\left|BBI_{sheet}\left(i\right) - BBI_{ref}\left(i\right)\right|$$

$$RMS_{error}\left(ms\right) = \sqrt{\frac{1}{N}\sum_{i=1}^{N}\left(BBI_{sheet}\left(i\right) - BBI_{ref}\left(i\right)\right)^2}$$

Another suitable figure for reporting the uncertainty of the result is using percentile units, which tells about the uncertainty of the true positive detections and is not affected by random false positives. We selected 99 percentile of the BBI signal's absolute error as the metrics of the BBI uncertainty. The average 99 percentile limit for the error when using all channel combinations and the force sensor information was 3.53 ms, which is less than one sample interval, 4 ms. As seen from the Table 1, using the force sensor does not have a clear effect on the BBIs' 99 percentile error in either way.

We also calculated the RMSE and MAE errors of the BBI results. The RMSE varied between 0.97 ms and 12.5 ms between the recordings, the arithmetic average RMSE being 5.81 ms. The average RMSE converted to the beats per minute was 0.36 bpm (0.07 – 0.78 bpm). The problem of using the RMSE is that a few erroneously detected R-peaks in a recording may have a large effect on the result even when all other BBIs are really close to the reference. Mean absolute error is less disturbed by random large errors. The BBI MAE of our recordings varied between 0.48 ms and 1.70 ms. The average was 1.12 ms. Conversion to the percentage units yields 0.05% and 0.16% as the minimum and maximum, and 0.11% as the average MAE percent from the reference BBI. As one can assume based on the nature of the monitoring method, the 0.11% MAE is clearly smaller than the smallest error reported for the ballistocardiographic method (0.34% in (Kortelainen *et al.,* 2011)). Also the RMS error reported in (Wu & Zhang, 2008) for a system using capacitive electrodes (0.66 ± 0.57 bpm) is outperformed by our 0.36 bpm RMSE. These error numbers were somewhat better in our earlier study with smaller dataset (Vehkaoja *et al.,* 2012) mainly due to the results of the subject 7 who had the bed sheet electrodes placed slightly too low in the test measurement and therefore relatively weak signal.

RCL Detection Coverage

Table 2 shows the performance characteristics of the breathing rate detection. The average respiration detection coverage has been improved from 74% presented in (Vehkaoja *et al.,* 2012) to 82%. The reason is the improved cluster density based RCL selection method, which allowed us to use shorter safety margins around the sections that include excessive movements. Earlier we selected the RCL just by taking the median of the suggestions, which forced us to use longer margins in order to avoid erroneous RCL detections.

Table 2. RCL detection coverage and error

Subject Number	Respiration Detection Performance						
	Cov[a]	***Correlation***[b]	***RMS***[c]	***MAE***[d]	***e<0.25***	***e<0.5***[e]	***e<1***[e]
1	93.3	0.996	0.113	1.51	98.7	99.7	99.8
2	64.0	0.954	0.394	2.79	92.7	98.1	98.8
3	61.4	0.905	0.231	2.42	95.6	99.2	99.5
4	69.3	0.911	0.165	2.37	94.4	99.5	99.9
5	90.5	0.967	0.133	2.21	93.9	99.6	100.0
6	83.6	0.966	0.138	1.84	96.7	99.6	99.8
7	74.5	0.967	0.063	1.16	99.6	99.9	99.9
8	97.5	0.901	0.216	2.01	96.6	98.7	99.2
9	91.5	0.990	0.217	2.47	90.4	97.2	99.4
10	94.5	0.907	0.116	2.12	96.5	99.4	99.8
Mean	82.0	0.946	0.179	2.09	95.5	99.1	99.6
ECG	39.6	0.777	0.378	5.60	71.2	89.7	97.0
Comb	85.0	0.925	0.216	2.29	94.6	98.7	99.5

a. Respiration cycle length detection coverage, %.
b. Concordance correlation of the respiration cycle lengths
c. Root-mean-square error (RMS) of the respiration cycle length in seconds per breath.
d. Mean absolute error (MAE) of respiration cycle length in percent.
e. Percent of the detected respiration cycle lengths where the error is smaller than 0.25s, 0.5s, and 1s.

A 200-second example of the respiration recording of subject 1 is shown in Figure 2. As seen from the subfigure b), the signal of the other force sensor has a deflection at the top especially during long respiration cycles. The deflection is attenuated and finally removed by filtering with different cut-offs. The deflections and other interferences cause a lot of erroneous respiration cycle length suggestions as seen in the subfigure c). The densest cluster of suggestions is searched and accepted as the respiration if the sum of square distances is below the threshold as seen in d). Subfigure e) shows a comparison of RCLs calculated from the force sensor signals and from the reference signal shown in a).

RCL Uncertainty

At the same time with increasing detection coverage, the RMSE of the detected RCL has been decreased from 0.24 s reported in (Vehkaoja *et al.,* 2012) to 0.18 s. The RMSE was erroneously presented as MAE in that paper. The average MAE for the ten subjects is 0.085 s, which equals an average of 2.1% of the reference RCL values. The most noticeable improvement to the performance of our algorithm has been the decrease of clearly erroneous RCL detections. Earlier the average of 97.3% of the RCLs was less than 0.5 s apart from the reference but this has been improved to 99.1%.

Cysarz *et al.* (2008) used a concordance correlation coefficient to describe the agreement between the respiration rate calculated in 5 minute windows from a single ECG lead and the reference air flow sensor. The regular Pearson correlation only considers the linear dependency of two variables and measures how far the observation pairs come from the best straight line fit. The concordance correlation also takes into account how well the actual values of the pairs correspond, i.e. how much the best fit differs from the 45-degree line that goes through the origin (Lin, 1989). The concordance correlation between two variables is calculated as:

$$\rho_c = \frac{2 \cdot s_{xy}}{s_x^2 + s_y^2 + \left(\mu_x - \mu_y\right)^2}$$

where s_{xy} is the covariance of the two variables, s_x and s_y are the variances and μ_x and μ_y are the means.

The average concordance correlation ρ_c in the ten recordings was 0.946, which is a good value. Cysarz *et al.* (2008) received ρ_c of 0.79 and 0.73 when detecting respiration rate in 5 minute epochs using RSA and RPA signals derived from ECG.

Combining the RCL Derived from ECG and Force Sensor Data

Table 2 shows the average results of ECG based RCL detections. As said earlier, the respiration information derived from the ECG signal has not been as reliable in the earlier studies as the results obtained with force sensors and this is the case also with our system. The ECG-based algorithm provided a respiration result on an average of 39.6% of time (approximately 50% of time when the ECG signal was available), which is less than a half of the coverage obtained using the force sensors. The error figures of the RCL results are worse than when using the force sensors as well. The results of the subject number seven were not included in the evaluation because the bad positioning of the sheet electrodes caused so weak ECG signal that the RPA signal did not correlate with the respiration and the RCL signal was only available during 3% of the time.

When combining the two results by using the ECG derived RCL values in cases where the force based value is missing, we were able to increase the detection coverage by 3 percent units. However, the accuracy of the RCL signal was decreased at the same time. We speculate that the reason why combining the two sensor modalities, at least this way, did not bring much advantage over using only the force sensors is that in the cases where the force sensor RCL data is missing, also the ECG based RCL information is more unreliable than on average because these cases are often related to movements.

CONCLUSION

We have presented an unobtrusive bed-integrated system for monitoring night-time physiological parameters. The results show a statistically significant improvement ($p < 0.05$) in the BBI detection coverage when the measurement channels were simply combined by adding their signals. We also tested if the performance can be improved by combining two sensor modalities. The results suggest that the BBI detection coverage can be further increased by combining the movement information to the analysis. We were, however, not able to yet find a technique for improving the force sensor based RCL detection by combining the ECG based RCL information to it. The results obtained from one hour long recordings with young healthy adults still show that the detection coverage and the accuracy of the received physiological parameters are so good that this information can be used in evaluation of the sleep structure and quality. Important aspects of the future work include the development and integration of sleep analysis algorithms for the estimation of sleep structure and the detection of sleep apnoea and other sleep disorders. Also more testing with a larger number of people of wider demographics and during the whole night is required.

ACKNOWLEDGMENT

We would like to acknowledge the volunteers who participated in the study. The work was partially funded by the Finnish Funding Agency for Technology and Innovation (TEKES) as a part of the project Monitoring and treatment of obesity-related sleeping disorders.

REFERENCES

Avci, C., Besli, S., & Akbas, A. (2011). Performance of the EDR methods: Evaluations using the mean and instantaneous respiration rates. In *Proceeding of 5th International Conference on Bioinformatics and Biomedical Engineering (iCBBE)* (pp.1-5).

Ayas, N., Pittman, S., MacDonald, M., & White, D. (2003). Assessment of a wrist-worn device in the detection of obstructive sleep apnea. *Sleep Medicine*, *4*(5), 435–442. doi:10.1016/S1389-9457(03)00111-4 PMID:14592285

Brüser, C., Stadlthanner, K., de Waele, S., & Leonhardt, S. (2011). Adaptive beat-to-beat heart rate estimation in ballistocardiograms. *Information Technology in Biomedicine*. *IEEE Transactions on*, *15*(5), 778–786.

Bulckaert, A., Exadaktylos, V., De Bruyne, G., Haex, B., De Valck, E., & Wuyts, J. et al. (2010). Heart rate-based nighttime awakening detection. *European Journal of Applied Physiology*, *109*(2), 317–322. doi:10.1007/s00421-010-1359-0 PMID:20094892

Cysarz, D., Zerm, R., Bettermann, H., Frühwirth, M., Moser, M., & Kröz, M. (2008). Comparison of respiratory rates derived from heart rate variability, ECG amplitude, and nasal/oral airflow. *Annals of Biomedical Engineering*, *36*(12), 2085–2094. doi:10.1007/s10439-008-9580-2 PMID:18855140

Devot, S., Bianchi, A., Naujokat, E., Mendez, M., Brauers, A., & Cerutti, S. (2007). Sleep monitoring through a textile recording system. In *Proc. 29th Annual Int Conf of the IEEE Engineering in Medicine and Biology Society (EMBC)* (pp. 2560–2563).

Hall, M., Vasko, R., Buysse, D., Ombao, H., Chen, Q., & Cashmere, J. D. et al. (2004). Acute stress affects heart rate variability during sleep. *Psychosomatic Medicine*, *66*(1), 56–62. doi:10.1097/01.PSY.0000106884.58744.09 PMID:14747638

Ishida, S., Shiozawa, N., Fujiwara, Y., & Makikawa, M. (2007). Electrocardiogram measurement during sleep with wearing clothes using capacitively coupled electrodes. In *Proc. 29th Annual Int Conf of the IEEE Engineering in Medicine and Biology Society (EMBC)* (pp. 2647–2650).

Ishijima, M. (1997). Cardiopulmonary monitoring by textile electrodes without subject-awareness of being monitored. *Medical & Biological Engineering & Computing*, *35*(6), 685–690. doi:10.1007/BF02510978 PMID:9538546

Keselbrener, L., Keselbrener, M., & Akselrod, S. (1997). Nonlinear high pass filter for R-wave detection in ECG signal. *Medical Engineering & Physics*, *19*(5), 481–484. doi:10.1016/S1350-4533(97)00013-1 PMID:9338889

Kortelainen, J., Mendez, M., Bianchi, A., Matteucci, M., & Cerutti, S. (2010). Sleep staging based on signals acquired through bed sensor. *Information Technology in Biomedicine*. *IEEE Transactions on*, *14*(3), 776–785.

Lim, Y., Kim, K., & Park, K. (2007). ECG recording on a bed during sleep without direct skin-contact. *Biomedical Engineering*. *IEEE Transactions on*, *54*(4), 718–725.

Lin, L. I. (1989). A concordance correlation coefficient to evaluate reproducibility. *Biometrics*, *45*(1), 255–268. doi:10.2307/2532051 PMID:2720055

Martin, J., & Hakim, A. (2011). Wrist actigraphy. *Chest*, *139*(6), 1514–1527. doi:10.1378/chest.10-1872 PMID:21652563

Orphanidou, C., Fleming, S., Shah, S. A., & Tarassenko, L. (2013). Data fusion for estimating respiratory rate from a single-lead ECG. *Biomedical Signal Processing and Control*, *8*(1), 98–105. doi:10.1016/j.bspc.2012.06.001

Paalasmaa, J., Leppakorpi, L., & Partinen, M. (2011). Quantifying respiratory variation with force sensor measurements. In *Proc. 33rd Annual Int Conf of the IEEE Engineering in Medicine and Biology Society (EMBC)* (pp. 3812–3815).

Peltokangas, M., Verho, J., & Vehkaoja, A. (2012). Night-time EKG and HRV monitoring with bed sheet integrated textile electrodes. *Information Technology in Biomedicine*. *IEEE Transactions on*, *16*(5), 935–942.

Puurtinen, M. (2012). *Precordial bipolar leads for mobile ECG applications*. Doctoral dissertation.

Roche, F., Gaspoz, J.-M., Court-Fortune, I., Pascal, M., Pichot, V., & Duverney, D. et al. (1999). Screening of obstructive sleep apnea syndrome by heart rate variability analysis. *Circulation*, *100*(3), 1411–1415. doi:10.1161/01.CIR.100.13.1411 PMID:10500042

Vehkaoja, A., Peltokangas, M., Verho, J., & Lekkala, J. (2012). Combining unobtrusive electrocardiography and ballistography for more accurate monitoring of sleep. In *Proceedings of the IEEE 12th International Conference on Bioinformatics & Bioengineering (BIBE)* (pp.202-207).

Wang, F., Tanaka, M., & Chonan, S. (2003). Development of a PVDF piezopolymer sensor for unconstrained in-sleep cardiorespiratory. *Journal of Intelligent Material Systems and Structures*, *14*(3), 185–190. doi:10.1177/1045389X03014003006

Wu, K.-F., & Zhang, Y.-T. (2008). Contactless and continuous monitoring of heart electric activities through clothes on a sleeping bed. In *Proceeding of Information Technology and Applications in Biomedicine* (pp. 282–285). ITAB. doi:10.1109/ITAB.2008.4570586

Zhengzhong, G., Fanxue, K., & Xu, Z. (2011). Accurate and rapid QRS detection for intelligent ECG monitor. In *Proceeding of Third International Conference* on *Measuring Technology and Mechatronics Automation (ICMTMA)* (pp. 298–301).

Antti Vehkaoja received the M.Sc. degree in electrical engineering from the Tampere University of Technology (TUT), Tampere, Finland, in 2004, where he is currently working toward the Ph.D. degree as a member of the Sensor Technology Research Group. He is currently a Teaching Associate in the Department of Automation Science and Engineering, TUT. His current research interests include sensors and measurement systems for physiological monitoring and processing of physiological signals.

Mikko Peltokangas was born in 1988 and received the B.Sc. degree from the Tampere University of Technology (TUT), Tampere, Finland, in 2011, where he is currently studying toward the M.Sc. degree. His research interests lie in physiological measurements and analysis of biosignals. He is currently working as a Research Assistant in the Department of Automation Science and Engineering, TUT.

Jarmo Verho is an undergraduate student working as a Research Assistant in the Department of Automation Science and Engineering, Tampere University of Technology, Tampere, Finland. He is specialized in low-noise electronics design and embedded systems. His other research interests include sensor networks, radio networks, short range inductive links, and capacitive sensing techniques.

Jukka Lekkala received his M.Sc. degree in electronics and D.Sc. (Eng) degree in biomedical engineering from Tampere University of Technology (TUT), Finland, in 1979 and 1984, respectively. Since 1991 he has been a docent of bioelectronics at University of Oulu, and a docent of biomedical engineering at TUT. He is a Professor of automation technology at the Department of Automation Science and Engineering, TUT. Currently, he also acts as the head of the department. His research interests include sensing systems and sensor materials, biochemical and chemical sensors, instrumentation, and modelling.

Publication IV

Vehkaoja, A., Peltokangas, M., and Lekkala, J., "Extracting the respiration cycle lengths from ECG signal recorded with bed sheet electrodes," *Journal of Physics: Conference Series, Joint IMEKO TC1–TC7–TC13 Symposium*, vol. 459, no. 1, 2013, 6 pages.

Extracting the respiration cycle lengths from ECG signal recorded with bed sheet electrodes

A Vehkaoja, M Peltokangas and J Lekkala
Department of Automation Science and Engineering,
Tampere University of Technology, Tampere, Finland

E-mail: antti.vehkaoja@tut.fi

Abstract. A method for recognizing the respiration cycle lengths from the electrocardiographic (ECG) signal recorded with textile electrodes that are attached to a bed sheet is proposed. The method uses two features extracted from the ECG that are affected by the respiration: respiratory sinus arrhythmia and the amplitude of the R-peaks. The proposed method was tested in one hour long recordings with ten healthy young adults. A relative mean absolute error of 5.6 % was achieved when the algorithm was able to provide a result for approximately 40 % of the time. 90 % of the values were within 0.5 s and 97 % within 1 s from the reference respiration value. In addition to the instantaneous respiration cycle lengths, also the mean values during 1 and 5 minutes epochs are calculated. The effect of the ECG signal source is evaluated by calculating the result also from the simultaneously recorded reference ECG signal. The acquired respiration information can be used in the estimation of sleep quality and the detection of sleep disorders.

1. Introduction and related work

Respiration is one of the most important physiological signals in sleep studies where the data is collected using polysomnography (PSG). It is used for the detection of breathing-related sleep disorders by following the amplitude of the breathing signal and comparing the breathing signals recorded with respiratory inductance plethysmography and temperature sensors. Respiration rate (RR) or respiration cycle length (RCL) can also be used in sleep staging because the variation of respiration rate is higher when a person is awake or during the rapid eye movement sleep stage and is decreased during deep sleep stages [1]. The respiration related features are even more important in novel unobtrusive systems developed for long term monitoring of sleep, like the one presented in [2]. The reason is that smaller amount of physiological signals are available through unobtrusive monitoring techniques and e.g. electroencephalogram and electrooculogram, which are normally used in sleep staging in PSG recordings cannot be measured unobtrusively.

Many authors have investigated the detection of the RR or RCL using ECG signal. In these studies, the ECG has been recorded using conventional electrodes attached to certain locations on the torso. The most commonly used ECG related features for the RR detection are respiratory sinus arrhythmia (RSA) and the modulation of the R-peak amplitude (RPA). The RSA is a result of the variation in the instantaneous heart beat intervals caused by the respiration related control of the autonomous nervous system, whereas the RPA is caused by the changes in the lead field and the heart orientation due to the breathing movement. [3–6]

We have earlier presented a system for recording night-time ECG unobtrusively using textile electrodes sewn on a bed sheet and used the data for detecting heart rate and heart rate variability parameters [7]. The current work investigates the usability of the recorded ECG in the detection of respiration cycle lengths. While other studies have investigated the detection of RR or RCL using conventional electrodes in fixed locations, the electrode locations do not stay constant when using the bed sheet integrated electrodes but change according to the sleeping posture and the measurement channel used. Also the quality of the ECG signal is not always as good as if using the regular gel electrodes.

2. Materials and Methods

2.1. ECG measurement system and R-peak detection algorithm

Our ECG measurement system consists of eight electrodes that are made by embroidering using silver coated polyamide yarn and are sewn on a bed sheet in 5 cm distances. The ECG is measured bipolarly between each adjacent electrode pair, which enables also combining the recorded ECG signals thus forming new ECG leads with wider inter-electrode distance. When recognizing the R-peaks and heart rate from the ECG, the ECG lead that produces the best signal is first selected and then used until the quality of the signal decreases too much. A detailed description of the channel selection and the R-peak recognition procedure is presented in [7] and the effect of combining the ECG channels in [8].

2.2. ECG derived respiration signals and RCL detection

We selected two commonly used respiration related features that are present in the ECG signal to determine the RCL: RSA and RPA. We also tested filtering the ECG signal with low, 0.6 Hz cut-off in order to reveal the baseline wandering caused by the breathing. The resulting signal however suffered from frequent interferences and did not provide as good results as the RSA and RPA signals.

The raw RSA and RPA signals contain one sample for each heartbeat. Both signals are first interpolated into constant 0.1 s sample interval using cubic spline interpolation. After this, the signals are filtered with different pass-bands in order to bring out the respiration related variation in the signals. Theoretically, both signals should contain a sinusoidal kind of variation at the frequency of the respiration but they also include interference components. Different pass-bands are used because the RCL usually varies between 2 s and 10 s, corresponding to the frequency range of 0.1–0.5 Hz. Depending on the respective value of the RCL, different pass-band will produce the best filtering result. The selected pass-bands are 0.1–0.22 Hz, 0.1–0.33 Hz, and 0.1–0.5 Hz. Forward-backward-filtering was used in order to eliminate the phase delay, which in this case could cause a significant distortion in the signals. The order of the Butterworth response filters was set as two. Using the forward-backward filtering then produces the overall filter order of four.

Next, the repetition intervals of each signal are calculated by searching local maxima and minima as well as rising and falling zero crossings and then calculating the repetition intervals of these features. This way, altogether 24 (respiration) interval signals are formed (2 ECG derived signals × 3 filters × 4 features). The interval signals are then linearly interpolated into 1000 ms sample interval. Finally, for each time instant a cluster of six RCL suggestions that are closest to each other is searched for. If the square sum of the distances is less than an empirically set threshold, the center of the cluster is chosen as the RCL for that time instant. If the smallest square distance of any six suggestions is higher than the threshold, no RCL value is chosen. Earlier we used a similar method for detecting the RCLs from the signals that were recorded using force sensors placed under a bed post [8].

2.3. Per epoch mean RCL detection

In addition to the instantaneous RCLs, we also tested how the presented method performs when the RCL values are used for calculating the mean RCL for epochs of certain length. The mean RCL is simply calculated by averaging all the RCLs detected during e.g. 1 or 5 minute epochs. If the mean RCL is calculated for all epochs that contain at least one detected instantaneous RCL, good coverage is achieved but the error of the result is probably higher. The error can be decreased by setting the minimum number of RCLs that must have been detected during an epoch before the mean RCL for the epoch is reported. The results were calculated using the overlaps of 50 and 240 seconds for the 60 and 300 second epoch lengths, respectively.

2.4. Reference respiration measurement

The reference respiration signal was measured using an NTC thermistor placed inside a breathing mask. The resistance of the thermistor was measured, converted into the temperature, and filtered. The respiration rate was calculated from the band-pass filtered temperature signal by finding the maximum from each separate segment that is above the zero level. These points correspond to the end of the inhale phase. Finally, the signals were visually inspected and false or missing detections were corrected. Short sections from the recordings of four test subjects were found, where the amplitude of the reference breathing signal was significantly decreased or the waveform distorted. These parts were discarded from the analysis because reliable reference was not available.

2.5. Test subjects and data collection

We made test measurements with eight male and two female subjects (subjects 6 and 10). The subjects were 23–33-year-old, normal weight and had no history of cardiovascular problems or sleeping related breathing disorders. The measurements were made in laboratory settings using an 80 cm wide spring mattress bed. The subjects were allowed to change their sleeping posture freely. The length of the recordings was approximately one hour and most of the subjects fell asleep during this time. In order to evaluate the effect of the ECG signal source to the performance of the proposed RCL detection algorithm, we also used the reference ECG signal that was recorded at the same time with disposable Ag/AgCl electrodes. The reference electrodes were placed under both clavicles so that they did not disturb the skin contact of the sheet electrodes in any posture.

3. Results

3.1. Instantaneous RCL detection results

Table 1 shows the results of instantaneous RCL detection for each subject. As seen in table 1, there is a significant variation in the performance of the method between the subjects. The best detection coverage was obtained with the data of subject 5, 83.2 % of the total recording time or 91.9 % of time when the source ECG signal was available. The average detection coverage for all the subjects is approximately 40 % of the whole recording time, which is nearly 50 % of the time the bed sheet ECG signal has been available. The ECG signal of the test subject 7 was so low in amplitude that the RPA signal was practically unusable and even when the R-peak detection algorithm was able to find the R-R-interval signal with 74 % coverage, the RCL detector found results that were reliable enough only 3 % of the time. The data of this subject was therefore excluded from the calculation of the average results.

The last two rows in table 1 present the instantaneous RCL detection results calculated using the reference ECG data. The coverage of the detected RCLs is higher when using the reference ECG than with the sheet ECG but this is explained by the fact that the RSA and RPA signals produced by the reference ECG are available almost 100 % of the time whereas the coverage of the sheet ECG based RSA and RPA is 82 % in average. Also the error figures for the reference ECG based RCL are slightly better than for the sheet ECG. The results of the subject 7 were now included because the reference ECG did not suffer from the same problems as the sheet ECG signal.

Table 1. Respiration recognition performance characteristics. The largest and smallest value of each parameter is boldfaced. The last two rows show the minimum, maximum, and the average of the results calculated for each test subject using the reference ECG signal.

	RRI Coverage (%)	*Respiration Coverage (%)*	*Concordance Correlation*	*RMSE [a] (s)*	*MAE [b] (s)*	*MAE [b] (%)*	*e < 0.5 s [c] (%)*	*e < 1 s [c] (%)*
1	93.3	32.1	0.770	**0.782**	**0.527**	**11.135**	**64.1**	**85.3**
2	64.0	42.4	0.948	0.367	0.176	3.744	96.1	99.1
3	**61.4**	28.6	0.791	0.307	0.183	4.714	97.1	99.6
4	69.3	28.3	**0.273**	0.579	0.398	9.871	73.3	93.7
5	90.5	**83.2**	0.929	0.194	0.148	**3.251**	98.1	**100.0**
6	83.6	47.1	0.902	0.224	0.145	3.492	97.5	99.3
7	*74.5*	*3.0*	*0.003*	*0.654*	*0.328*	*10.369*	*86.4*	*90.0*
8	**97.5**	24.4	0.655	0.434	0.239	5.863	88.9	98.0
9	91.5	**19.0**	**0.973**	0.356	0.212	4.621	93.2	98.3
10	94.5	51.2	0.749	**0.169**	**0.131**	3.689	**99.2**	**100.0**
Mean	82.0	39.6	0.777	0.379	0.240	5.598	89.7	97.0
Min-Max Ref ECG	98.5–100.0	13.0–83.6	0.184–0.991	0162–0.588	0.116–0.241	2.678–5.683	94.7–99.3	97.2–100.0
Mean Ref ECG	99.6	47.8	0.777	0.309	0.165	4.144	97.1	98.9

a Root-mean-square error of the instantaneous and interpolated RCL values.
b Mean absolute error of the instantaneous and interpolated RCL values.
c Percentage of the RCL values that are within 0.5 second and 1 second from the reference.

Figure 1 shows as an example, the histogram of the RCL error for the test subject 5. As seen in figure 1, the error produced by the presented method has a Gaussian distribution with zero mean, which shows that the method does not produce any bias to the result. Figure 2 shows the scatter plot of the sheet ECG based instantaneous RCL values and the thermistor reference values for the same person. The concordance correlation is a measure of the deviation of the variable pairs from the 45-degree line drawn through the origin (the grey line in figure 2).

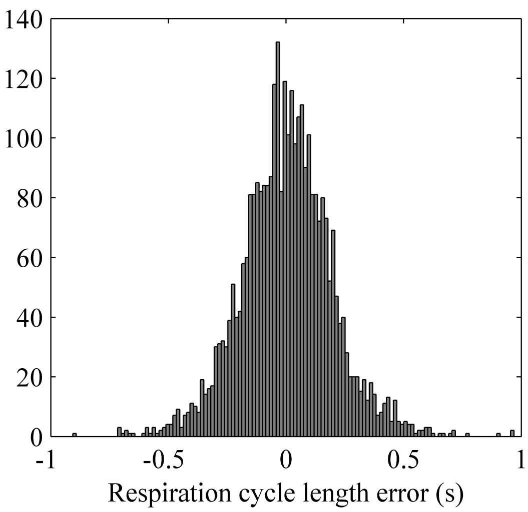

Figure 1. Histogram of the error of the detected respiration cycle lengths (subject 5).

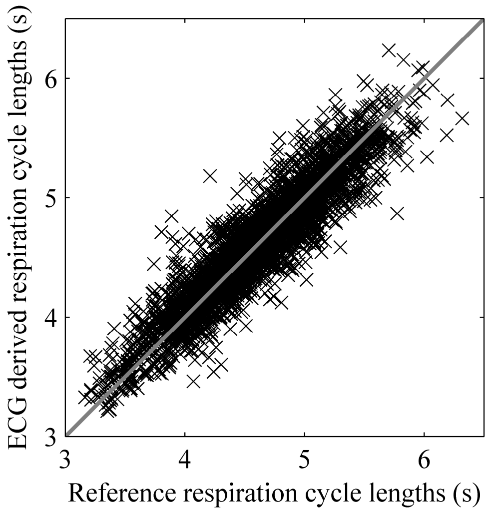

Figure 2. Scatter plot of the respiration results (subject 5).

3.2. Mean RCL detection results

Figure 3 shows the coverage and the mean absolute error (MAE) of the mean RCL values as a function of the minimum required number of the instantaneous RCLs in an epoch. The results in figure 3 are calculated for 1 minute epoch length and using 50 seconds overlap between epochs. 88.4 % of all epochs calculated using the sheet ECG data contained at least one RCL value and the average relative MAE for the mean RCL was 6.6 %. Somewhat better mean RCL coverage is achieved by using the reference ECG signal because the reference signal is always available. The average MAE is slightly smaller for the reference ECG when all possible epochs are considered but when the minimum number of the required RCLs in an epoch is increased, both signals produce similar errors.

Orphanidou *et al.* received 4.8 % average relative MAE for 1 minute mean respiration rate with young subjects when they combined the RSA and RPA signals by selecting as the result the one that has the higher magnitude of the pole in the autoregressive spectrum [3]. They did not calculate the results for all the available data but used a criterion for choosing the parts where a high quality reference signal was available. In this way they used 71 % of the available data. Similar coverage is achieved by the sheet ECG data when setting a 10 % minimum value for the within epoch RCL coverage. The average relative MAE is then approximately the same as in [3]. The reference ECG yields approximately 3.3 % MAE when using the same criterion.

Cysarz *et al.* used the concordance correlation coefficient (CCC) to describe the agreement between the respiration rate calculated in 5 minute time windows from a single ECG lead and the reference air flow sensor [4]. The regular Pearson correlation only considers the linear dependency of two variables but concordance correlation also takes into account the difference of the exact values of the tested variables. Cysarz *et al.* received the night-time CCC values of 0.79 and 0.73 younger group of subjects when using only RSA and RPA signals, respectively. They did not consider the epochs where the valid R-peaks were available less than 75 % of the time.

Table 2 shows the CCCs between the 1 and 5 minute mean RCLs and the thermistor based reference RCL. The average CCC of 0.63 was achieved with both sheet and reference ECG when all available epochs were considered. The CCCs are considerably improved (0.82 and 0.86 for the sheet and the reference ECG) when only the epochs that contain at least 25 % of the RCLs are considered. The mean RCL coverages are however then decreased to 64 and 79 %.

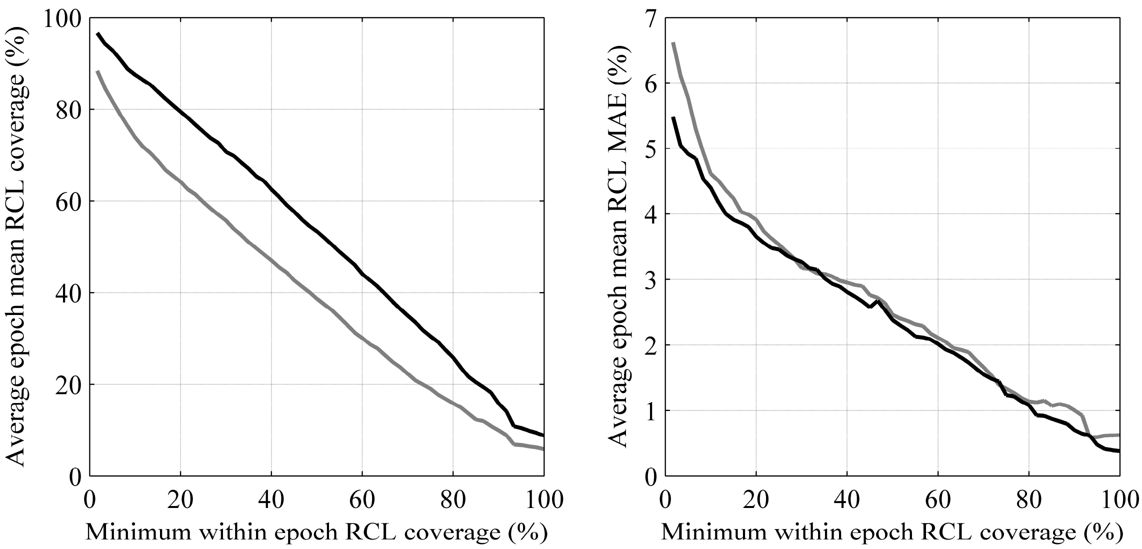

Figure 3. The average dependency of the coverage (left) and the MAE of the mean RCL values (right) for one minute epochs for all subject. The results calculated from the reference ECG are shown in black and the results calculated from the sheet ECG in grey.

Table 2. Average per epoch mean RCL recognition coverage and concordance correlation coefficients for 1 and 5 minute epoch lengths.

		Coverage Sheet (%)	*Coverage Reference (%)*	*Concordance Correlation Sheet*	*Concordance Correlation Reference*
1 minute epoch length	**All epochs**	88.4	96.6	0.69	0.59
	Epochs > 25 %	58.3	73.7	0.89	0.87
	Epochs > 50 %	37.4	51.9	0.94	0.95
	Epochs > 75 %	17.7	29.2	0.96	0.98
5 minute epoch length	**All epochs**	99.8	100	0.63	0.63
	Epochs > 25 %	64.2	79.2	0.82	0.86
	Epochs > 50 %	36.1	56.6	0.85	0.87
	Epochs > 75 %	13.3	23.8	0.96	0.87

Epochs > 25 %, 50 % or 75 %: only epochs that include more than the specified amount of recognized instantaneous RCL values are considered.

4. Conclusions

A method for detecting instantaneous respiration cycle lengths from an ECG signal recorded with bed sheet integrated textile electrodes or regular ECG electrodes has been presented. Also mean RCLs are calculated for 1 and 5 minute epochs and the results compared with methods found in the literature. The proposed method performs well with both sheet ECG and reference ECG signals at least with the test subjects who were younger than 35 years.

The future work includes the evaluation of the proposed method with people of wider demographics. It has been concluded that the RSA phenomenon attenuates along with aging and that parameter is not as efficient for estimating the RCL with older people [4].

References

[1] Chung G, Choi B, Lee J, Lee J, Jeong D and Park K S 2009 REM sleep estimation only using respiratory dynamics *Physiological Measurement* **30** 1327–40

[2] Paalasmaa J, Waris M, Toivonen H, Leppäkorpi L and Partinen M 2012 Unobtrusive online monitoring of sleep at home *Proc. 34th Ann. Int. Conf. IEEE Engineering in Medicine and Biology Society* (San Diego, CA, USA, 28 August–1 September 2012), pp 3784–88

[3] Orphanidou C, Fleming S, Shah S A and Tarassenko L 2013 Data fusion for estimating respiratory rate from a single-lead ECG *Biomedical Signal Processing and Control* **8** 98–105

[4] Cysarz D, Zerm R, Bettermann H, Frühwirth M, Moser M and Kröz M 2008 Comparison of Respiratory Rates Derived from Heart Rate Variability, ECG Amplitude, and Nasal/Oral Airflow *Annals of Biomedical Engineering* **36** 2085–94

[5] O'Brien C and Heneghan C 2007 A comparison of algorithms for estimation of a respiratory signal from the surface electrocardiogram *Computers in Biology and Medicine* **37** 305–14

[6] Boyle J, Bidargaddi N, Sarela A and Karunanithi M 2009 Automatic Detection of Respiration Rate From Ambulatory Single-Lead ECG *Transactions on Information Technology in Biomedicine* **13** 890–6

[7] Peltokangas M, Verho J and Vehkaoja A 2012 Night-Time EKG and HRV Monitoring With Bed Sheet Integrated Textile Electrodes *Transactions on Information Technology in Biomedicine* **16** 935–42

[8] Vehkaoja A, Peltokangas M., Verho J and Lekkala J 2012 Combining unobtrusive electrocardiography and ballistography for more accurate monitoring of sleep *Proc. IEEE 12th Int. Conf. on Bioinformatics and Bioengineering* (Larnaca, Cyprus, 11–13 November 2012) pp 202–7

Publication V

Vehkaoja, A., Salo, A., Peltokangas, M., Verho, J., Salpavaara, T., and Lekkala, J., "Unconstrained night-time heart rate monitoring with capacitive electrodes," in *Proceedings of XIII IFMBE Mediterranean Conference on Medical and Biological Engineering and Computing 2013*, vol. 41, 2014, pp. 1511–1514.

Unconstrained night-time heart rate monitoring with capacitive electrodes

A. Vehkaoja, A. Salo, M. Peltokangas, J. Verho, T. Salpavaara and J. Lekkala

Department of Automation Science and engineering, Tampere University of Technology, Tampere, Finland

Abstract—**An unobtrusive measurement system for night-time heart rate (HR) monitoring is presented. The system uses capacitive electrodes that do not require galvanic skin contact, thus allowing user to wear clothes while being monitored. The electrodes are located transversely on the bed and the electrocardiographic signals are measured between each electrode and a common reference. The signals are then combined in order to remove the common mode movement artifacts and the best one is selected for HR detection.**

The average RR-interval detection coverage with five test subjects in one hour long measurements was 81.0 %. The average mean absolute error compared to the reference ECG signal was 1.78 ms in average.

Keywords— **Night-time heart rate, capacitive electrode, physiological monitoring**

I. Introduction and motivation

Night-time physiological information, especially the heart rate, the respiration rate and the movements can be used for example in screening of medical disorders like sleep apnea [1] and evaluation of sleeping quality [2] or detecting psychophysiological stress [3]. Many potential applications would benefit or even require continuous monitoring for detecting long term changes in sleeping pattern and sleep parameters. In these cases, it is important that the measurement equipment is unobtrusive and requires little effort from the user. Comfort is increased if the user does not need to wear the measurement equipment but the sensors are e.g. integrated into the bed.

There are several sensor options for such an unconstrained monitoring system. Heart rate and respiration can be extracted from ballistographic signals that are recorded using force sensors e.g. [4] or from the electrocardiogram (ECG) that can be measured with contact electrodes attached to a shirt or to the bed sheet as e.g. in [5]. The drawback of the ballistographic technique is that it is very sensitive to all kinds of movements. For example, movements caused by another person sleeping in the same bed can disturb the measurement and cause erroneous results. In addition, the ballistographic signal does not have as distinguishable and consistent features as the ECG's R-peak, which increases the uncertainty to the beat-to-beat interval detection. Contact ECG recorded e.g. with textile electrodes attached to the bed sheet enables monitoring of heart rate and heart rate interval generally with better coverage and accuracy than the ballistographic technique but its drawback is the requirement for direct skin contact which, in practice, prevents the user from wearing a shirt during the measurement. Using capacitive non-contact electrodes for measuring the ECG signal combines the good features of these two techniques by measuring the signal that enables accurate detection of the heart rate, yet allowing the user to wear clothes while being monitored.

II. Related work

ECG recording using capacitive bed-integrated electrodes has been studied by several researchers. Wu and Zhang used wide electrode strips made of conductive textile and placed them on the bed in transversal direction. They measured the ECG between two strips while the third strip acted as an active ground electrode [6]. They received good results when making the test measurements in an electrically shielded room. More than 98 % of the recorded data was artifact free by visual inspection. They however reported the heart rates as a mean value for one minute so it is not possible to say the amount of correctly recognized individual R-peaks. An interesting detail in their approach was that they used a high-pass cut-off frequency as high as 8 Hz when filtering the measurement signal. Usually the high-pass filter is set below 1 Hz frequency in ECG recordings.

Similar electrode setup was also used by Ishida *et al* in [7]. They also tested the effect of a layer of electrically shielding material under the electrodes. Despite that the shielding decreased the coupling of electrical interference, they were able to detect the heart rate only 27 % of the time during one night measurement.

Lim *et al.* developed a capacitive ECG measurement system that uses several active electrodes placed transversally on top of the mattress and a large sized common reference electrode located under the lower body [8]. They stated that the capacitive measurement is very sensitive to motion artifacts and that the main sources for these are the changes of the electrode and the grounding capacitances and the triboelectrical effect caused by friction of the clothes. The morphology of the ECG signal measured with a similar electrode setup has also been successfully used for detecting sleeping posture [9].

III. Materials and Methods

A. The measurement setup

Our ECG monitoring system consists of four capacitive active electrodes and a large common reference electrode. The active electrodes are located transversally so that they are approximately at the location of the chest. The inter-electrode distance is set to 5 cm. The whole width of the bed cannot be covered when using such small inter-electrode distance and only four measurement electrodes, but this has not been a major problem in the laboratory measurements, where the position of the test person can be controlled. More electrodes are, however, needed if the system is used at home in overnight measurements. The capacitive reference electrode is made of a conductive fabric and it is placed under the bed sheet thus covering the whole area of the bed.

In previous studies we have measured ECG with contact electrodes attached transversally to the bed sheet by using bipolar measurement between the electrodes [5]. When using capacitive electrodes, the high-pass cut-off frequency of each electrode depends on the skin-electrode capacitance and the input resistance of the active electrode. The skin-electrode capacitances may vary during the measurement and are not necessarily the same in all electrodes. Having different cut-off frequencies in the electrodes would decrease e.g. the common mode rejection ratio of a bipolar measurement and therefore we decided to use the unipolar measurement between each active electrode and a common reference electrode.

The reference electrode is made as large as possible in order to maximize its capacitance with the body, thus making the capacitive grounding as strong as possible. If the body is in galvanic contact with the electrode, the grounding is further improved and the measurement noise decreases. Fig. 1 shows the measurement setup used.

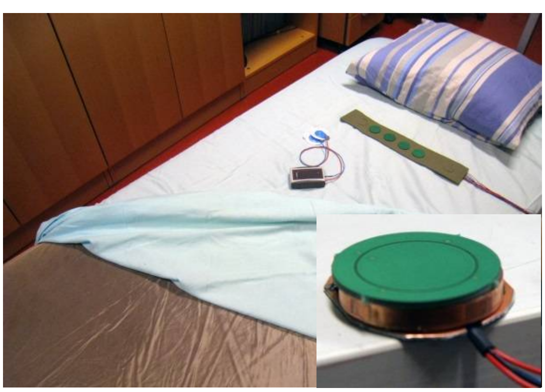

Fig. 1 Capacitive ECG system and a close-up view of one electrode. The wireless contact ECG reference device is also seen on the bed.

B. The capacitive active electrodes

An important aspect, when designing a measurement system that uses capacitive electrodes, is to provide high input resistance with respect to the electrode capacitance. We chose OPA129 from Texas Instruments as the operational amplifier for the active electrodes because it has extremely low input bias current (±30 fA typical) thus enabling the use of extremely high resistance in the bias current path and therefore also high input impedance in the capacitive electrode.

In order to increase the input impedance of the amplifier connection, the bias current is taken from the amplifier's output using so called bootstrap connection. This effectively multiplies the value of the bias resistor R1 in the Fig. 2 by the ratio of resistors R5 and R4:

$$R_{in} = (\frac{R5}{R4} + 1) \cdot R1 + R3 \quad (1)$$

The benefit of the bootstrap connection is that the effects of the leakage currents on the circuit board are minimized because the value of the actual resistor can be set smaller and the voltage across the resistor is smaller. The drawback of the bootstrap circuit on the other hand is that it increases the noise and the offset voltage of the amplifier. However, the frequency bandwidth required in ECG monitoring is so small that the increased noise density is seldom a critical issue.

The diameter of our active electrodes is 25 mm. When the person being measured is wearing 0.5 mm thick cotton shirt, assuming relative permittivity of 2, the capacitance of the electrode becomes approximately 20 pF and the high-pass cut-off frequency then about 0.1 Hz.

Because of the extremely high input impedance, it is important to carefully protect the amplifier input from leakage currents that might cause the input voltage to wander uncontrolled. A guard trace is therefore placed everywhere around the electrode surface and the op amp on the layout. Special pinout of the OPA129 also supports efficient guarding.

The guard also decreases the parasitic capacitance of the circuit board layout, but the input capacitance of the amplifier component is still present. In order to minimize the remaining parasitic capacitance we used an active positive feedback for compensating it. The gain of the feedback is adjusted by the trimmer resistor R2 so that when a square wave signal is fed capacitively to the electrode, its waveform should not be distorted, besides the distortion caused by the high-pass filter in the electrode input. Similarly, the amplitude should match the gain of the active electrode, 0.9 in our case.

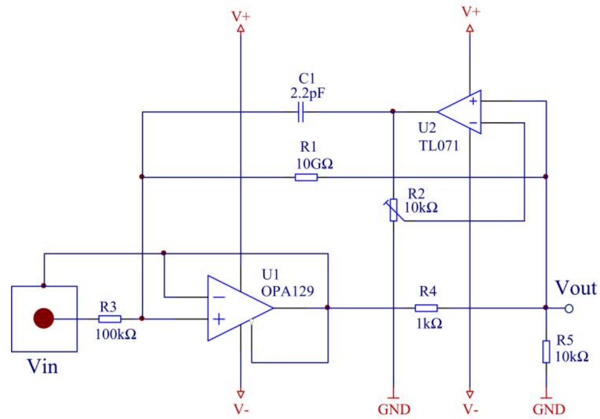

Fig. 2 The schematic of the capacitive active electrodes.

C. Data acquisition

The four capacitive active electrodes, along with the common reference electrode, are connected to a custom made data acquisition (DAQ) device. The input voltage range of the DAQ is ± 0.436 V with a resolution of 13.4 μV when the DAQ's internal amplifier, that has a gain of 5, is used. The RMS noise level of the DAQ is less than 1 digital unit.

The DAQ is capable of transmitting the measurement data to the PC either through a USB or by a wireless Bluetooth link. We used the Bluetooth mode in the tests. The maximum sampling rate is 1 kHz per channel but 250 Hz was found high enough for the capacitive ECG recording.

D. Signal processing

The capacitive ECG measurement is very sensitive to movements. Large movements, e.g. changing the sleeping posture or even a movement of a limb causes so strong disturbance to the measured signal that recognition of R-peaks is impossible. Even the ballistographic movements caused by heart beats and breathing may cause interference that is higher in amplitude than the electrical ECG signal as seen in the upper figure of Fig. 3. Luckily, often the movement artifact is seen similarly in multiple channels while the ECG component in the signals is different because of the different electrode location on the body. We therefore combine the measurement channels by subtracting their signals and let a channel selection algorithm to select the best signal for R-peak detection. Also the original signals are used as possible candidates in the selection phase.

We used same signal processing algorithm for finding the R-peaks, selecting the best channel, and calculating the heart rate as we have earlier used for processing ECG signal recorded with contact electrodes attached on a bed sheet. A detailed description of the algorithm can be found from [5]. All digital signal processing was done off-line using MATLAB®.

E. Reference ECG measurement

When testing sensitive capacitively coupled ECG measurement systems, care must be taken that the reference measurement does not affect the capacitive measurement. For example, the reference device should not be connected in such a way that galvanic ground current path would be provided through its electrodes. Therefore we used a wireless ECG measurement system for recording the reference data. Disposable Ag-AgCl electrodes were attached below left and right clavicles and the reference ECG was measured between them. The reference and the capacitive ECG data were synchronized manually. The reference recording system has been presented in [10].

F. Test measurements

We evaluated the operation of the system with five test subjects in one hour long recordings. All subjects were normal weight healthy male adults (25-33 years) with no history of cardiovascular diseases. Subjects spent 15 minutes in each main sleeping posture (supine, left side, prone, and right side) and they were wearing t-shirt made of cotton. Any galvanic contact to the measurement device was prevented.

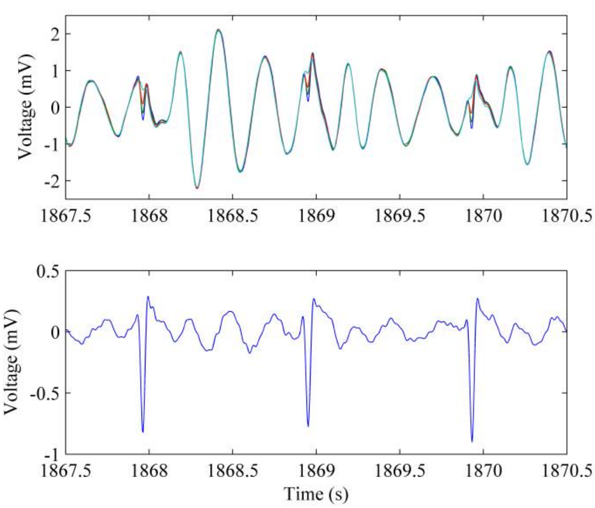

Fig. 3 Four signals recorded with the capacitive electrodes (upper figure). Large common mode artifacts are caused by the ballistographic movements caused to the heartbeats. The lower figure shows how the R-peaks are emphasized when subtracting two signals (blue and cyan).

IV. Results

Table 1 shows the results calculated from the five test measurements. The RR-interval detection coverage varied between 62 % and 96 % between the subjects during the whole one hour measurement period. The average coverage was 81 %.

The average mean absolute error (MAE) of the detected RR-intervals was 1.78 ms, which can be considered a good result. Recordings of the test subjects 3 and 5 both contained 3 false positive R-peak detections, which increase the MAE slightly. The error is also partially explained by the small temporal drift between the signals of the capacitive and reference recording devices. This results from the different sampling clocks between the two devices. The drift was only approximately 0.1 seconds during the one hour measurements so we decided not to correct it.

A. The effect of the sleeping posture

The Table 1 also presents the detection coverage figures for each sleeping posture separately. As seen from the results, the capacitive heart rate monitoring system performs well in all other sleeping postures but is not as reliable when the person is lying on the right side. For the subject number three, the RR-intervals were detected only 8 % of the time spent on the right side and for the subject number five, the algorithm was not able to find any R-peaks. A visual inspection of the data of the subject number five showed that the ballistographic movement component was seen in the signal but the ECG component wasn't different enough between the channels to produce usable results. A possible explanation for the missing electrical difference component is that because the heart is located on the left side of the body, the difference signal between any two electrodes at the right side was not strong enough for the R-peak detection.

The rightmost column in the table shows the average detection coverage of all postures. The time period of changing the posture is not considered in this data.

Table 1 Performance figures of the capacitive ECG monitoring system.

Subject number	Coverage	MAE (ms)	Cov. supine	Cov. left	Cov. prone	Cov. right	Mean Cov.
1	84.77	1.88	90.77	72.53	93.02	91.69	87.0
2	89.82	1.62	97.85	91.48	98.47	85.91	93.4
3	62.66	1.96	92.49	87.20	70.85	8.42	64.7
4	95.96	0.92	99.28	99.87	99.82	96.63	98.9
5	71.90	2.51	99.88	99.88	97.58	0.00	74.3
Average	81.0	1.78	96.1	90.2	91.9	56.5	83.7

V. Conclusions

A bed integrated system for capacitive monitoring of the ECG signal was proposed. The system performs well in other sleeping postures but has sometimes problems in detecting R-peaks from the ECG signal recorded when the subject is lying on the right side. Testing the monitoring system in overnight measurements is a part of the future work, as well as finding a solution for the R-peak detection in right side sleeping posture.

Acknowledgment

The authors would like to thank the test subjects for their participation.

References

1. Roche F, Gaspoz J-M, Court-Fortune I et al. (1999) Screening of obstructive sleep apnea syndrome by heart rate variability analysis. Circulation, 100(3):1411–1415
2. Bulckaert A, Exadaktylos V, De Bruyne G et al (2010) Heart rate-based nighttime awakening detection. Eur J. Appl. Physiol. 109(2):317–322
3. Hall M, Vasko R, Buysse D et al (2004) Acute stress affects heart rate variability during sleep. Psychosom Med 66(1):56–62
4. Brüser C, Stadlthanner K, de Waele S, Leonhardt S (2011) Adaptive beat-to-beat heart rate estimation in ballistocardiograms. IEEE Trans. on Inf. Tech. Biom. 15(5):778–786
5. Peltokangas M, Verho J, Vehkaoja A (2012) Night-Time EKG and HRV Monitoring With Bed Sheet Integrated Textile Electrodes. IEEE Trans. on Inf. Tech. Biom. 16(5):935–942
6. Wu K-f, Zhang Y-t (2008) Contactless and continuous monitoring of heart electric activities through clothes on a sleeping bed. Proc. vol. 5, Int. Conf. on Inf. Tech. Appl. Biom. ITAB, Shenzhen, China, 2008, pp 282–285
7. Ishida S, Shiozawa N, Fujiwara Y, Makikawa M (2007) Electrocardiogram measurement during sleep with wearing clothes using capacitively coupled electrodes. Proc. vol. 29 Ann. Int. Conf. IEEE Eng. Med. Biol. Soc. in Engineering in Medicine and Biology Society, Lyon, France, 2007, pp 2647 –2650
8. Lim Y G, Kim K K, Park K S (2007) ECG recording on a bed during sleep without direct skin-contact. IEEE Trans. on Biomed. Eng. 54(4):718–725
9. Lee H, Hwang S, Lee S et al. (2013) Estimation of Body Postures on Bed Using Unconstrained ECG Measurements. IEEE J. Biomed. and Health Inf. (in press)
10. Vehkaoja A, Verho J, Cömert A et al. (2012) Wearable System for EKG Monitoring - Evaluation of Night-Time Performance. Revised Selected Papers from Mobihealth 2011, Lecture Notes of the Institute for Computer Sciences, Social Informatics and Telecommunications Engineering, 83:119-126

Author: Antti Vehkaoja
Institute: Tampere University of Technology
Street: Korkeakoulunkatu 3
City: Tampere
Country: Finland
Email: antti.vehkaoja@tut.fi

Tampereen teknillinen yliopisto
PL 527
33101 Tampere

Tampere University of Technology
P.O.B. 527
FI-33101 Tampere, Finland

ISBN 978-952-15-3470-6
ISSN 1459-2045